Constraint Relaxations: Analyzing the Impacts on System Reliability, Dynamics, and Markets

Final Project Report

Power Systems Engineering Research Center

Empowering Minds to Engineer
the Future Electric Energy System

Constraint Relaxations: Analyzing the Impacts on System Reliability, Dynamics, and Markets

Final Project Report

Project Team

Kory W. Hedman, Project Leader
Arizona State University

Vijay Vittal
Arizona State University

James McCalley
Iowa State University

Graduate Students

Yousef M. Al-Abdullah, Ahmed Salloum, Jonghwan Kwon
Arizona State University

Xian Guo
Iowa State University

PSERC Publication 15-04

September 2015

For information about this project, contact

Kory W. Hedman
Arizona State University
School of Electrical, Computer, and Energy Engineering
P.O. BOX 875706
Tempe, AZ 85287-5706
Phone: 480 965-1276
Fax: 480 965-0745
Email: kory.hedman@asu.edu

Power Systems Engineering Research Center

The Power Systems Engineering Research Center (PSERC) is a multi-university Center conducting research on challenges facing the electric power industry and educating the next generation of power engineers. More information about PSERC can be found at the Center's website: http://www.pserc.org.

For additional information, contact:

Power Systems Engineering Research Center
Arizona State University
527 Engineering Research Center
Tempe, Arizona 85287-5706
Phone: 480-965-1643
Fax: 480-965-0745

Notice Concerning Copyright Material

Acknowledgements

This is the final report for the Power Systems Engineering Research Center (PSERC) research project titled “Constraint Relaxations: Analyzing the Impacts on System Reliability, Dynamics, and Markets” (project M-29). We express our appreciation for the support provided by PSERC’s industry members and by the National Science Foundation under grant NSF EEC 9908690 received under the Industry / University Cooperative Research Center program.

The authors thank industry collaborators including Juan Castaneda (SCE); Hong Chen (PJM); Erik Ela (EPRI), Robert Entriken (EPRI); David Gray (Southwest Power Pool); Marissa Hummon (National Renewable Energy Laboratory); Jay Liu (PJM); Muhammad Marwali (New York ISO); Khosrow Moslehi (ABB); Jim Price (California ISO); Alva Svoboda (PG&E); Michael Swider (New York ISO); Xing Wang (ALSTOM Grid); Li Zhang (Midcontinent ISO); and Feng Zhao (ISO New England).

Executive Summary

Today, system operators enable constraint relaxations by allowing the constraint to be violated for a set penalty, i.e., price. Including constraint relaxation practices in market models provides several benefits, such as providing a mechanism to cap the market clearing prices in the energy market models, possible gains in social welfare (market surplus), and assisting the market model to find good feasible solutions. The primary goal of this report is to examine the impact of constraint relaxation practices on market outcomes, system reliability, and system stability. In addition, the report investigates the market implications of enabling constraint relaxations with appropriate price cap on shadow prices and proposes alternative mechanisms. Finally, this report investigates the practice of risk-based constraint relaxation in handling infeasibility in real-time market model. The report is presented in two parts.

Part I: Analyzing the Impacts of Constraint Relaxations on System Reliability, Dynamics, and Markets

Part I of the final report on PSERC project M-29 reviews and implements the practice of including constraint relaxations in market models similar to those an Independent System Operator (ISO) might perform. Part I of this report contains an analysis of market implications, alternative penalty price schemes, a methodology to price thermal line limit constraints, and discusses the effects on system reliability and stability.

While constraint relaxation practices are disclosed to market participants, overall, the benefits of constraint relaxation practices are not well understood and analyzed. Moreover, the implications these practices have on market outcomes have not been thoroughly investigated either. In this report, using a standard IEEE test case and a 15,000 bus test case based on proprietary data from PJM, the effect of constraint relaxation practices were investigated. This report shows that:

- Constraint relaxations allow ISOs to handle approximations inherent within market models and aid the market in converging to a feasible solution.
- The practices of allowing constraint relaxations in market models enable a market operator to model select constraints as soft constraints, which would otherwise be unnecessarily strictly enforced as a hard constraint.
- Constraint relaxations are a mechanism for price control.
- There are different forms of constraint relaxation practices that could be utilized by ISOs today. However, these forms should be practical to the ISO and negotiated with market participants.
- Penalty prices for line thermal limit constraints can be determined more accurately based upon risk associated with to the conductor degradation.
- While constraints that are violated within the market model (e.g., a system operating limit, SOL) are generally corrected after the market closes (operators

modify the market solution to eliminate the violation), constraint relaxation practices can result in actual violations during real-time operations.

- The utilization of constraint relaxation practices allows for further transfer capability, which enables added economic gains but results generally in fewer generators being typically committed. As a result, reactive power availability from the proposed market solution was limited and out-of-market corrections were needed to fix base-case and post-contingency voltage violations.
- Thermal limit line relaxations in the proposed market solution will usually appear as an overload in real-time, if not corrected in the post-processing phase.
- Constraint relaxations that are allowed to appear in real-time did not cause instability for the test cases utilized. However, the system suffered from higher post-contingency rotor angle oscillations, which implies narrower stability margins.

In closing, although constraint relaxation practices are widely utilized by ISOs today and although these practices are disclosed, further transparency is recommended and further understanding of the implications of these practices is recommended as well. In terms of transparency, the steps taken by ISOs to modify the market solutions to remove violations after the market closes are not clearly communicated. Furthermore, the frequency and duration by which constraint relaxations show up in actual system operations (exist during actual operations) is not widely known, which makes it difficult to assess the impact on system reliability, security, and stability. Moreover, current penalty prices set by ISOs are determined through negotiations with market participants. However, more accurate penalty prices should be determined based on the overall impact on market surplus while considering the risk associated to system reliability and security.

Part II: Risked-Based Constraint Relaxation for Security Constrained Economic Dispatch

Part II of the final report on PSERC project M-29 reviews and implements the practice of including constraint relaxations in security constrained economic dispatch (SCED) in industry; it proposes and illustrates the practice of risk-based constraint relaxation (RBCR) in handling infeasibility in SCEDs. Part II of this report contains state of art in handling infeasibilities in SCEDs, definition of the risk metric used, formulations and illustration of RBCR, and analysis of the interaction between constraint relaxations and electricity markets, with particular focus on locational marginal prices.

While the current form of constraint relaxation is convenient to implement in practice, it has three significant weaknesses. First, it does not facilitate the control of, or even monitoring of, increased system stress that may result from constraint relaxation. Second, it requires the selection of a penalty price when constraints are violated, where the penalty price selection method is ad-hoc. Third, use of the penalty price results in geographically variable and temporally volatile locational marginal prices. In this report, using an IEEE six-bus network, we have illustrated these weaknesses; in addition, we have extended the previously developed risk-based SCED (RB-SCED) in developing the RBCR. RB-SCED has been developed over the past ten years as an implementation of SCED which enables

increased levels of security with increased levels of economy by constraining system risk while relaxing risk associated with post-contingency flows on individual circuits. A key feature of RB-SCED is that it exerts redispatch control for all "heavy" post-contingency flows (and not just those exceeding their limits) in proportion to each post-contingency flow's loading level (e.g., redispatch control is greater for a 110% post-contingency overload than for a 95% post-contingency overload, but both are controlled). The work described in this report shows that:

- Constraint relaxations is an effective and feasible way to conduct infeasibilities in SCED, which otherwise would be infeasible.
- Risk is a probabilistic metric to quantify the likelihood and severity, which is related to the expectation of the sum, over all 'N-1' contingencies, of normalized flows on post-contingency heavily loaded circuits, thus, risk is a useful metric for quantifying system security level.
- The practice of RBCR allows two alternative formulations, risk as a part of the objective function, which enables minimization of cost and risk simultaneously; and risk as a constraint to realize controlled risk level with enhanced economy.
- The practice of RBCR also monitors critical contingency risk and second contingency circuit risk; this provides that the system under any first contingency or corresponding second contingency does not introduce excessive risk.
- The approach of RBCR achieves lower geographical variability and temporal volatility in the LMP, that is to say, it could smooth LMP distribution.
- The approach of RBCR results in more secure operating conditions with little increase in production cost, and perhaps even with a decrease in production costs.

We make the case in this work that RBCR is a promising way to addressing the infeasible SCED problem. Future work in a PSERC-funded follow-on project includes constraint relaxation by dynamic line rating, constraint relaxation under normal condition and constraint relaxation for corrective security constrained economic dispatch.

Project Publications

Y. M. Al-Abdullah, A. Salloum, K. W. Hedman, V. Vittal, "Analyzing the Impacts of Constraint Relaxations in Electric Energy Markets," *IEEE Transactions on Power Systems*, - under review

Y. M. Al-Abdullah, J. Kwon, G. L. Labove, K. W. Hedman, V. Vittal, "Examination of Penalty Policies in Electric Energy Markets," *Electric Power System Research*, to be submitted.

Y. Al-Abdullah, M. Abdi-Khorsand, and K. W. Hedman, "Analyz-ing the impacts of out-of-market corrections," *in 2013 IREP Symp.*, pp. 1-10, Crete, Greece, Aug. 2013.

Y. M. Al-Abdullah, M. Abdi-Khorsand, K. W. Hedman, “The role of out-of-market corrections in day-ahead scheduling,” *IEEE Trans. Power Syst*., accepted for publication.

J. Kwon and K. W. Hedman, "Risk-based penalty price determination for thermal constraint relaxation," *IEEE transactions on power systems*, to be submitted.

A. Salloum and K. W. Hedman, “Base case and post contingency constraint relaxations impacts on system security,” *Arizona State University Reading and Conference*, 2015.

A. Salloum and K. W. Hedman, “Constraint relaxations impacts on power system performance,” *Electric Power Systems Research*, to be submitted.

X. Guo and J. McCalley, “Risk-based constraint relaxation for security constrained economic dispatch,” *North American Power Symposium*, 2015.

Student Theses

Yousef M. Al-Abdullah. *Implications of Constraint Relaxation and Out-of-Market Correction Practices in Electric Energy Markets*. PhD dissertation, Arizona State University, Tempe AZ, expected in February 2016.

Ahmed Salloum. *Constraint Relaxations Impacts on Power System Performance*. PhD dissertation, Arizona State University, Tempe AZ, expected in May 2016.

Jonghwan Kwon. *Economic Assessment of Thermal Constraint Relaxation along with the Conductor Degradation Model within the Transmission Expansion Planning Problem*. PhD dissertation, Arizona State University, Tempe AZ, expected in February 2017.

Intentionally Blank Page

Part I

Analyzing the Impacts of Constraint Relaxations on System Reliability, Dynamics, and Markets

Yousef M. Al-Abdullah
Ahmed Salloum
Jonghwan Kwon
Kory W. Hedman
Vijay Vittal

Arizona State University

For information about this project, contact

Kory W. Hedman
Arizona State University
School of Electrical, Computer, and Energy Engineering
P.O. BOX 875706
Tempe, AZ 85287-5706
Phone: 480 965-1276
Fax: 480 965-0745
Email: kory.hedman@asu.edu

Power Systems Engineering Research Center

The Power Systems Engineering Research Center (PSERC) is a multi-university Center conducting research on challenges facing the electric power industry and educating the next generation of power engineers. More information about PSERC can be found at the Center's website: http://www.pserc.org.

For additional information, contact:

Power Systems Engineering Research Center
Arizona State University
527 Engineering Research Center
Tempe, Arizona 85287-5706
Phone: 480-965-1643
Fax: 480-965-0745

Notice Concerning Copyright Material

Table of Contents

List of Figures

List of Tables

Nomenclature

Indices and Sets

g	Index of generators, $g \in G$.
$g(n)$	Set of generators connected to node n.
$H(g)$	Set of hydro-generators.
i	Index of generator segments, $i \in I$.
j	Index of penalty price segments, $j \in J$.
k	Index of transmission lines, $k \in K$.
n	Index for buses, $n \in N$.
t	Index for time periods, $t \in T$.
$\delta^+(n)$	Set of lines specified as to node n.
$\delta^-(n)$	Set of lines specified as from node n.

Parameters

B_k	Electrical susceptance of line k.
B_{im}	Imaginary part of admittance of element between i and m.
C_k^{end}	End of service cost.
c_{gi}^{OP}	Operational cost of unit g (\$/MWh) segment i.
c_g^{NL}	No-load cost of unit g.
c_g^{SD}, c_g^{SU}	Shutdown and startup cost of unit g.
d	Conductor diameter.
d_{nt}	Demand at bus n in period t.
Deg_T	Loss of tensile strength of a conductor.
FS_g	Indicator for unit g as a fast-start unit.
G_{im}	Real part of admittance of element between i and m.
$I^2R(T_C)$	Joule heat gain.

J	Jacobian matrix.
J_r	Reduced Jacobian matrix.
P_{gi}^{Limit}	Max output of unit g for segment i.
P_g^{max}	Max output of unit g.
P_i	Real power consumed at bus i.
P_k^{max}	Thermal rating of transmission line k.
P^k	Penalty for relaxing transmission constraints.
P^N	Penalty for relaxing node balance constraint.
P^R	Penalty for relaxing operating reserve constraints.
$PTDF_{nk}^{REF}$	Power transfer distribution factor for an injection at n sent to the reference bus, for flow on line k.
Q_c	Forced convection heat loss.
Q_i	Reactive power consumed at bus i.
Q_r	Radiated heat loss.
Q_s	Solar heat gain.
$R(T_C)$	Line resistance at T_C.
R_g^{HR}, R_g^{10}	Max hourly and 10-min ramp rates of unit g.
RS_{al}	Residual tensile strength of an aluminum strand.
Si	Complex power consumed at bus i.
STR_{al}	Initial strength of aluminum strands.
STR_{st}	Initial strength of steel cores.
STR_T	Initial strength of a conductor.
T_C	Line temperature.
T_a	Ambient temperature.
UT_g, DT_g	Minimum up time and down time of unit g.
W_a	Wind speed.

x	State vector of the system.
Y	Admittance matrix.
α	Percent of total supply required for operating reserve for period *t*.
β	Percent of non-hydro supply required for operating reserve for period *t.*
Variables	
I_i^*	The conjugate current injected at bus i.
P_{git}	Real power output for unit g, segment i, period t.
P_{gt}^{total}	Total real power output for unit g in period t.
P_{nt}^{inj}	Net power injection at bus n for time period t.
r_{gt}^{NS}	Non-spinning reserve for unit g in period t.
r_{gt}^{SP}	Scheduled spinning reserve for unit g in period t.
r_t^{req}	Required level of spinning reserve in period t.
s_{kt}^{k+}, s_{kt}^{k-}	Violation in the flow limits of line k in period t.
s_{nt}^{n+}, s_{nt}^{n-}	Violation in the node limit of node n in period t.
s_t^{SP}, s_t^{NS}	Violation in the operating reserve in period t.
u_{gt}	Unit commitment binary variable for unit g in period t.
V_i	Voltage at bus i.
v_{gt}, w_{gt}	Startup and shutdown variables for unit g in period t respectively.
θ_i	Voltage angle at bus i.
θ_{nt}	Voltage angle at bus *n* in period *t.*
λ_{kt}^{FGP}	Flowgate marginal price of line *k* in period *t.*
λ_{nt}^{LMP}	Locational marginal price at bus *n* in period *t.*
λ_t^{RMP1}	Reserve marginal price component in period *t.*
λ_t^{RMP2}	Reserve marginal price component in period *t.*

Terms

AC	Alternating Current
ACSR	Alloy Aluminum Conductor Steel Reinforced
ACOPF	Alternating Current Optimal Power Flow
CAISO	California Independent System Operator
DAM	Day-ahead Market
DC	Direct Current
DCOPF	Direct Current Optimal Power Flow
EMS	Energy Management System
ERCOT	Electric Reliability Council of Texas
FMP	Flowgate marginal price
HVDC	High Voltage Direct Current
IFM	Integrated Forward Market (CAISO)
IPP	Independent Power Producer
ISO	Independent System Operator
ISO-NE	Independent System Operator New England
LP	Linear Program
LMP	Locational Marginal Price
LSE	Load Serving Entity
MILP	Mixed Integer Linear Program
MISO	Midcontinent Independent System Operator
MMS	Market Management System
MVL	Marginal Value Limit (MISO)
N-1	NERC standard reliability criterion regarding the loss of a single system component
NERC	North American Electric Reliability Corporation
NYISO	New York Independent System Operator

OMC	Out-of-Market Correction
OPF	Optimal Power Flow
PJM	Pennsylvania Jersey Maryland Interconnection
PSCOPF	Preventive Security Constrained Optimal Power flow tool from PSS/E
PSS/E	Power System Simulator for Engineering (Siemens)
PTDF	Power Transfer Distribution Factor
RAC/RUC	Reliability Assessment/Unit Commitment
RCP	Reserve clearing price
RTCA	Real-time Contingency Analysis Tool
RTO	Regional Transmission Organization
RTS-96	Reliability Test System 1996 version
SCED	Security Constrained Economic Dispatch
SCUC	Security Constrained Unit Commitment
SCUC-CR	Security Constrained Unit Commitment with constraint relaxations
SCUC-FP	Security Constrained Unit Commitment with fixed penalty price relaxations
SCUC-SP	Security Constrained Unit Commitment with stepwise penalty price relaxations
VAr	Volt Ampere reactive
WECC	Western Electricity Coordinating Council

1. Introduction

1.1 Research Premise

Electric power grids are among the most complex engineered systems today. To ensure a reliable and continuous supply of electric power, operators attempt to control their portion of the electric grid in the most efficient manner possible regardless of whether the operator works for an independent system operator (ISO), a regional transmission operator (RTO), or a vertically integrated utility. Operators must manage their generation fleet, which has complex operating requirements, while maintaining system synchronism and managing transmission assets throughout their control area. Operators must also cope with the increasing presence of variable generation (e.g., photovoltaic solar and wind power) and limited energy storage capability all while meeting stringent reliability standards. The North American Electric Reliability Corporation (NERC) has many standards guiding operator action. One such required standard is *N*-1 reliability, where the loss of a single generator or non-radial transmission asset does not cause involuntary load shedding. NERC states that operators must check for any potential *N*-1 violations every 30 minutes and if there is a potential violation, regain *N*-1 reliability within 30 minutes [1]-[2]. The Western Electric Coordinating Council (WECC), a regional authority, advises *N*-1 reliability be checked every 15 minutes [3]. Since *N*-1 reliability is checked at various time intervals, this standard is not continually enforced; furthermore, the operator must regain *N*-1 reliability 30 minutes after observing that the criterion has not been met. As a result, there are situations when operators allow short-term violations to occur, but later correct for those violations in order to meet *N*-1 requirements.

System operators, who manage the auction of wholesale energy, cannot incorporate all of these requirements into their market management systems (MMS) due to the added computational complexity. Even with a linearized market, some constraints become too costly to meet or may create an infeasibility. With the incorporation of constraint relaxations into the MMS, operators can attain a market solution. The market solution is then corrected to meet local and federal standards or the constraint is allowed to occur in actual operations for a short time period.

In this report, an investigation is conducted into the current constraint relaxations practices utilized by ISOs, the potential market outcomes of these practices, and finally their effect on system reliability.

1.2 Research Scope

Today, market models can only approximate some of these complex operating, reliability, and transmission requirements while trying to optimize the dispatch of the generation fleet. Even with continued advances in algorithmic performance and hardware, such optimization problems continue to require an engineered market structure with various approximations that impact the schedule of energy and ancillary services along with the corresponding market prices and settlements. Therefore, instead of forcing market models

to abide by strict, although approximated, constraints, market designers choose to relax some of these constraints by adding slack variables. However, to discourage the optimization algorithm from readily choosing to violate the constraint with no consequence, the system must pay a pre-determined penalty price, i.e., the slack variables show up in the objective function with a chosen penalty price. Although these practices have been approved and implemented today, little is understood regarding the impacts on market solutions, reliability, and stability of the system. Furthermore, there has been limited evaluation of the impacts of such market design practices.

System operators can potentially receive several benefits from employing constraint relaxations practices in market models. First, constraint relaxations allow for the potential to obtain gains in market surplus with small relaxations. At times, strictly enforcing a constraint, which is an approximation itself, can substantially increase the operating costs while the enforcement of that constraint to such a stringent requirement may serve a minimal purpose. Furthermore, the approximations themselves may result in the optimization model being infeasible even if a real-world solution were to exist.

Another benefit of constraint relaxations in market models is that these practices allow operators to manage prices. Previously, markets were designed with a bid cap, which would limit the bid (the price) that market participants could submit to the market for their service. This approach was intended to place a cap (a ceiling) on market prices, the locational marginal prices (LMP). To the surprise of early market designers, the LMPs were not (and are not) limited by imposing a restriction on the bid values themselves; instead, LMPs can be limited by relaxing the node balance constraint with slack variables and then placing a penalty on the slack. This makes it more economical to always have the slack artificially create production at a bus if the delivery cost exceeds the penalty price. As a result, the penalty price becomes a cap on the LMP. The process is demonstrated using a simple linear programming formulation, provided in Chapter 2.3.

1.3 Report Organization

The rest of part one for this two part report is summarized as follows. Chapter 2 presents background material regarding optimal power flow, security constrained unit commitment, and constraint relaxations in linear programs. The contribution of this work is first a summary and description of constraint relaxation practices, given in Chapter 3. As yet, limited work has been done to investigate the impacts of constraint relaxation practices on markets, reliability, and stability. This report examines the issue: market outcomes. To demonstrate the impacts of these practices, a day-ahead deterministic security constrained unit commitment (SCUC) model is solved in Chapter 4.1 with and without constraint relaxations on two different test cases; one of these test cases is developed from data given by PJM, which is based upon a large-scale model of actual market data. The resulting dispatch solutions are then corrected using PSS/E and its preventive security optimal power flow (PSCOPF) tool [4], such that the dispatch solutions become not only AC feasible, but also *N*-1 reliable. A comparison between these corrected dispatch solutions and the original SCUC dispatch solutions with and without constraint relaxations will be presented in

Chapter 4.5. Subsequently, a study on constraint relaxation penalty price schemes is presented in Chapter 5. Initially, a SCUC model is solved without relaxations; based on the values of the dual variables, penalty prices are chosen for the SCUC models with relaxations. The market solutions are compared based upon market outcomes. In Chapter 6, a methodology is proposed to determine the penalty prices for transmission thermal limits. This methodology considers line degradation effects and attempts to accurately capture the physical impact of operating the conductor at elevated temperatures due to the relaxation of the thermal limits via constraint relaxation practices. In Chapter 7, constraint relaxation impacts on system performance are analyzed. The impact of constraint relaxations on system stability are investigated following severe contingency events. Moreover, the reactive power availability was assessed and compared to cases with no relaxations. Finally, the conclusions and future work are discussed in Chapter 8.

2. Background

To replicate the approach that an ISO or RTO might take for allocating resources in the day-ahead setting, the fundamental practices must be stated, especially the approximations these organizations make when solving a deterministic security constrained unit commitment model (SCUC). To account for the transmission network, a derivation of the linearized direct current optimal power flow (DCOPF) is described in Chapter 2.1 and is subsequently followed by one formulation for a day-ahead SCUC in Chapter 2.2. Finally this chapter includes an example of the inclusion of constraint relaxation and its effect on the dual variable in Chapter 2.3.

2.1 Optimal Power Flow

The process to optimally schedule the delivery of power is a challenging problem for system operators today. Day-ahead markets operated by ISOs, operators seek a dispatch solution that delivers power with the least cost while guaranteeing reliability. Due to the complexity of the problem, some assumptions must be made. One main assumption is how the transmission network is modeled. In the unit commitment models developed in this report, a DCOPF formulation is utilized and derived based on [5].

A true representation of the network would include an Alternating Current Optimal Power Flow (ACOPF). Starting with the π-equivalent circuit of a transmission line shown in Figure 2.1, the real and reactive power flow equations over an individual line can be derived. Note that the index, *k*, represents the particular transmission line, while *m* and *n* represent the 'from' and 'to' buses that are connected by the transmission line.

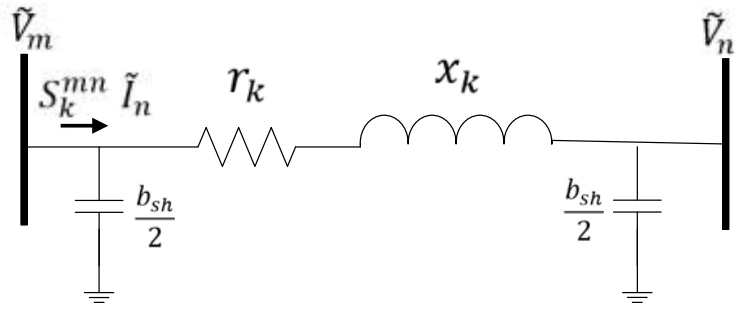

Figure 2.1. The π-equivalent circuit of a transmission line.

$$z_k = r_k + jx_k \tag{2.1}$$

$$y_k = \frac{1}{z_k} = \frac{1}{r_k+jx_k} \times \frac{r_k-jx_k}{r_k-jx_k} = \frac{r_k-jx_k}{r_k^2+x_k^2} = \frac{r_k}{r_k^2+x_k^2} - \frac{jx_k}{r_k^2+x_k^2} = g_k + jb_k \tag{2.2}$$

$$\tilde{V}_m = |V_m|\angle\theta_m = |V_m|(cos\theta_m + jsin\theta_m) \tag{2.3}$$

$$\tilde{V}_n = |V_n|\angle\theta_n = |V_n|(cos\theta_n + jsin\theta_n) \tag{2.4}$$

$$\tilde{I}_m = \tilde{V}_m\left(\frac{jb_{sh}}{2}\right) + \frac{\tilde{V}_m - \tilde{V}_n}{z_k} = \tilde{V}_n\left(\frac{jb_{sh}}{2}\right) + y_k\left(\tilde{V}_m - \tilde{V}_n\right) \tag{2.5}$$

$$\tilde{I}_m = \tilde{V}_m\left(\frac{jb_{sh}}{2}\right) + (g_k + jb_k)\left(\tilde{V}_m - \tilde{V}_n\right) = \tilde{V}_m\left(g_k + jb_k + \frac{jb_{sh}}{2}\right) - \tilde{V}_n(g_k + jb_k) \tag{2.6}$$

$$S_k^{mn} = \tilde{V}_m\tilde{I}_m^* = \tilde{V}_m\left(\tilde{V}_m\left(g_k + jb_k + \frac{jb_{sh}}{2}\right) - \tilde{V}_n(g_k + jb_k)\right)^* \tag{2.7}$$

$$S_k^{mn} = |V_m|^2\left(g_k - jb_k - \frac{jb_{sh}}{2}\right) - V_m\tilde{V}_n(g_k - jb_k) \tag{2.8}$$

$$S_k^{mn} = |V_m|^2\left(g_k - jb_k - \frac{jb_{sh}}{2}\right) - (|V_m||\tilde{V}_n|\angle\theta_m - \theta_n)(j_k - jb_k) \tag{2.9}$$

$$S_k^{mn} = |V_m|^2\left(g_k - jb_k - \frac{jb_{sh}}{2}\right) - |V_m||V_n|(\cos(\theta_m - \theta_n) + j\sin(\theta_m - \theta_n))(g_k - jb_k) \tag{2.10}$$

$$S_k^{mn} = |V_m|^2\left(g_k - jb_k - \frac{jb_{sh}}{2}\right) - |V_m||V_n|(g_k\cos(\theta_m - \theta_n) - jb_k\cos(\theta_m - \theta_n) + jg_k\sin(\theta_m - \theta_n) + b_k\sin(\theta_m - \theta_n)) \tag{2.11}$$

$$S_k^{mn} = |V_m|^2\left(g_k - jb_k - \frac{jb_{sh}}{2}\right) - |V_m||V_n|(g_k\cos(\theta_m - \theta_n) + jb_k\sin(\theta_m - \theta_n)) - j|V_m||V_n|(g_k\sin(\theta_m - \theta_n) - b_k\cos(\theta_m - \theta_n)) \tag{2.12}$$

From (2.12), the complex power sent from bus *m* to bus *n* was derived. The associated real and reactive power flows can now be separated as follows,

$$S_k^{mn} = P_k^{mn} + jQ_k^{mn} \tag{2.13}$$

$$P_k^{mn} = |V_m|^2 g_k - |V_m||V_n|(g_k\cos(\theta_m - \theta_n) + b_k\sin(\theta_m - \theta_n)) \tag{2.14}$$

$$Q_k^{mn} = -|V_m|^2\left(b_k + \frac{b_{sh}}{2}\right) - |V_m||V_n|(g_k\sin(\theta_m - \theta_n) - jb_k\cos(\theta_m - \theta_n)). \tag{2.15}$$

Now that equations have been derived for real and reactive power flow, an ACOPF dispatch problem can be completed. The control variables associated with the power flow equations in the ACOPF are the voltages (V_m and V_n) and the bus angles (θ_m and θ_n). It is typically assumed that voltage levels must remain within five percent of their rated values and this is reflected in (2.20). Another criterion is that the angle difference between two buses cannot exceed the stability limit, approximately 0.52 radians. Equations (2.13) to (2.22) represent the ACOPF.

$$minimize\ \sum_g c_g P_g \tag{2.16}$$

$$\sum_{k\epsilon\delta^+(n)} P_k - \sum_{k\epsilon\delta^-(n)} P_k + \sum_{g\epsilon g(n)} P_g = d_n \qquad \forall n \tag{2.17}$$

$$\sum_{k\epsilon\delta^+(n)} Q_k - \sum_{k\epsilon\delta^-(n)} Q_k + \sum_{g\epsilon g(n)} Q_g = q_n \qquad \forall n \tag{2.18}$$

$$P_k^2 + Q_k^2 \leq (S_k^{max})^2 \qquad \forall k \qquad (2.19)$$

$$0.95 \leq V_n \leq 1.05 \qquad \forall n \qquad (2.20)$$

$$-0.52 \leq \theta_m - \theta_n \leq 0.52 \qquad \forall n \qquad (2.21)$$

$$0 \leq P_g \leq P_g^{max} \qquad \forall \qquad (2.22)$$

Due to the added complexity of the unit commitment models, operators linearize the power flow equations to derive what is called a DCOPF. The assumptions for the DCOPF are as follows: (1) reactive power is ignored; (2) conductance (g_k) in the transmission lines is much smaller than the susceptance (b_k) and, therefore, it is assumed that the conductance is negligible ($g_k = 0$); (3) the angle difference between bus (i) and (j) is relatively small and, therefore, approximations are made to simplify the trigonometric terms: $\cos(\theta_i - \theta_j) \approx 1$ and $\sin(\theta_i - \theta_j) \approx (\theta_i - \theta_j)$; (4) the voltages of V_i and V_j are assumed to be 1 per unit. With a linear objective function, the DCOPF is a linear program (LP). The DCOPF formulation becomes,

$$minimize \ \sum_g c_g P_g \qquad (2.23)$$

$$\sum_{k \epsilon \delta^+(n)} P_k - \sum_{k \epsilon \delta^-(n)} P_k + \sum_{g \epsilon g(n)} P_g = d_n \qquad \forall n \qquad (2.24)$$

$$-P_k^{max} \leq P_k \leq P_k^{max} \qquad \forall k \qquad (2.25)$$

$$P_k - b_k(\theta_n - \theta_m) = 0 \qquad \forall k \qquad (2.26)$$

$$0 \leq P_g \leq P_g^{max}. \qquad \forall g \qquad (2.27)$$

2.2 Security Constrained Unit Commitment

The security constrained unit commitment (SCUC) model, used for this study, is a deterministic mixed integer program, which resembles the deterministic SCUC that is used in day-ahead market models. Its solution is used to produce the day-ahead market solution. The model presented is a mixed integer linear program, with the objective of,

$$minimize \ \sum_g \sum_t \left(c_g^{op} P_{gt} + c_g^{NL} u_{gt} + c_g^{SU} v_{gt} + c_g^{SD} w_{gt} \right). \qquad (2.28)$$

The total system cost (2.28) is represented by linear cost term in $c_g^{op} P_{gt}$, where c_g^{op} is the linear fixed cost and P_{gt} is the supply for each generator during each time period. The fixed costs are represented by binary variables (whose value could only be 0 or 1) in u_{gt}, v_{gt}, and w_{gt}, which represent the generator status, startup indicator, and shutdown indicator. Therefore, the term $c_g^{NL} u_{gt}$ represents the fixed no-load cost term and $c_g^{SU} v_{gt} + c_g^{SD} w_{gt}$ represent the startup and shutdown costs, respectively.

The binary variables v_{gt} and w_{gt} are related to the status binary, u_{gt}, which represents the periods that a unit is committed. A generator turned on during a specific time period is

represented by the binary v_{gt}, the startup variable, whereas a de-committed generator is represented by w_{gt}, the shutdown variable. These variables are restricted to a binary output because the formulation presented in Chapter 3 does not guarantee a binary output.

$$v_{gt} \geq u_{gt} - u_{gt-1} \qquad \forall g, t \qquad (2.29)$$

$$w_{gt} \geq u_{gt-1} - u_{gt} \qquad \forall g, t \qquad (2.30)$$

The SCUC replicates generator operating constraints. For example, the minimum and maximum production levels are represented by the parameters P_g^{min} and P_g^{max} respectively. In (2.31) and (2.32), a committed generator must be between its minimum and maximum production level. The variable r_{gt}^{SP} represents the spinning reserve acquired for a given generator during a specific time period and, therefore, the production level plus the spinning reserve must be less than the maximum supply level since, in the event of a contingency, a generator cannot provide power greater than its maximum production level. Thus, the reserve acquired plus the production level must be less than the maximum production level. These operational constraints are represented below,

$$P_{gt} \geq P_g^{min} u_{gt} \qquad \forall g, t \qquad (2.31)$$

$$P_{gt} + r_{gt}^{SP} \leq P_g^{max} u_{gt}. \qquad \forall g, t \qquad (2.32)$$

Operational generator requirements extend beyond minimum and maximum production levels. Another set of requirements include minimum time up and down that a committed/de-committed generator has after a unit has been turned on or off. This is represented in (2.33) and (2.34), where the summation of the startup and shutdown binary variable is over the minimum up and down time requirement, respectively.

$$\sum_{s=t-UT_g-1}^{t} v_{gs} \leq u_{gt} \qquad \forall g, t \qquad (2.33)$$

$$\sum_{s=t-DT_g-1}^{t} w_{gs} \leq 1 - u_{gt} \qquad \forall g, t \qquad (2.34)$$

Another generator operational constraint included in the SCUC is the hourly ramp rate. For simplicity, startup and shutdown ramp rates are assumed to be the generator's max production level, P_g^{max}. The ramp up and down constraints, using only hourly ramp rates, are shown in (2.35) and (2.36),

$$u_{gt-1} R_g^{HR} + v_{gt} P_g^{max} \geq P_{gt} - P_{gt-1} \qquad \forall g, t \qquad (2.35)$$

$$u_{gt} R_g^{HR} + w_{gt} P_g^{max} \geq P_{gt-1} - P_{gt}. \qquad \forall g, t \qquad (2.36)$$

Apart from generator operational constraints, the unit commitment model seeks to ensure *N*-1 reliable dispatch by also acquiring reserve. Committed generators could have their production level reduced to provide spinning reserve in the case of a contingency. Reserve could also be provided in the form of non-spinning reserve from fast-start generators. The total reserve acquired from the system during a given time period must be at least 7% of

the total demand during that specific hour and greater than the largest generator production level plus any spinning reserve acquired from that generator, represented in (2.37) and (2.38) (2.35) and (2.36). The total reserve acquired is also constrained to be at least half from spinning reserve, shown in (2.39). Furthermore, the total reserve for the given time period is also constrained to 7% of the total load, which follows [6].

$$r_t^{total} \geq \sum_n 0.07\, d_{nt} \qquad \forall n, t \qquad (2.37)$$

$$r_t^{total} \geq P_{gt} + r_{gt}^{SP} \qquad \forall g, t \qquad (2.38)$$

$$\sum_g r_{gt}^{SP} \geq 0.5\, r_t^{total} \qquad \forall t \qquad (2.39)$$

The amount of spinning reserve acquired for a committed unit is further constrained by the emergency ramp rate of the specific generator. This restriction is needed because, in case of a contingency, a generator can only move within the emergency ramp rate. Any spinning reserve acquired in the unit commitment model must be also be constrained to the emergency ramp rate.

$$r_{gt}^{SP} \leq R_g^{10} u_{gt} \qquad \forall g, t \qquad (2.40)$$

Non-spinning reserve can only be acquired by fast-start generators. A binary parameter FS_g is set to 1 to indicate a fast-start generator and 0 otherwise. Paired with this binary parameter, the non-spinning reserve acquired is constrained between a generator's minimum and maximum production levels for units that are not committed.

$$0 \leq r_{gt}^{NS} \leq R_g^{10}\big(1 - u_{gt}\big) FS_g \qquad \forall g, t \qquad (2.41)$$

$$r_{gt}^{NS} \leq P_g^{max}\big(1 - u_{gt}\big) FS_g \qquad \forall g, t \qquad (2.42)$$

Based on a DCOPF, the transmission network included in the unit commitment model are constrained by (2.43) to (2.44), where (2.45) is a node balance constraint. Alternatively, the line flow constraints could be formulated with the power transfer distribution factors (PTDFs) of the transmission network.

$$P_{kt} - B_k(\theta_{nt} - \theta_{mt}) = 0 \qquad \forall k, t \qquad (2.43)$$

$$-P_k^{max} \leq P_{kt} \leq P_k^{max} \qquad \forall k, t \qquad (2.44)$$

$$\sum_{k \epsilon \delta^+(n)} P_{kt} - \sum_{k \epsilon \delta^-(n)} P_{kt} + \sum_{g \epsilon g(n)} P_{gt} = d_{nt} \qquad \forall n, t \qquad (2.45)$$

$$u_{gt}, v_{gt}, w_{gt} \in \{0,1\} \qquad \forall g, t \qquad (2.46)$$

There are several forms and modifications that can be made to better represent the system. For example, in another formulation presented in Chapter 4.1, the generator operation constraints governing the minimum up and down time requirements are updated such that in the day-ahead unit commitment model, the beginning and ending periods depend on each other. There are several different reserve requirement rules that could be used in an

attempt to guarantee *N*-1 reliability, but these reserve requirements do not necessarily guarantee reliability.

2.3 Example of Constraint Relaxation in a Linear Program

In a linear program (LP) or mixed integer linear program (MILP), a constraint relaxation is incorporated into the problem by adding a slack variable to the particular constraint and to the objective with a penalty price. Formulating the LP or MILP in this manner limits the dual variable associated with the relaxed constraint. As long as the slack variable is not limited, the penalty price is the maximum value of the dual variable.

When applied to a market model, which will presented in Chapter 4.1, the dual variable in the associated constraints will also be limited by the penalty price. Constraint relaxation is a mechanism to managing prices. Early deregulated electric energy markets only limited the bid price of market participants (generators). However, this policy does not limit the locational market price (LMP), which is the price used for settling the market at that node. The LMP can be limited allowing relaxations on the node/power balance constraint in the market model. If a particular node is relaxed, the LMP is limited to the penalty price; additionally, the LMP will not exceed the set penalty price. Below is an example in Figure 2.2 and Figure 2.3.

Standard Primal Problem	Corresponding Dual Formulation
$minimize$: $c_1x_1 + c_2x_2$ $a_{11}x_1 + a_{12}x_2 \geq b_1\ (\lambda_1)$ $a_{21}x_1 + a_{22}x_2 \geq b_2\ (\lambda_2)$ $x_1 \geq 0$ $x_2 \geq 0$	$maximize$: $b_1\lambda_1 + b_2\lambda_2$ $a_{11}\lambda_1 + a_{21}\lambda_2 \leq c_1\ (x_1)$ $a_{12}\lambda_1 + a_{22}\lambda_2 \leq c_2\ (x_2)$ $\lambda_1 \geq 0$ $\lambda_2 \geq 0$
Primal Problem with Constraint Relaxation	Corresponding Dual Formulation of Primal with Constraint Relaxations
$minimize$: $c_1x_1 + c_2x_2 + P_1s_1 + P_2s_2$ $a_{11}x_1 + a_{12}x_2 \geq b_1 - s_1\ (\lambda_1)$ $a_{21}x_1 + a_{22}x_2 \geq b_2 - s_2\ (\lambda_2)$ $x_1 \geq 0$ $x_2 \geq 0$ $s_1 \geq 0$ $s_2 \geq 0$	$maximize$: $b_1\lambda_1 + b_2\lambda_2$ $a_{11}\lambda_1 + a_{21}\lambda_2 \leq c_1\ (x_1)$ $a_{12}\lambda_1 + a_{22}\lambda_2 \leq c_2\ (x_2)$ $\lambda_1 \leq P_1\ (s_1)$ $\lambda_2 \leq P_2\ (s_2)$ $\lambda_1 \geq 0$ $\lambda_2 \geq 0$

Figure 2.2. LP example to demonstrate the effects of constraint relaxations on dual variables.

The "Standard Primal Problem" exhibits hard constraints that cannot be violated, i.e., any solution found for the primal variables x_1 and x_2, must stay within the set bounds. Notice that in the corresponding Dual Formulation, the dual variables λ_1 and λ_2, are only restricted to be greater than zero. In the "Primal Problem with Constraint Relaxations," constraints are relaxed by adding the slack variables s_1 and s_2. However, relaxing the constraint means that a penalty price must be paid, P_1 and P_2 in this example. In the

corresponding dual formulation, the dual variables, λ_1 and λ_2, are now restricted and cannot exceed the corresponding penalty price, P_1 and P_2.

As demonstrated, relaxing a constraint while imposing a penalty price restricts the corresponding dual variables. When this occurs on the node balance constraint in the market model and the LMP, the basis of system settlements is restricted to the penalty price. Therefore, when CAISO performs its pricing run with a constraint relaxation on the node balance constraint with a penalty price of 500 $/MWh, a price cap is imposed on the LMP by relaxing the SCUC formulation.

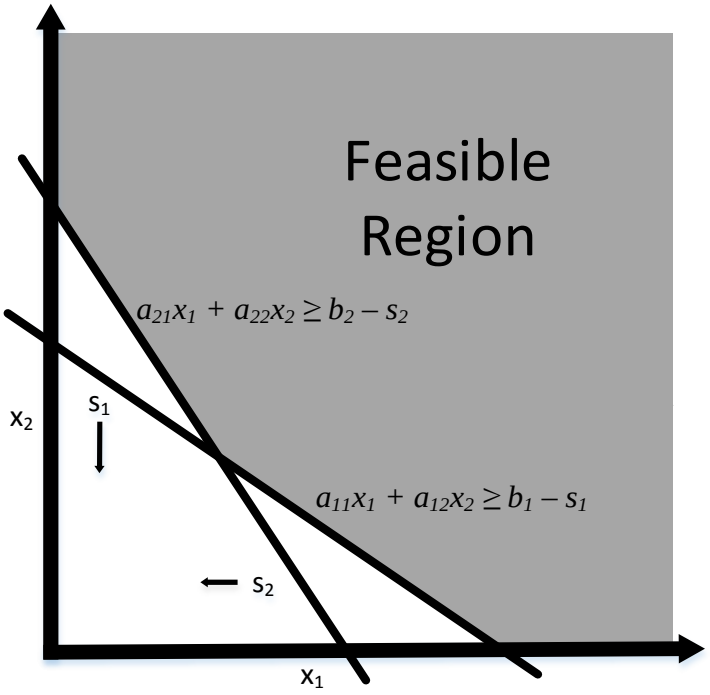

Figure 2.3. Graphical interpretation of relaxing a constraint.

2.4 Conclusions

The DCOPF represents an approximation of the real power flow throughout the transmission network. The approximations made to attain the DCOPF are necessary; otherwise, the SCUC model would not be a mixed integer linear program due to the non-linear constraints that would have been included through an ACOPF formulation. The day-ahead SCUC model presented is similar to what an ISO, RTO, or even a vertically integrated utility might use to determine which generators to commit the next day. Other formulations could be used.

3. Literature Review

While both market management systems (MMS) and constraint relaxation practices vary among industry members, the general process is similar to that shown in Figure 3.1. Details of the different market software tools that ISOs utilize are given in [7]. Initially, ISOs will collect bids for the day-ahead market (DAM), where market participants bid to either purchase or supply energy and ancillary services. Participants, typically known as load-serving entities (LSEs), purchase energy in the day-ahead market while participants, known as independent power producers (IPPs), sell energy. A virtual bidder could take either position in the market. The ISO attempts to maximize the market surplus based on these offers relative to operating and reliability requirements. Due to the complexity of these requirements, approximations must be made in the market SCUC model. This includes using a DCOPF formulation instead of a non-linear ACOPF formulation. Similarly, proxy reserve requirements are implemented in an attempt to guarantee *N*-1 reliability instead of explicitly modeling all *N*-1 scenarios in the SCUC; note that implementing the latter creates a stochastic program. Approximations are needed even for smaller systems because the computational complexity would increase immensely. Different methods for the SCUC are detailed in [8].

Even though ISOs approximate operating and reliability requirements in the SCUC, these organizations allow constraints to be relaxed. When a constraint is relaxed, the market pays a penalty, which must be offset by greater benefits in terms of market surplus. Relaxations allow ISOs to obtain solutions that would otherwise be infeasible due to approximations made within the SCUC. ISOs then modify the proposed market-based dispatch solution until a feasible solution is obtained. Most frequently, the solution is not AC feasible because of the assumptions made regarding power flow (using a DCOPF formulation). Operators will make any changes that are necessary, including running contingency analysis, to obtain a feasible dispatch solution. This process can be viewed in Figure 3.2 [9].

Once the DAM is solved, awards are given to generators to produce power and load-serving entities must pay for power acquired in the day-ahead market. However, some LSEs might not have purchased adequate capacity to serve their customers throughout the entire day and would have to acquire the additional energy in the real-time market.

To ensure adequate capacity is available during real-time operations, after solving the DAM SCUC, ISOs will solve a reliability unit commitment (RUC), also referred to as a residual unit commitment problem using an ISO-based forecasted demand and will remove all artificial bids from virtual bidders. The RUC is one of many additional steps that take place during the adjustment period in the day-ahead scheduling process [10]. A natural separation in forward and spot prices can occur because the day-ahead (forward) market and RUC are separate and the RUC solution will influence the real-time (spot) market [11]. For the purpose of both improving the overall system efficiency as well as reducing this potential market distortion, note that at least one ISO (CAISO) is considering merging their RUC model with their DAM model to create a unified DAM-RUC model [12].

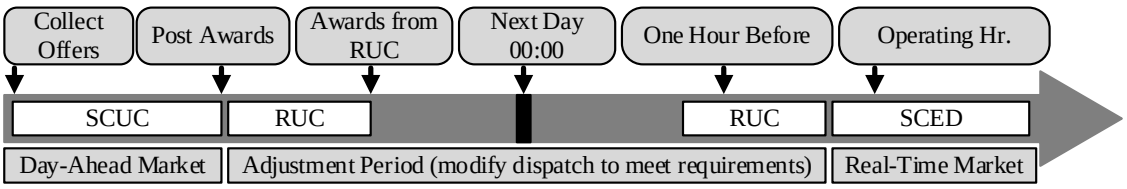

Figure 3.1. General day-ahead to real-time market process adapted from ERCOT [13].

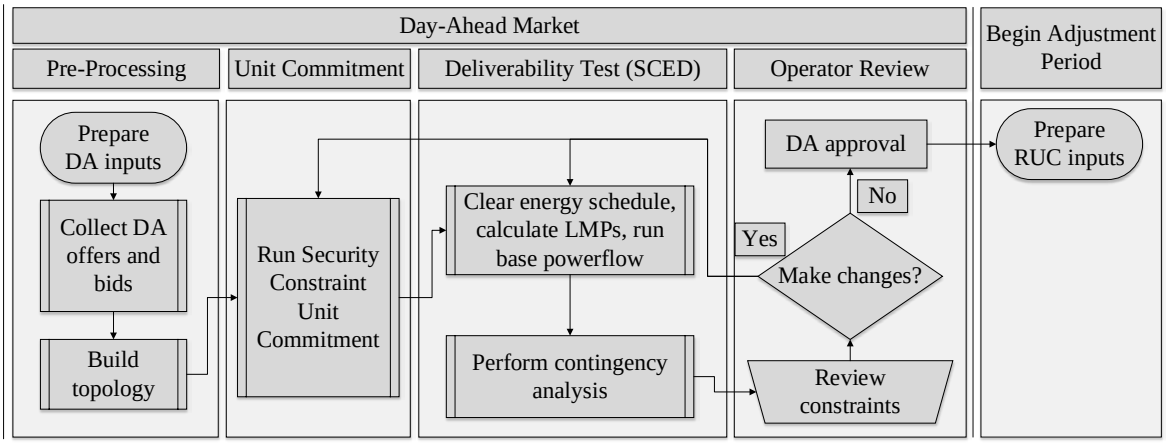

Figure 3.2. Modified day-ahead market process for MISO [9].

The real-time (spot) market opens after the day-ahead market has cleared. During real-time operations, ISOs typically solve a security constrained economic dispatch (SCED) problem and the SCED includes constraint relaxations as well. The SCED only models a portion of the transmission network as the operator will choose what constraints to enforce based on the flags provided by the real-time contingency analysis (RTCA) tool and the energy management system (EMS). Since the market SCED model also includes constraint relaxations, when the operators choose what constraints to model within the SCED, the operator may de-rate transmission thermal limits (steady-state limits) to ensure the SCED does not result in a constraint relaxation that violates the actual steady-state limits; this is possible since the EMS has a bias factor built into it that the operator can adjust (the operator can adjust this bias factor to de-rate the line's thermal rating or the operator can use the bias factor to allow the flow to exceed the thermal limit). However, operators managing the SCED may not include all requirements so that operators will have to correct for approximations and relaxations. For example, if a transmission line's flow is close to its limit, the EMS will warn the operator that actions are necessary to correct for the violations to ensure that the system is secure, including de-rating the transmission line the next time the operator runs the SCED.

3.1 California Independent System Operator (CAISO)

CAISO has both a forward market and a spot market for energy transactions known as the Integrated-Forward Market (IFM) and the Real-time Market (RTM), respectively [14]. As part of their day-ahead procedures, CAISO also runs a RUC. CAISO applies constraint

relaxations in all three stages. In both markets operated by CAISO, the IFM and RTM are solved twice. The first time either market is solved is known as the "scheduling-run," for which CAISO applies large penalty prices to ensure that the market attempts to utilize the bids posted by the market participants before relaxing any of the constraints [15]. The outputs of the scheduling runs are used to determine the dispatch schedule. The results are then passed to the pricing run where only small deviations from the scheduling run's dispatch schedule are allowed. The pricing run is different as the penalty prices are much lower in the pricing run. For example, within both the IFM and RTM, the energy/node balance constraint can be relaxed at a penalty price of 6,500 $/MWh within the scheduling run; however, when solving the pricing run, the penalty is lowered to 500 $/MWh. As such, the scheduling run can be interpreted to determine the primal solution (dispatch schedule) while the pricing run is used to determine the dual solution (the market prices) [16]. While this procedure has been approved by the Federal Energy Regulatory Commission (FERC) and agreed upon by the stakeholders in CAISO, this could be seen as price distortion. The scheduling run is being determined with constraint relaxations based on higher penalty prices; the resulting primal solution is kept the same but the resulting prices from the scheduling run are not used even though those prices are based on the dual solution that corresponds to the scheduling run's primal solution. Instead, the prices are based on what comes from the pricing run, where there are much lower penalty prices, resulting in much lower price caps (i.e., this is done for the purpose of price control).

After obtaining results from the scheduling and pricing run, CAISO solves a RUC model to ensure adequate capacity is acquired for the next day. Like the IFM, the RUC includes constraint relaxations, including the relaxation of the energy/node balance constraint and transmission limit constraints.

Due to the approximations made in these models, CAISO has to perform "exceptional dispatches" to guarantee reliability. In 2011 and 2012, CAISO paid out $43 and $34 million, respectively, for exceptional dispatches. CAISO even recognized that some of the constraint relaxation practices utilized in their markets could have resulted from the need for exceptional dispatches [17].

3.2 Midcontinent Independent System Operator (MISO)

MISO's reach is the largest among ISOs in North America [18]. Once MISO determines the cleared energy and ancillary services from the DAM SCUC, operators subsequently check system reliability by performing contingency analysis. The resulting output from the contingency analysis is reviewed. If operators determine the day-ahead schedule is unreliable, the operator will either choose to resolve the SCUC or perform out-of-market correction [9], [19]-[20].

After the MISO DAM process is completed and the schedule has been approved, MISO begins the process anew with the reliability assessment commitment (RAC), also known as a RUC. Similarly, MISO uses their version of the RUC to commit additional generation capacity to ensure adequate supply for the next operating day.

During the RTM, MISO solves a SCED to re-dispatch generators to fulfill demand and manage congestion. Due to time constraints, operators will ignore certain constraints, which might include ignoring portions of the transmission network. As a result, violations could occur in real-time. MISO has indicated that operators will attempt to avoid violations by manually de-rating line ratings when solving the SCED to avoid overloads that could be violated due to the constraint relaxation procedures [21].

Previously, MISO discontinued the use of a "constraint relaxation algorithm" [22]-[23]. In [24], the authors state that the constraint relaxation procedures artificially decrease the actual congestion present in the system during real-time operations. Today within SCED, constraints are assigned marginal value limits (MVL), which is the same as applying a penalty price. The MVL caps the dual variable of the corresponding constraint. MISO has declared these values in [24].

In [25], MISO has updated some of the MVLs to stepwise demand curves. For example, a transmission line with a voltage level greater than 161kV has an MVL of 1000 $/MWh when the constraint exceeds its limit until it reaches 102% of its rating. Above that level, the model sets the penalty price at 2000 $/MWh. Transmission lines at other levels have different MVL prices, but still exhibit a stepwise curve.

3.3 Electric Reliability Council of Texas (ERCOT)

The DAM managed by ERCOT, which acquires energy and ancillary services [13], is solved by utilizing a multi-hour mixed integer programming algorithm that seeks to maximize market surplus for the entire day. The DAM is a unit commitment optimization problem that utilizes constraint relaxation practices similar to other ISOs and where the market penalizes the system when violating these constraints, typically with a set penalty price.

However, ERCOT uses a different constraint relaxation structure with its node balance constraint. Like other ISOs, it can be violated either positively, when more generation is acquired artificially, or negatively, when generation is reduced artificially. However, unlike other ISOs, violations are penalized via a step-wise function [26]. As for transmission constraints, their penalty prices are dependent on the voltage level. Furthermore, ERCOT stipulates that the penalty factors used in the DAM can be set (adjusted) by the operator. Similar practices occur in real-time operations [27].

3.4 New York Independent System Operator (NYISO)

NYISO employs constraint relaxation practices in both their SCUC and real-time scheduling models by utilizing demand curves that reflect scarcity [28] and serve the same purpose as constraint relaxations used for price control. Some of these demand curves are either fixed or stepped. For instance, NYISO sets a "Demand Curve Price" of 4000 $/MWh for relaxing any transmission constraint. Conversely, the price for relaxing the 30 minute reserve requirement in the New York Control Area is stepped, i.e., for the first 200 MW,

the system pays a penalty price of 50 $/MWh, for the next 200 MW, the system pays 100 $/MWh, and for the rest, the system pays 200 $/MWh [28]-[29]. The NYISO operator may acquire additional reserve in real-time at any quantity or price point [29].

3.5 Independent System Operator of New England (ISO-NE)

ISO-NE also utilizes constraint relaxations in their market operations. Specifically, ISO-NE implements penalty prices for reserves, known as "reserve constraint penalty factors." The constraints for different reserve products have different prices. For example, relaxing the 10-minute non-spinning reserve requirement previously cost 850 $/MWh, but now costs the system 1,500 $/MWh. Additionally, the 30-minute operating reserve was priced at $500/MWh, but now costs 1,000 $/MWh [30].

ISO-NE relaxes other constraints, but provides little detail regarding such practices. In [5], it is stated that the relaxation of transmission constraints occurs in a separate process that includes very high penalties. Furthermore, in [31], ISO-NE discusses the consequences of allowing for constraint relaxations; in the example provided, ISO-NE shows that relaxations on interface limits among the northeastern ISOs allows cheaper generation from other ISOs to be dispatched.

3.6 PJM Interconnection (PJM)

PJM utilizes constraint relaxation practices similar to that of other ISOs, where one set penalty price for each constraint is applied. According to [7], these penalty prices included a cost of 1000 $/MWh for the power balance constraint, 50,000 $/MWh for ramping constraints, 5000 $/MWh for normal and emergency operation constraints, and 1000 $/MWh for transmission constraints.

In [6], penalty prices have been updated by PJM. This includes the penalty price for primary and synchronized reserves in each region, which is set to 850 $/MWh because PJM witnessed reserve costs exceeding 800 $/MWh regularly during peak hours. Furthermore, PJM states that it has a bid cap of 1000 $/MWh and a maximum LMP of 2700 $/MWh.

During previous conference calls with industry participants, PJM indicated a need to analyze the consequences of these relaxations practices. PJM has even indicated that relaxations at times can occur in actual operations due to inadequate procurement of capacity or when operators are not concerned about short-term overloads on particular constraints [19].

3.7 Summary

Reliable and economic deployment of a generation fleet to satisfy demand is a complex problem. Independent system operators (ISOs) and regional transmission operators (RTOs) solve complex unit commitment and economic dispatch models to determine appropriate

resources to deploy at various time stages. Due to the complexity of power systems, several approximations are made within optimization models, including approximations of the transmission network with a linearized formulation known as the direct current optimal power flow (DCOPF) instead of the more realistic alternating current optimal power flow (ACOPF) formulation. Furthermore, approximations occur in these models by relaxing specific constraints in the model, i.e., the constraint is allowed to be violated based on a predetermined penalty price. By doing so, the ISO/RTO receives several benefits, including the ability to manage prices and clear the market as well as the potential to obtain gains in social welfare (market surplus). This report described the constraint relaxation practices of ISOs in their unit commitment models and will analyze the corresponding consequences resulting from these practices.

4. Effects of Constraint Relaxation Practices on Market Outcomes

ISOs apply constraint relaxations to several constraints throughout the scheduling process. In this report, two test cases are used to analyze the potential impacts constraint relaxations have on market outcomes. The first test case used is the RTS-96 test case [32]. A day-ahead SCUC is formulated and solved with and without constraint relaxations. The only constraint relaxations applied for the RTS-96 test case study was on the line flow limits. The resulting market dispatch solutions are subsequently modified utilizing tools within PSS/E to achieve an AC feasible and *N*-1 reliable dispatch schedule. At this point, a comparison is performed on how the modifications made with the tools within PSS/E affect potential market outcomes. This comparison is performed by calculating the settlements from the market LMPs, which are from the SCUC market model, and the ex-post LMPs after all corrections were made to the market solution, as shown by Figure 4.1.

The second test case used to evaluate constraint relaxations is based upon data provided by PJM. With this test case, a SCUC is solved similar to that used for the RTS-96 test case; however, it is only solved for two separate time periods, an on-peak and off-peak hour and, as before, the test case is solved with and without relaxations. The test case is solved with the original penalty prices used by PJM, which resulted in fewer relaxations, and a set of lower penalty prices. For the PJM study, both the node balance constraints and the line flow limit constraints are relaxed. The resulting dispatches are corrected for AC and *N*-1 feasibility and a comparison on market settlements is performed based on the market LMPs.

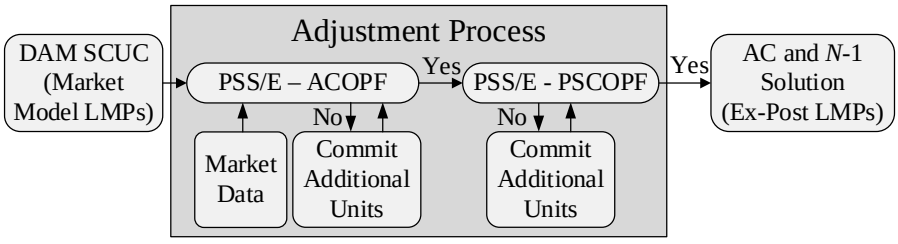

Figure 4.1. Two stage process to achieve AC and *N*-1 feasible dispatch solution.

4.1 Security Constrained Unit Commitment with Constraint Relaxations

The SCUC objective (4.1) is to minimize the total system cost while using a linear-piecewise cost curve that requires the segmentation of the power output of the generators, which is exhibited in (4.2)-(4.4). The proxy reserve requirements (4.5)-(4.12) are based on CAISO's rules [33]. They specify that the total reserve must be greater than the largest contingency, (5), as well as greater than a combination of load (α) and load met by non-hydro resources (β), (6). In [33], CAISO specifies that operating reserves must exceed 5% of the load met by hydro resources and 7% of load met by non-hydro, which translates to $\alpha = 0.05, \beta = 0.02$ in (4.6). The total reserve reflects the spinning and non-spinning reserve, (4.7), and at least half of the operating reserve must come from spinning reserves,

(4.8). While these rules are based on CAISO's rules, these reserve requirement rules are similar to the rules used by many systems.

Additional generator constraints include minimum up- and down-time as well as ramp rate requirements. Note that while the startup and shutdown variables are binary, prior work has proven that with (4.13)-(4.15) and (4.25), it is possible to treat these binary variables as continuous variables, i.e., (4.23)-(4.24), and still guarantee a binary solution for the startup and shutdown variables [34]. Finally, in the DCOPF formulation, the line flow is calculated with the PTDFs where the total power flow into or out of a bus is represented by a net-injection variable, denoted as P_{nt}^{inj}. The unit commitment could have its line flow constraints violated, accomplished by the addition of the slack variables s_{kt}^{k+} and s_{kt}^{k-}. If these slack variables are anything other than zero, the objective is penalized by the penalty price, PP^K, which is set to 100 $/MWh within this formulation. This SCUC is solved with and without line limit constraint relaxations using the RTS-96 test case [32].

$$min\ \sum_g \sum_t \sum_i \left(c_{gi}^{op} P_{git}\right) + \sum_g \sum_t (c_g^{NL} u_{gt} + c_g^{SU} v_{gt} + c_g^{SD} w_{gt}) + \sum_k \sum_t P^K \left(s_{kt}^{k+} + s_{kt}^{k-}\right) \quad (4.1)$$

$$P_{git} = u_{gt} P_{gi}^{Limit} \qquad \forall g, i = 1, t \qquad (4.2)$$

$$0 \le P_{git} \le u_{gt} P_{gi}^{Limit} \qquad \forall g, i > 1, t \qquad (4.3)$$

$$P_{gt}^{total} = \sum_i P_{git} \qquad \forall g, t \qquad (4.4)$$

$$P_{gt}^{total} + r_{gt}^{SP} \le r_t^{req} \qquad \forall g, t \qquad (4.5)$$

$$r_t^{req} \ge \alpha \sum_g P_{gt}^{total} + \beta \sum_{g \epsilon H(g)=0} P_{gt}^{total} \qquad \forall g, t \qquad (4.6)$$

$$r_t^{req} \le \sum_g \left(r_{gt}^{SP} + r_{gt}^{NS}\right) \qquad \forall t \qquad (4.7)$$

$$0.5 r_t^{req} \le \sum_g r_{gt}^{SP} \qquad \forall t \qquad (4.8)$$

$$0 \le r_{gt}^{SP} \le P_g^{max} - P_{gt}^{total} \qquad \forall g, t \qquad (4.9)$$

$$r_{gt}^{SP} \le R_g^{10} u_{gt} \qquad \forall g, t \qquad (4.10)$$

$$0 \le r_{gt}^{NS} \le P_g^{max} (1 - u_{gt}) \qquad \forall FS_g = 1, g, t \qquad (4.11)$$

$$r_{gt}^{NS} \le R_g^{10} (1 - u_{gt}) \qquad \forall FS_g = 1, g, t \qquad (4.12)$$

$$v_{gt} - w_{gt} = u_{gt} - u_{gt-1} \qquad \forall g, t \qquad (4.13)$$

$$\sum_{s=t-UT_g+1}^{t} v_{gs+T} + \sum_{s=t-UT_g+1}^{t} v_{gs} \le u_{gt} \qquad \forall g, t \qquad (4.14)$$

$$\sum_{s=t-DT_g+1}^{t} w_{gs+T} + \sum_{s=t-UT_g+1}^{t} w_{gs} \le 1 - u_{gt} \qquad \forall g, t \qquad (4.15)$$

$$u_{gt-1}R_g^{HR} + v_{gt}P_g^{max} \geq P_{gt}^{\text{total}} - P_{gt-1}^{total} \qquad \forall g,t \qquad (4.16)$$

$$u_{gt}R_g^{HR} + w_{gt}P_g^{max} \geq P_{gt-1}^{\text{total}} - P_{gt}^{total} \qquad \forall g,t \qquad (4.17)$$

$$-P_{nt}^{inj} + \sum_{g\in g(n)} P_{gt}^{total} = d_{nt} \qquad \forall n,t \qquad (4.18)$$

$$\sum_n P_{nt}^{inj} PTDF_{nk}^{REF} \leq P_k^{max} + s_{kt}^{k+} \qquad \forall k,t \qquad (4.19)$$

$$-P_k^{max} - s_{kt}^{k-} \leq \sum_n P_{nt}^{inj} PTDF_{nk}^{REF} \qquad \forall k,t \qquad (4.20)$$

$$\sum_n P_{nt}^{inj} = 0 \qquad \forall t \qquad (4.21)$$

$$0 \leq v_{gt} \leq 1 \qquad \forall g,t \qquad (4.22)$$

$$0 \leq w_{gt} \leq 1 \qquad \forall g,t \qquad (4.23)$$

$$s_{kt}^{k+}, s_{kt}^{k-} \geq 0 \qquad \forall \text{n}, k,t \qquad (4.24)$$

$$u_{gt}\epsilon\{0,1\} \qquad \forall g,t \qquad (4.25)$$

4.2 RTS-96 Test Case

A modified version of the RTS-96 test case [32] was used to solve the SCUC unit commitment with line thermal limit relaxations. These modifications include reducing the transmission thermal limits by ten percent without including the HVDC line. Furthermore, for the purposes of this simulation, the load for the peak day was increased by ten percent as well. These actions were taken to increase the number of relaxations the SCUC market model obtained with relaxations.

After the initial SCUC was solved with and without relaxations, these market dispatch solutions were corrected for AC and *N*-1 feasibility. Part of this requirement was to ensure that the voltage deviated no more than +/- 5% of voltage rating.

4.3 PJM Test Case

Using a similar formulation, a SCUC is solved for an on- and off-peak hour, based on a 15,000 bus test case of the PJM system including actual market data from various operating days. Areas outside PJM were included to accurately account for the tie-line flows. In total, there were over 20,000 lines that appeared in the PJM data set, but ratings were only enforced for lines at or above 138kV. While PJM relaxes many different constraints within their market model, we focus on the relaxation of the line limits and the node balance constraints. These relaxations were penalized in the model with two sets of penalty prices: i) with the original PJM penalty prices of 1000 $/MWh and 2700 $/MWh and ii) with a lower set of 100 $/MWh and 250 $/MWh for the line limits and node balance constraints respectively. Finally, the reserve requirements are modified to resemble those of PJM [35].

The reserve requirements include acquiring total reserve (spinning and non-spinning reserve), which must be at least 150% of the single largest generator contingency. At least half of the total reserve must be spinning reserve and the total spinning reserve must be greater than the largest generator. The other reserve requirements are similar to those in the previous formulation, which include (4.10)-(4.12).

4.4 Correction Process to Attain AC and *N*-1 Feasibility

To attain a base-case AC feasible solution that has no voltage or transmission violations, the PSS/E optimal power flow (OPF) package was used. Market dispatch solutions with and without constraint relaxations are the initial starting point for the AC power flow, which utilizes network controls, such as switchable shunts and transformers' tap settings. In some peak load cases, the adjustment of network controls is not sufficient and, thus, additional units must be committed in order to eliminate large reactive power mismatches.

The approximations incorporated within the market model were corrected by using PSS/E's ACOPF. Using an ACOPF, which assimilates market data and minimizes cost while utilizing shunts and taps controls, ensured that AC related quantities, such as reactive current flow, losses, and voltage limits, were incorporated in the new base-case AC solution. All violations of any defined limits were removed. This process is the first step of the adjustment process in Figure 4.1.

The new AC dispatch solutions provided a feasible base-case solution with no violations. However, *N*-1 contingency analysis revealed that the system was susceptible to various voltage and flow violations following certain contingencies. Additional corrections to AC dispatch solutions were required in order to achieve an *N*-1 reliable solution.

To implement these preventive actions, the following control options were used: switchable shunts, transformers' tap setting adjustments, dispatched generators' active and reactive power output, and committing offline generators. An AC *N*-1 contingency analysis was performed to identify the most severe contingencies that needed to be considered in the preventive correction process. Post-contingency violations were subsequently removed using the previously stated control actions; post-contingency limits for voltages were set to ±5% deviation from rated values for the RTS-96 test case and ±20% for the PJM test case. In both cases, line flows were permitted to exceed their thermal ratings by 25%. Contingency analysis was performed again to confirm the effectiveness of the corrective actions and ensure that other contingencies had not been negatively affected. This iterative process was automated throughout this work using the built-in preventive security constrained OPF (PSCOPF) feature in PSS/E. Using PSCOPF also ensured consistency in identifying preventive corrective actions [4]. The result of this process was the achievement of not only AC feasible, but also *N*-1 reliable dispatch solutions and is the final step in Figure 4.1.

4.5 Market Implications

To demonstrate the impact of constraint relaxation practices, the deterministic unit commitment program was solved with and without relaxations. The mipgap used to solve these unit commitment programs was set to 1%. Two distinct test cases (RTS-96 and PJM) were used to evaluate the possible market impacts of these relaxation practices.

4.5.1 RTS-96 Test Case Results

The first test case used was the RTS-96 test case, which was solved twice based on (4.1)-(4.25): once without relaxations (SCUC) and once with relaxations (SCUC-CR). The relaxed transmission limits produced from this program are given in Table 4.1.

Table 4.1. Relaxed transmission line limits produced by SCUC-CR.

Line	Time Period Relaxed	Amount Above Rating (MW)	Percentage (above rating)
25	22	9.96	3.2%
65	7	32.21	10.3%
65	23	25.98	8.3%
104	7	14.18	4.5%
104	8	15.85	5.0%
104	23	16.92	5.4%

The dispatch solutions produced by the SCUC and SCUC-CR solutions are not AC feasible nor *N*-1 reliable. After correcting both of these dispatch solutions to attain AC feasibility and *N*-1 reliability, system settlements were calculated with the market model LMPs (i.e., the LMPs that would come out of the market model and correspond to the approximate solution that is not *N*-1 feasible nor AC feasible) and then again with the final dispatch solution LMPs (i.e., the marginal cost to deliver one MW after all post-market corrections are established, which reflects ex-post LMP pricing [36]). Table 4.2 presents these three sets of solutions for both cases with and without constraint relaxations; the original market SCUC solutions are presented along with what are listed as the *N*-1 corrected solutions, which are both AC feasible and *N*-1 reliable.

The system settlements, particularly for generators, were determined for these solutions and can be seen in Table 4.2. There is a slight difference in the total system cost in the SCUC and SCUC-CR solutions. Note that the total system cost for the SCUC-CR solution includes the penalty cost for relaxing transmission limit constraints. Since the solution from SCUC-CR was able to produce constraint relaxations, it produced a cheaper solution compared to the SCUC solution with no relaxations. These results emulated those produced from market models employed today.

The market solution for the SCUC had a resulting optimality gap of 0.27%; the SCUC solution's lower bound is higher than the best incumbent solution obtained for the SCUC-

CR market solution, whose resulting optimality gap was 0.1%. While the SCUC-CR optimal solution must be as cheap, if not cheaper, than the non-relaxed solution, there is no guarantee that the incumbent solution will be cheaper if the problems are not solved to optimality. Even though the market models are not solved to optimality today due to time restrictions, it is still expected that the relaxed solution has a lower market cost. However, it is important to keep in mind that such a solution involves relaxations, which are considered to be actual violations. Therefore, the emphasis needs to be placed on the actual cost to operate an AC feasible and *N*-1 reliable system, which are the costs after all of the corrections have been made.

Comparing the two AC feasible and *N*-1 reliable solutions, the solution with relaxations had a lower system cost than the solution without relaxations. The difference in total cost was approximately $245,000, or roughly 5%, over the entire day, much larger than the difference in the market solution costs of 0.3%. The final difference in costs (5%) between the two solutions is not due to just the relaxations but are obviously also dependent on the corrections made within the adjustment phase. While the adjustment phase itself is imprecise (i.e., due to the complexity, an optimal adjustment is not determined), this process replicates industry practices and it is important to capture whether the practice of constraint relaxations increases the reliance on out-of-market corrections. This issue is left for further review in the discussion section of Table 4.2.

The day-ahead SCUC solution (without relaxations) exhibited a cost increase of $700,000 between the original market solution and the final corrected solution that is AC feasible and *N*-1 reliable. The day-ahead SCUC-CR solution (with relaxations) exhibited a lower increase in cost between the original market solution and the final AC feasible and *N*-1 reliable solution, a cost of only $490,000. This result is somewhat counterintuitive; it may be expected that the solution with relaxed constraints would cost more to obtain a proper AC feasible and *N*-1 solution. However, this result intriguingly shows that this is not always the case. When you have two infeasible solutions, it is not possible to guarantee which solution will cost less to correct to achieve feasibility. A solution with more overall relaxations may very well be cheaper once feasibility is achieved. This result also then translates to the SCUC-CR solution having a lower overall cost, meaning that this practice improves the overall social welfare even after all corrections have been made. While this is only one result, it roughly confirms one argument in support of constraint relaxations: it is questionable to impose such strict requirements when the model itself is a rough approximation.

With all the corrections made to both dispatch solutions, generator profit decreased as expected. When utilizing the ex-post LMPs that reflect the implemented out-of-market changes made to guarantee AC feasibility and *N*-1 reliability (during the day-ahead scheduling process), the generators were able to make a profit with the final SCUC dispatch solution. However, the final solution for the SCUC-CR indicated that generators would incur a loss over the entire 24 hour time horizon. Note this profit is determined by LMP payments alone and does not include the subsequent uplift payments, whose calculation is similar to that in [20]. This would only occur if there were no deviation during real-time operations. Today, operators post day-ahead market results based upon the original LMPs

from the day-ahead market model. In this case, both dispatch solutions exhibited generators making a profit over the entire operating day.

Table 4.2. Market results in ($k) for SCUC-CR and SCUC.

SCUC-CR market solution and resulting *N*-1 corrected solution				
	Total Cost	Gen. Revenue	Uplift	Gen. Profit + Uplift
Market SCUC Solution	4,082	11,457	297	7,684
N-1 Corrected (Market Model LMPs)	4,557	11,682	564	7,688
N-1 Corrected (Ex-Post LMPs)	4,557	4,456	2,071	1,969
SCUC market solution and resulting *N*-1 corrected solution				
Market SCUC Solution	4,095	11,518	303	7,726
N-1 Corrected (Market Model LMPs)	4,803	11,734	799	7,730
N-1 Corrected (Ex-Post LMPs)	4,803	5,391	2,103	2,691

If the day-ahead market settlements were based on the resulting LMPs that come after the out-of-market corrections, which happen during the day-ahead scheduling process (this is analogous to ex-post real-time pricing), then the generator revenue and profit would be much lower (compared to market model LMPs) for both cases with and without constraint relaxations. The uplift payments are also much higher with ex-post pricing. The results provide a mechanism to analyze how market settlements are impacted when constraints are relaxed within the market model but are later corrected outside of the market (auction) engine by operators. These results first show that the main impacts on settlements are not primarily the constraint relaxations that occur but the inaccuracies within the market models associated with not having an ACOPF or an explicit representation of all contingencies. This can be observed since both results with and without constraint relaxation have substantially lower generator profits after the correction phase; note, however, that such results do not guarantee this as a general outcome. With that said, there is still a difference between the solutions that employ constraints relaxations and those that do not. Furthermore, the practice of constraint relaxations influences system operating costs, as shown by Table 4.2.

4.5.2 PJM Test Case Results

Extending the analysis performed on the RTS-96 test case, another test case was constructed from data provided by PJM. A single period SCUC model, with and without relaxations, is solved for an off-peak period and an on-peak period. The market solutions were then modified to achieve AC and *N*-1 feasibility. Additionally, SCUC-CR was solved with line limit relaxations and node balance relaxations for two sets of penalty prices: i) with lower prices of 100 $/MWh and 250 $/MWh and ii) with PJM's original penalty prices of 1000 $/MWh and 2700 $/MWh for line limit and nodal relaxations respectively. Note

that when a nodal relaxation occurs in the model, the dual variable (LMP) is limited by the penalty price. In the SCUC model solution, no relaxations were allowed and, thus, the highest LMPs exhibited in the system were $1473 and $2754 for the off- and on-peak hours respectively.

For the off-peak hour, the SCUC-CR solution, with lower penalty prices resulted in 57 MW of nodal relaxations, which is less than 0.1% of demand. The total line limit relaxations for the off-peak hour were 743 MW on nine lines. Furthermore, when solving with the SCUC-CR model for the off-peak hour, the model chose not to relax any constraints with the original penalty prices.

For the on-peak hour, the SCUC-CR with lower penalty prices chose a greater amount of nodal relaxations, approximately 5400 MW. These relaxations occurred but were not limited to the areas controlled by PJM (i.e., some relaxations occurred outside of PJM's territory due to model approximations). These nodal relaxations represent 3.5% of the total load for PJM's system and the outside areas that were also represented during the on-peak hour. Furthermore, due to these nodal relaxations, the LMP is limited only to $250 at several nodes, thereby controlling prices. The market chose to relax eight lines for the line thermal limit relaxations, but only overloaded these lines by a total of 490 MW. Unlike the RTS-96 test case results, the initial gap between the market solutions is much greater when comparing the SCUC and SCUC-CR solutions with the lowered penalty prices. The difference in total system cost between the initial market solutions for off- and on-peak hours are 3.9% and 8.3%, respectively, with the SCUC-CR solutions being cheaper. The difference in total system costs between the final AC and *N*-1 feasible solutions for the off- and on-peak hours are 10% and 2.5%, respectively, this time with the SCUC solutions being cheaper. For market solutions with relaxations, the off- and on-peak hours required changes to the dispatch solution to the point that the total system cost changed dramatically. While the penalty prices are lower than what PJM employs, these results demonstrate what can happen to the costs and market settlements once an infeasible solution with relaxations is corrected by the operator.

When the on-peak hour is solved with the original penalty prices (2700 $/MWh for node and 1000 $/MWh for line relaxations), the SCUC-CR solution had a relaxation of 340 MW total on seven lines. There were no nodal relaxations because the highest LMP obtained only reached $905 because the model was able to find a cheaper cost solution with only line relaxations. As expected, the relaxed market solutions produce lower overall costs than the market solutions without relaxations. The initial SCUC-CR market solution only has a 1.3% difference with the cost of the initial market SCUC solution. With the original penalty prices, few relaxations occur, and the relaxations that did occur were not due to feasibility requirements, because a solution was obtainable without relaxations in this test case, but rather to the economic benefit of relaxing the constraint for the specified penalty price. Finally, the overall total cost after obtaining AC feasibility and *N*-1 reliability is higher for the relaxed market solution compared to the market solution without relaxations. While such a result is not guaranteed, a solution with relaxations is expected to cost more in the end, as the relaxed solution is likely to rely more on costly out-of-market corrections by the operator. Additional results regarding market settlements can be seen in Table 4.3 and

in Figure 4.2, which further demonstrate how constraint relaxation practices can substantially influence market settlements.

When comparing the market solutions, for the on-peak hour between the two SCUC-CR models with low penalty prices and the original penalty prices, the initial market solution corresponding to the low penalty price model was approximately 7% cheaper than the SCUC-CR with the original penalty prices. The low penalty price model has a penalty on the node balance constraint of 250 $/MWh, which causes this result. While the lower penalty price market based solution will have a cheaper market-based cost (higher market surplus), both solutions must be corrected to achieve an *N*-1 AC feasible solution. After correcting these dispatch solutions to achieve AC and *N*-1 feasibility, the final cost for the SCUC-CR with low penalties was cheaper only by 0.9%. There were far more corrections required for the SCUC-CR solution with low penalties due to the high number of nodal relaxations (5400 MW) as well as 490 MW of line relaxations. In comparison, the SCUC-CR solution with the original penalty prices had no nodal relaxations and 340 MW of line relaxations. Such a result demonstrates that while the penalty prices may be substantially lower to produce a market solution that is more efficient, the actual efficiency gains may still be modest; solutions with more relaxations are naturally expected to require more corrections.

The two market solutions are also distinguishable as the low penalty price model substantially limits the LMPs to 250 $/MWh since the LMP cap is much lower, so there is an obvious difference in the settlements. The results also show that there is a much wider range of LMPs across the system. For instance, for the on-peak hour, the SCUC solution without relaxations has a standard deviation for the LMPs above 100, the SCUC-CR with the original penalties has a standard deviation at roughly 70, and the low penalty case has a standard deviation at about 15. The congestion rent in the low penalty case is also half of the congestion rent for the original penalty case. Another important result is that the uplift payments are also much higher for the case with a low penalty price; lowering the price cap then reduces profits and more generators need to receive a side payment (uplift) as a result. Thus, the original prices result in much higher settlements, which includes the generator revenue, generator profit, congestion rent, and the load payment. The results in Figure 4.2 and Table 4.3 illustrate how the chosen prices influence settlements dramatically while the costs to operate the system do not experience such a wide variation between the results. Constraint relaxation is thus shown to be very influential in settlements as well as imposing price control.

It should be noted that the difference in total system cost between the market solution and its corresponding AC and *N*-1 feasible solution is likely greater than what would be expected. Commercial grade market management systems are tailored to the system to account for system specific limitations to improve the approximation of the SCUC model (e.g., the inclusion of reliability must run units or nomograms). Thus, the market solution should be closer to the final solution than what is reported within this work. With that said, the comparative results with the same SCUC model except for relaxations demonstrate that constraint relaxations can substantially impact market settlements.

Table 4.3. Market results for PJM market and resulting *N*-1 final feasible solutions.

	Time Period	Total Cost	Gen. Revenue	Uplift	Gen. Profit + Uplift
SCUC (no relaxations)					
Market	Off	5,720	10,601	948	5,829
	On	16,649	42,255	63	25,669
N-1 Feasible	Off	10,499	11,852	5,547	6,899
	On	22,529	44,665	4,910	27,045
SCUC-CR low penalty prices					
Market	Off	5,499	10,602	43	5,235
	On	15,329	31,781	96	17,961
N-1 Feasible	Off	11,620	11,452	5,939	5,771
	On	23,106	35,147	6,700	18,740
SCUC-CR PJM original penalty prices					
Market	On	16,431	40,194	23	23,819
N-1 Feasible	On	23,315	42,695	4,879	24,259

Note that to obtain AC feasibility and *N*-1 reliability, additional units are only committed after all other control options have been exhausted. For the off-peak hour, the PJM SCUC market results required an additional 14 generators to achieve AC and *N*-1 feasibility whereas the PJM SCUC-CR market results with low penalties required 28 additional generators. For the on-peak hour to achieve AC and *N*-1 feasibility, the PJM SCUC market results required 22 generators to be committed and PJM SCUC-CR with low penalties required 74 generators. For the latter results where the relaxed case needed what seemed to be an abnormally high amount of additional generators, this amount only accounted for an additional 7% of generation. Regarding the PJM SCUC-CR with original penalties, this market solution required an additional 62 generators to be committed to attain AC and *N*-1 feasibility.

As for generator revenue, every scenario exhibited an increase when comparing the initial market solution and the final AC and *N*-1 feasible solution based upon market LMPs; this is due to the fact that additional units are committed while the market settlements for generators committed based on the market solution are maintained. The uplift payments also increase as well. The highest increase is exhibited for the on-peak hour when the market solution was initially relaxed with the lower penalty prices. The greatest increase in profit occurred for the on-peak hour when no relaxations were allowed. Both relaxed market solutions end up with higher costs in the end than the solution without relaxations; however, the generation revenue, generation profit, and load payments are all lower for the relaxed solutions. This is, in part, a result of the fact that relaxations cap market clearing prices. These results can be viewed in Table 4.3 as well as in Figure 4.2.

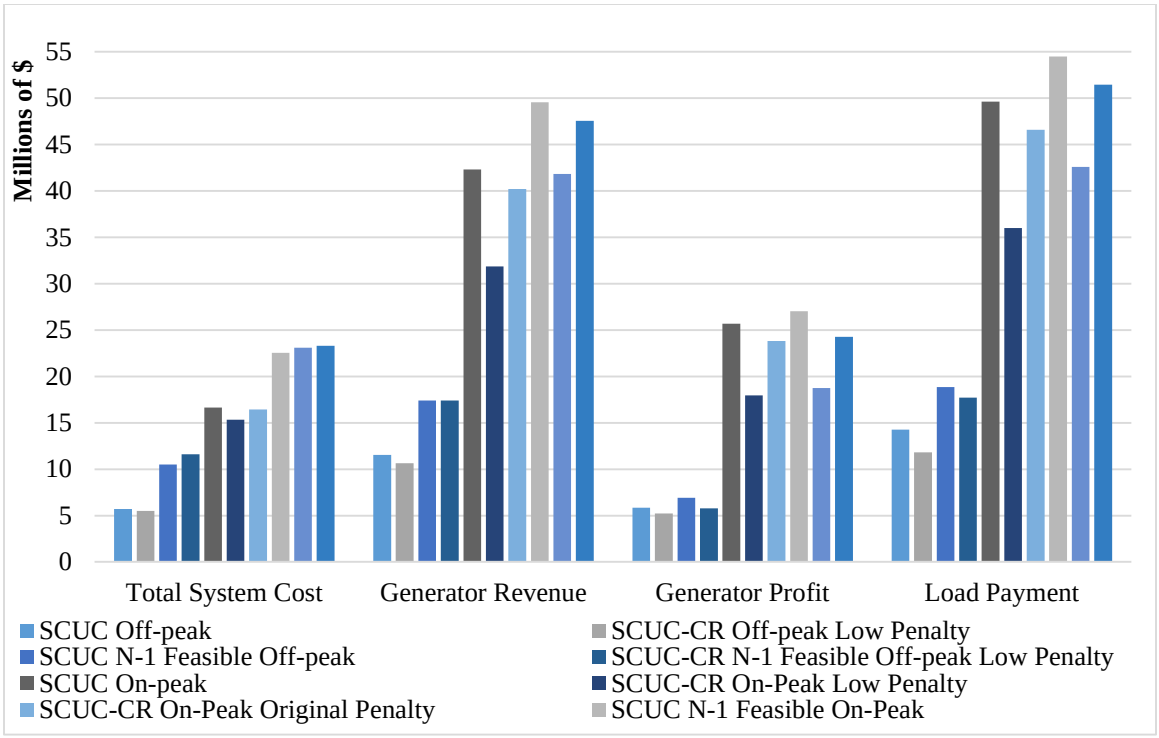

Figure 4.2. System settlement results for both on and off-peak hours, with and without relaxations; generator revenue, generator profit as well as load payment include the uplift payments.

4.5.3 Discussion

When the market model involves constraint relaxations, the optimal solution to the SCUC-CR model is at least as good, if not better, than the optimal solution of the SCUC model without relaxations. However, the simulations conducted for this study demonstrate that it is not possible to conclude what method will produce a lower cost at the final stage of the process after each solution is modified to be AC feasible and *N*-1 reliable. While the SCUC-CR solution is considered to be infeasible due to the relaxations, both solutions are infeasible due to the DC approximation and the proxy reserve requirements that do not guarantee *N*-1. The results show that the final solutions are not just dependent on the solution produced by the market engine but that they are also dependent on the procedures taken to modify the solutions to get reliable solutions. Overall, the results demonstrate that it may not be beneficial to have an overly precise market model since the market model has other approximations embedded in it anyway. One result demonstrates that the final cost ($23,315k) for the PJM market solution with PJM's original relaxation prices that, resulted in minimal relaxations is higher than the final cost ($23,106k) for the PJM market solution with much lower relaxation prices while having many more relaxations in the market solution.

On the other hand, having more relaxations in the market solution can result in more corrections needed outside the market environment. For the PJM on-peak hour, the market solution that contained relaxations required twice as many additional units to be committed during the adjustment process (i.e., taking the market solution and modifying it to obtain an AC feasible, *N*-1 solution). Such adjustments are based on ad-hoc operator influenced modifications, which are not clearly established or published, leaving more ambiguity relative to the overall process, which is not preferred by market participants, especially when the results demonstrate that these practices influence market settlements.

4.6 Summary

This report includes an overview of existing constraint relaxation practices of the ISOs within the United States. SCUC models are formulated with and without relaxations in order to assess the overall impact on market costs and market settlements as a result of constraint relaxations. Results are presented for two test cases: i) an IEEE test case and ii) a large-scale model of the PJM system with actual market data used in this study. All market SCUC solutions were then modified to attain an AC feasible and *N*-1 reliable solution. The results, thus, demonstrate whether relaxations within the market engine require additional operator based costly out-of-market corrections to occur, which can substantially impact not only the market efficiency but also market settlements.

It was expected that after applying these corrections the dispatch schedule, which allowed for constraint relaxations, would result in a higher cost schedule because more costly out-of-market corrective actions would be anticipated to be necessary. In the RTS-96 test case, that did not occur and the final feasible dispatch solution whose market solution contained relaxations had a lower total cost than the final dispatch solution whose market solution did not contain relaxations. As for the PJM test case, the dispatch results that initially contained constraint relaxations did need more adjustments to attain *N*-1 reliability and, as expected, the total cost solution for the dispatch without relaxations had a lower total cost in the end when comparing *N*-1 reliable dispatch solutions. For the PJM results, not only are the final costs higher, but the generation revenue, generation profit, and load payment are all lower. Thus, the sacrifice for price control seems to be higher overall system costs, lower profits for generators, and lower payments for the load.

Even though market participants have previously agreed to such practices, one aspect that is generally not preferred is the lack of transparency. While the structure of market models and settlement schemes are widely known, the process operators take to correct solutions produced by the market engine that are not feasible is far less transparent. While there is no guarantee, intuitively, the more relaxations that occur the more corrections are expected in this adjustment phase leading to less transparency.

5. Penalty Price Analysis

To replicate the process of choosing potential penalty prices and schemes, a similar security constrained unit commitment model is presented in Chapter 4.1. Originally this formulation, (4.1)-(4.25), was a fixed price relaxation on the line thermal limits. In the following sections, modifications to this formulation are presented.

One method to determine penalty prices is to analyze the dual solution to the original problem without constraint relaxations and to choose potential penalty prices such that expected market outcomes do not deviate too much while taking advantages of constraint relaxation practices. To aid in choosing potential penalty prices and schemes, a traditional security constrained unit commitment (SCUC) model is presented in Chapter 5.1. With this formulation, the RTS-96 test case is solved for the entire year [32]. This formulation optimizes both energy and acquired operating reserve. The prior SCUC formulation presented, (4.1)-(4.25), is modified to represent a fixed priced penalized and a stepwise penalized SCUC in the subsequent sections below. Constraint relaxations are applied to the node balance constraints, thermal limit constraints, and operating reserve requirements. First, the SCUC is solved and dual values of the constraints to be relaxed are recorded and analyzed. Penalty prices are then chosen on the basis of price control and eliminating extremely high dual values for both SCUC models with constraint relaxations (fixed price and stepwise). Furthermore, these penalty prices were chosen such that no generator resource, energy or reserve, was disqualified, i.e., the penalty price for the constraints was set above the highest generator cost to provide energy and reserve. The mipgap was set to 1%.

5.1 SCUC without Relaxations

The unit commitment model, without relaxations (SCUC), is similar to (4.1)-(4.25). However, slack variables are removed. Additionally, the objective is modified to (5.1a), which minimizes the cost of acquired energy and operating reserves. Operating reserve is assumed to be 25% and 15% of the final generator cost segment for spinning and non-spinning reserve, respectively.

When solving the SCUC model with the replace objective, the dual variables of (4.7)-(4.8) are recorded for the entire year. The sum of these dual variables is known as the reserve clearing price (RCP), which is the price used to pay for operating reserves. The RCP components are displayed in (5.2a) and (5.3a).

The SCUC formulation is slightly modified to have a B-theta to represent the line flow throughout the network. As a result, (4.18)-(4.20) are modified to (5.4a)-(5.5a). The dual variable of (5.29a) represents the LMP and the dual of (5.5a) represent the FMP.

$$min \sum_g \sum_t \sum_i \left(c_{gi}^{op} P_{git}\right) + \sum_g \sum_t (c_g^{NL} u_{gt} + c_g^{SU} v_{gt} + c_g^{SD} w_{gt}) + \sum_g \sum_t (0.25 c_{gI}^{op} r_{gt}^{sp} + 0.15 c_{gI}^{op} r_{gt}^{NS}) \quad (5.1a)$$

$$r_t^{req} \leq \sum_g \left(r_{gt}^{SP} + r_{gt}^{NS}\right) \quad [\lambda_t^{RMP1}] \quad \forall t \quad (5.2a)$$

$$0.5 r_t^{req} \leq \sum_g r_{gt}^{SP} \quad [\lambda_{kt}^{RMP2}] \quad \forall t \quad (5.3a)$$

$$\sum_{g \in g(n)} P_{gt}^{total} + \sum_{k \in \delta_n^+} P_{kt} - \sum_{k \in \delta_n^-} P_{kt} = d_{nt} \quad [\lambda_{nt}^{LMP}] \quad \forall n, t \quad (5.4a)$$

$$-P_k^{max} \leq P_{kt} \leq P_k^{max} \quad [\lambda_{kt}^{FGP}] \quad \forall k, t \quad (5.5a)$$

5.2 SCUC with Fixed Penalty Relaxations

A modified SCUC version, a formulation with fixed penalty prices, is presented below by (5.1b)-(5.6b). For this formulation only the objective (5.1a), operating reserve constraints of (5.2a)-(5.3a), the node/energy balance (5.4a), and the line flow limits (5.5a) are modified from the original formulation in (4.1)-(4.25).

The objective (5.1a) is modified to include the slack variables in order to penalize the model from choosing to relax its associated constraint. Although relaxations are being introduced, the penalty prices prevent the model from readily choosing to relax constraints. This modification is shown in (5.1b), where the penalty prices on the nodal, line and reserve relaxations are represented by P^N, P^K, and P^R respectively.

To include operating reserve relaxations, the original SCUC without relaxations is modified to have (5.2b)-(5.3b) instead. This modification includes adding the associated slack variables s_t^{SP} and s_t^{NS}, which correspondingly relaxes the spinning and non-spinning reserve acquired during each period. The total reserve might require 400 MW; however, the amount of reserve acquired from the various generators can be less through these additional slack variables.

As for the node balance constraint, (5.4b) is instead included. The slack variable s_{nt}^{n+} represents the additional acquirement of demand, e.g., instead of a node having 100 MW of load, it can now have an additional 10 MW if the model finds it beneficial. This rarely happens, yet the slack variable s_{nt}^{n-} represents artificial generation and could decrease the load at a bus by 10 MW instead.

The line flow was originally restricted by the thermal limit of the line. The addition of the slack variables s_{kt}^{k+} and s_{kt}^{k-} to (5.5b) allow these limits to be violated. Therefore, cheaper generation that was previously restricted by congestion, can now be dispatched at a higher level because the model is allowed to relax these limits.

The added slack variables in (5.1b), (5.2b)-(5.3b), and (5.4b)-(5.5b) allow the SCUC with fixed price penalties (SCUC-FP) model to choose to relax these constraints, but with a penalty price. These relaxations will typically result in a cheaper total system cost solution

than the SCUC solution or at least the same solution as the one without relaxations. Note that all slack variables are greater than or equal to zero, as indicated by (5.6b).

$$min\ \sum_g \sum_t \sum_i \left(c_{gi}^{op} P_{git}\right) + \sum_g \sum_t (c_g^{NL} u_{gt} + c_g^{SU} v_{gt} + c_g^{SD} w_{gt}) + \sum_g \sum_t (0.25 c_{gI}^{op} r_{gt}^{sp} + 0.15 c_{gI}^{op} r_{gt}^{NS}) + \sum_n \sum_t P^N (s_{nt}^{n+} + s_{nt}^{n-}) + \sum_k \sum_t P^K (s_{kt}^{k+} + s_{kt}^{k-}) + \sum_t P^R (s_t^{SP} + s_t^{NS})$$

(5.1b)

$$r_t^{req} \leq \sum_g \left(r_{gt}^{SP} + r_{gt}^{NS}\right) + s_t^{SP} + s_t^{NS} \qquad [\lambda_t^{RCP1}] \qquad \forall t \qquad (5.2b)$$

$$0.5 r_t^{req} \leq \sum_g r_{gt}^{SP} + s_t^{SP} \qquad [\lambda_{kt}^{RCP2}] \qquad \forall t \qquad (5.3b)$$

$$\sum_{g \in g(n)} P_{gt}^{total} + \sum_{k \in \delta_n^+} P_{kt} - \sum_{k \in \delta_n^-} P_{kt} = d_{nt} + s_{nt}^{n+} - s_{nt}^{n-} \qquad [\lambda_{nt}^{LMP}] \qquad \forall n, t \qquad (5.4b)$$

$$-s_{kt}^{k-} - P_k^{max} \leq P_{kt} \leq P_k^{max} + s_{kt}^{k+} \qquad [\lambda_{kt}^{FGP}] \qquad \forall k, t \qquad (5.5b)$$

$$s_{nt}^{n+}, s_{nt}^{n-}, s_{kt}^{k+}, s_{kt}^{k-}, s_t^{SP}, s_t^{NS} \geq 0 \qquad \forall n, k, t \qquad (5.6b)$$

5.3 SCUC with Stepwise Penalty Relaxations

The SCUC with stepwise penalty relaxations (SCUC-SP), modifies the original SCUC, similar to the SCUC-FP. However, instead of adding one slack variable, three slack variables are added and are indexed by j, each of which has a monotonically increasing penalty price. Furthermore, the first two slack variables are limited, whereas the third and final slack is not limited. For nodal relaxations, the first two slack variables can only relax the model by 2 and 5 MW, respectively. The same is true for the first two slack variables associated with spinning and non-spinning reserve. Finally, line relaxations are limited based on the percentage of line capacity. The first two slack variables cannot take on a value higher than 2% and 5% of the line's rated capacity. These modifications are shown below in (5.1c)-(5.10c).

$$Min\ \sum_g \sum_t \sum_i \left(c_{gi}^{op} P_{git}\right) + \sum_g \sum_t (c_g^{NL} u_{gt} + c_g^{SU} v_{gt} + c_g^{SD} w_{gt}) + \sum_g \sum_t (0.25 c_{gI}^{op} r_{gt}^{sp} + 0.15 c_{gI}^{op} r_{gt}^{NS}) + \sum_n \sum_t \sum_j P_j^N (s_{ntj}^{n+} + s_{ntj}^{n-}) + \sum_k \sum_t P_j^K (s_{ktj}^{k+} + s_{kth}^{k-}) + \sum_t P_j^R (s_{tj}^{SP} + s_{tj}^{NS})$$

(5.1c)

$$r_t^{req} \leq \sum_g \left(r_{gt}^{SP} + r_{gt}^{NS}\right) + \sum_j s_{tj}^{SP} + s_{tj}^{NS} \qquad [\lambda_t^{RMP1}] \qquad \forall t \qquad (5.2c)$$

$$0.5 r_t^{req} \leq \sum_g r_{gt}^{SP} + \sum_j s_{tj}^{SP} \qquad [\lambda_{kt}^{RMP2}] \qquad \forall t \qquad (5.3c)$$

$$\sum_{g \in g(n)} P_{gt}^{total} + \sum_{k \in \delta_n^+} P_{kt} - \sum_{k \in \delta_n^-} P_{kt} = d_{nt} + \sum_j (s_{ntj}^{n+} - s_{ntj}^{n-}) \qquad [\lambda_{nt}^{LMP}] \qquad \forall n, t \qquad (5.4c)$$

$$-\sum_j s_{ktj}^{k-} - P_k^{max} \le P_{kt} \le P_k^{max} + \sum_j s_{ktj}^{k+} \qquad [\lambda_{kt}^{FGP}] \qquad \forall k,t \qquad (5.5c)$$

$$s_{ntj}^{n+}, s_{ntj}^{n-}, s_{ktj}^{k+}, s_{ktj}^{k-}, s_{tj}^{SP}, s_{tj}^{NS} \ge 0 \qquad \forall n,j,k,t \qquad (5.6c)$$

$$s_{ntj}^{n+}, s_{ntj}^{n-}, s_{tj}^{SP}, s_{tj}^{NS} \le 2 \qquad \forall n, j = 1, k, t \qquad (5.7c)$$

$$s_{ntj}^{n+}, s_{ntj}^{n-}, s_{tj}^{SP}, s_{tj}^{NS} \le 5 \qquad \forall n, j = 2, k, t \qquad (5.8c)$$

$$s_{ktj}^{k+}, s_{ktj}^{k-} \le 0.02 P_k^{max} \qquad \forall n, j = 1, k, t \qquad (5.9c)$$

$$s_{ktj}^{k+}, s_{ktj}^{k-} \le 0.05 P_k^{max} \qquad \forall n, j = 2, k, t \qquad (5.10c)$$

5.4 Dual Analysis of SCUC and Penalty Price Selection

Initially, the SCUC (without relaxations) is solved for the entire year. The dual variables of SCUC are recorded for the entire year and are respectively known as the RCP, LMP, and the flowgate marginal price (FMP). Note the RCP is the sum of the dual variables from (5.2a)-(5.3a). With the value of these dual variables accessible over the entire year, penalty prices for the relaxed SCUC models can be determined.

The objective of this paper is to demonstrate that even with constraint relaxations, market solutions are relatively similar. The selection of the penalty is crucial because when the penalty chosen is relatively small (even though above the highest generator bid), relaxations will readily occur. This result is undesirable. Thus, the two penalty price schemes are demonstrated, i.e. the SCUC-FP and SCUC-SP.

For the year that was analyzed, the LMPs generally stayed under the highest generator's cost of 218 $/MWh. In Figure 5.1, the LMPs are shown for values over the highest generator cost. The figure shows the frequency at which the value all LMPs take throughout the network during the entire year.

If the desire was to cap the LMP at the highest generator cost/bid, then a penalty price of 225 $/MWh would be chosen. In the RTS-96 test case, the LMPs rise above this price a total of approximately 500 times over all nodes (73) and all time periods (8736). The high LMPs are due to system congestion.

For SCUC-FP, the penalty price for the nodal/energy balance constraint is set to 300 $/MWh. As for SCUC-SP, the penalty prices were 250, 350, and 500 $/MWh. Note that the SCUC-SP model can only have 2 MW and 5 MW relaxed at a particular node for 250 $/MWh and 350 $/MWh, respectively. At 500 $/MWh, SCUC-SP can choose to relax the penalty at any MW amount. These penalty prices were chosen for the different model so that the model would still exhibit some relaxations, but not unnecessarily. These nodal approximations are warranted due to inaccuracies in demand forecasts. Therefore, there is no reason to force the market model to strictly enforce this equality constraint.

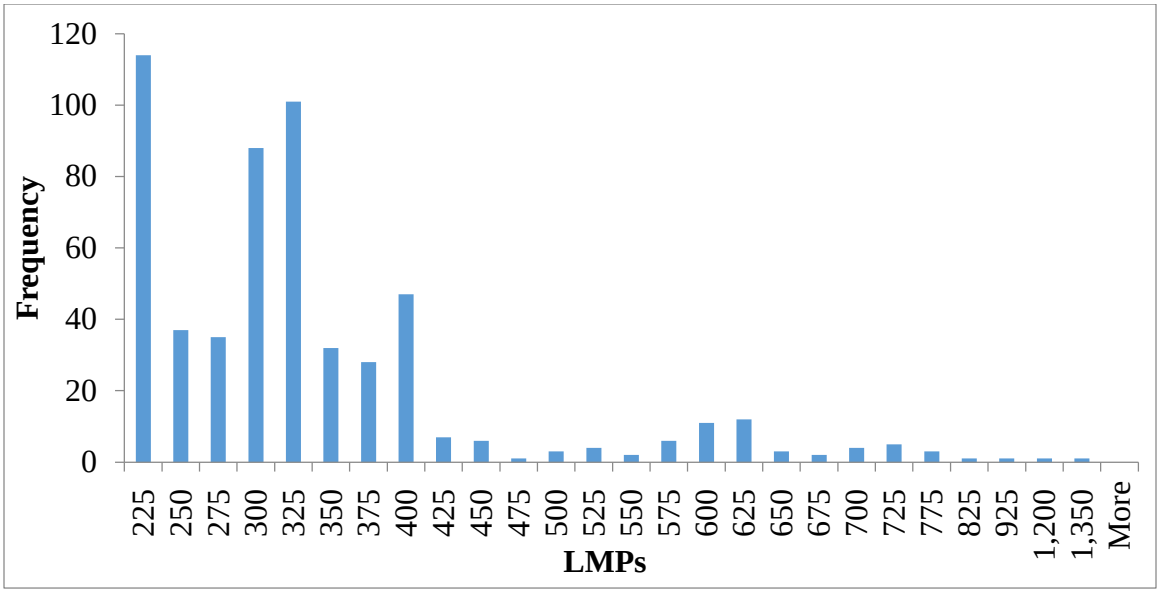

Figure 5.1. Histogram of LMPs above highest generator cost.

In order for the RTS-96 test case to exhibit congestion when the transmission lines are at their rated capacity, transmission line thermal limits were lowered by 15%. Other lines were de-rated further. These changes only resulted in a total of four lines being at capacity. If these changes were not made, then the line thermal limit, (5.5a), would not be binding and, thus, the dual would be zero.

Most of the FMPs, the value of the dual variables of (5.5a), even in this modified version of the RTS-96 test case are zero because most lines are not at their respective limit. Even for the four lines that exhibit some congestion, overall the FMPs were relatively low with the average at approximately 35 $/MWh.

In Figure 5.2, FMPs are above this average. Based on the value of these dual values for the SCUC (without relaxations), a penalty price of 100 $/MWh was chosen for the SCUC-FP. As for the SCUC-SP, the line relaxation penalty prices were 65, 150, and 500 $/MWh.

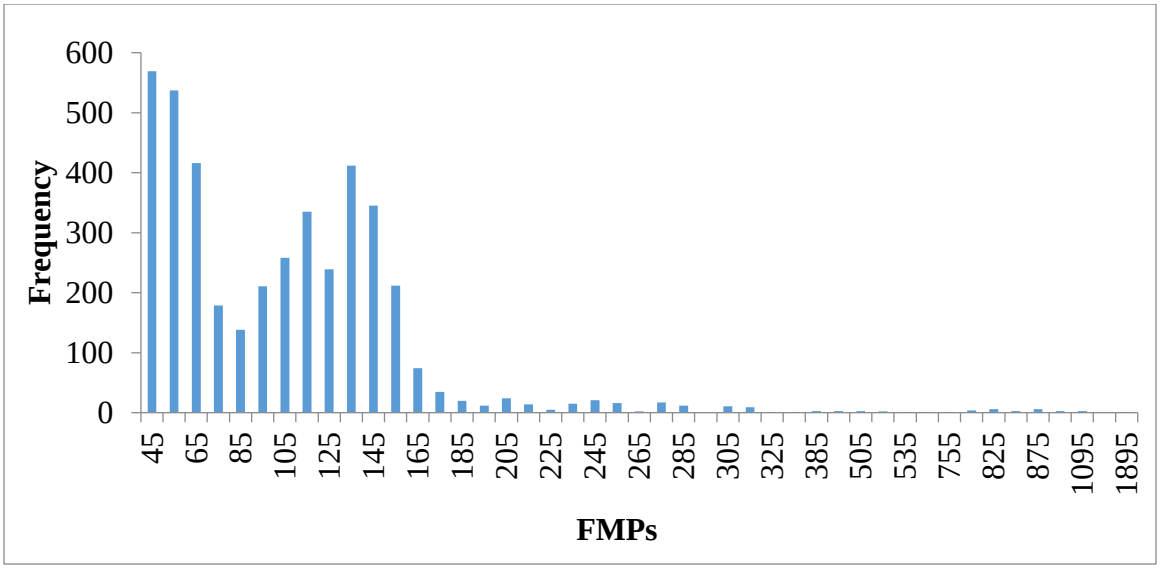

Figure 5.2. Histogram of FMPs starting at the average value of non-zero FMPs.

The assumed prices of spinning and non-spinning reserve were to be 25% and 15% of the particular generator's last segment cost based on the assumption that the highest spinning reserve cost was approximately 28 $/MWh and non-spinning reserve was approximately 33 $/MWh. Therefore, penalty prices for these constraints must also be selected above these costs, such that the model still has these resources available.

Upon examination, the RCP, the sum of (5.2a)-(5.3a), is frequently around 15 $/MWh and is due to the market being able to acquire reserve at lower prices, especially during hours when the system is lightly loaded. During hours when the system is more restricted, the RCP will go beyond 33 $/MWh (Figure 5.3). For the entire year, this occurred during approximately 1300 hours. Therefore, for the SCUC-FP, a penalty price for reserve was chosen 40 $/MWh while, for the SCUC-SP, penalty prices were chosen as 35, 50, and 100 $/MWh for the monotonically increasing price function.

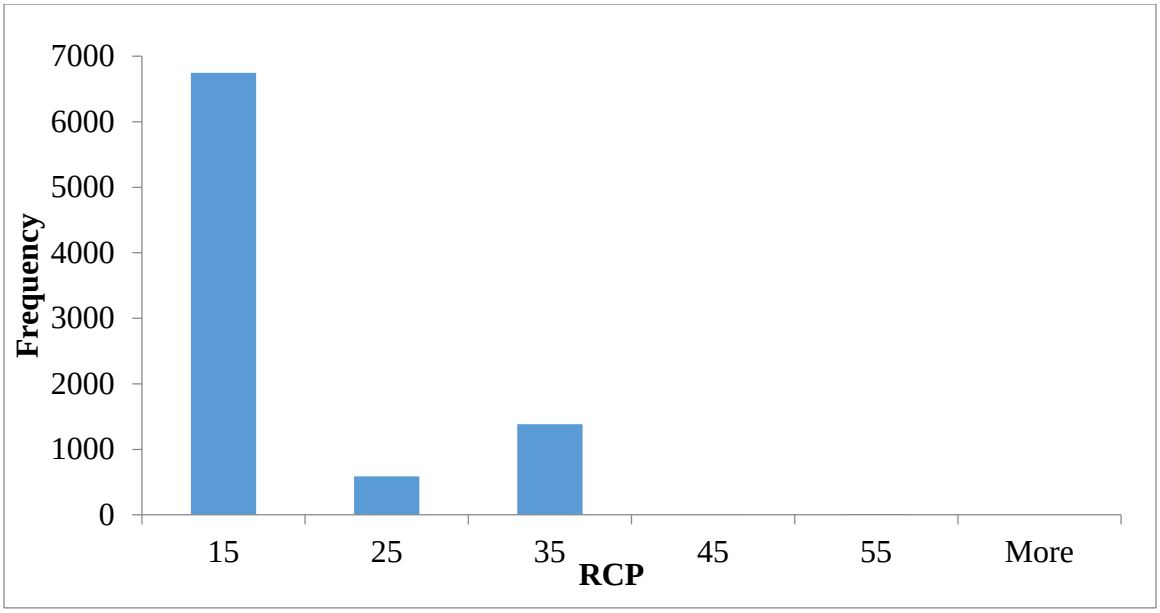

Figure 5.3. Histogram of RCPs.

5.5 Results

With the penalty prices, chosen SCUC-FP and SCUC-SP are also solved for the entire year with the same load and line ratings. The constraint relaxations observed for both penalty schemes are vastly different due to the structure of the penalty schemes and the chosen penalty prices.

For node relaxations, the SCUC-FP only chose to relax a single node during the entire testing period, for a total of approximately 11 MW. As for the SCUC-SP, a total of approximately 3,300 MW over all nodes were relaxed. Bus 62 had the highest relaxation at 247 MW. These relaxations might seem high, but over the entire year the total node relaxations accounted for less than 0.01% of the total load. With the choice of either pricing scheme or utilizing a similar method of choosing the penalty price, relatively few relaxations will occur that need to be corrected for an adjustment phase, which occur anyway due to the inherent linearized nature of the market model. With both pricing schemes, operators will be guaranteed a solution from the market as well as price control. For SCUC-FP, the LMP cannot go above 300 $/MWh while for SCUC-SP, the highest LMP observed was 500 $/MWh due to the model choosing to relax that node at a value above 7 MW (the sum of the relaxations of the first two steps).

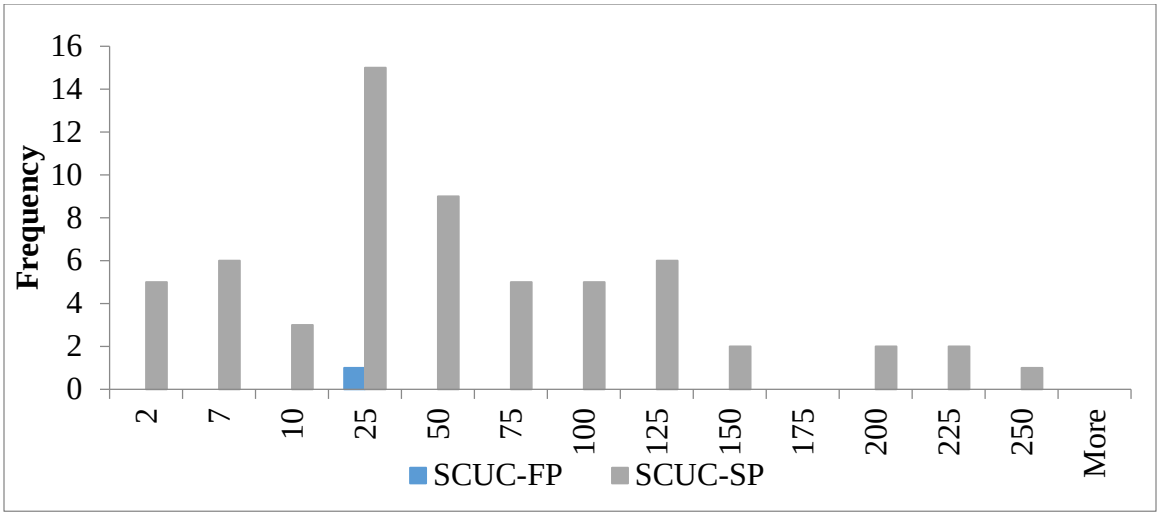

Figure 5.4. Histogram of node relaxations for SCUC-FP and SCUC-SP.

Unlike node relaxations, SCUC-FP chooses to relax line thermal limits often. In Figure 5.5 below, SCUC-FP chooses to relax a total of 35,500 MW approximately over the entire year. Most of these relaxations are on line 65, which is a line close to several generators. The relaxation of this line allows for additional power from these generators to be dispatched. Furthermore, the highest overload across all time periods was 15%.

Similarly, SCUC-SP chooses to relax the same lines at a total of approximately 20,000 MW over the entire year. Examining line 65, which also has the most relaxations, the highest overloaded was 7% above the rated value. In either case penalty scheme, these transmission line overloads from the market solution will need to be corrected. Since the market solution must be adjusted anyway, correcting for these overloads can be handled in the post-processing phase because the market solution does not meet all system requirements, such as AC feasibility.

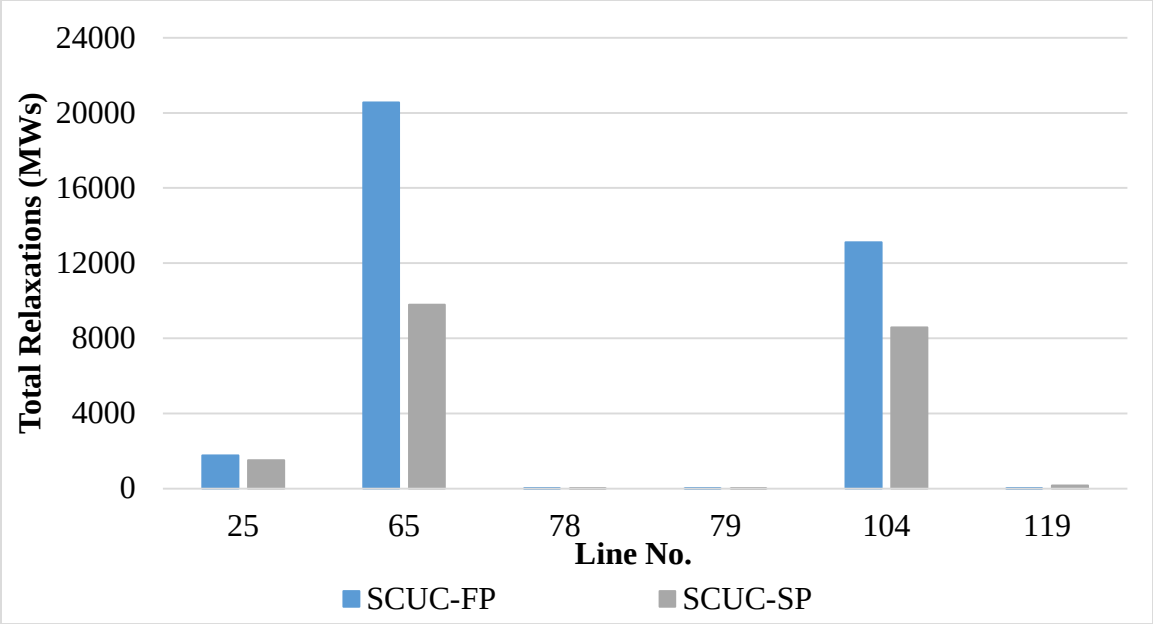

Figure 5.5. Total line relaxations over entire year.

Regarding operating reserve relaxations as seen in Figure 5.2, SCUC-FP had the most relaxations. Even though the relaxation price was chosen in between the first and second penalty prices for SCUC-SP, the model found that it was much more advantageous to relax the operating reserve requirement and instead allow cheaper generation to dispatch at higher levels. Instead of withholding capacity for reserves, generators could now be dispatched more. It is obvious, from these results, that the stepwise penalty price function is more suitable for reserve relaxations. Furthermore, according to some industry members, without reserve relaxation curves, there is no way to price reserves [21]. It should be noted that the SCUC, SCUC-FP, and SCUC-SP will have to be modified to attain *N*-1 reliability because acquiring reserve does not guarantee *N*-1 reliability.

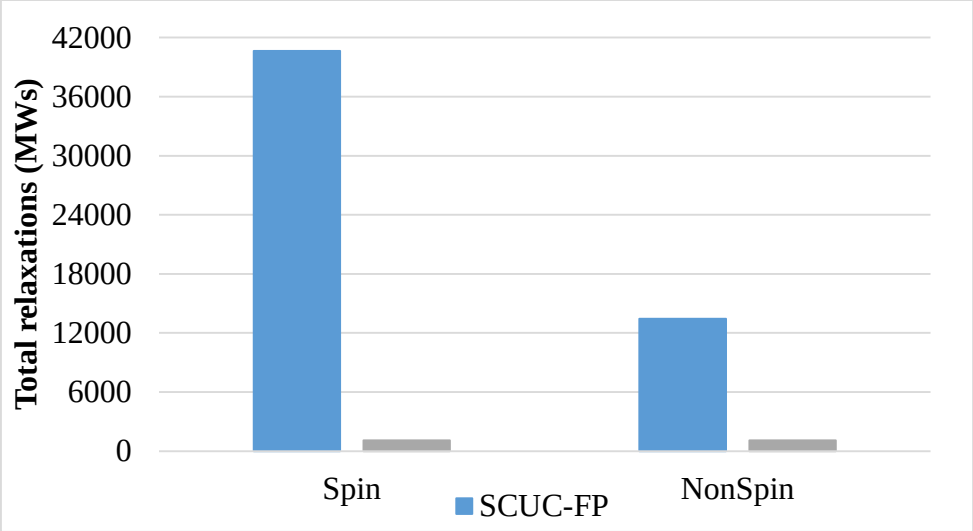

Figure 5.6. Total operating reserve relaxations over entire year.

When comparing market settlements, the SCUC-FP and SCUC-SP solutions do not differ greatly from traditional SCUC without relaxations. For example, the deviation in total cost over the entire year is 0.43% and 0.22% for the SCUC-FP and SCUC-SP compared to SCUC, respectively. Furthermore, when compared daily, the total cost difference between SCUC-FP and SCUC-SP to SCUC was at most a decrease of 1.83% and 1.52%, respectively. This means that even with relaxations, neither dispatch solution deviated too far from the SCUC solution (without relaxations) in terms of the objective to minimize total system cost.

Other settlements did have larger deviations compared to the non-relaxed SCUC solution. One notable aspect is that with SCUC-FP and SCUC-SP, generators were generally receiving higher settlements, which can be seen from the revenue and profit acquired through the entire year. SCUC-FP had an increase of about 6% in terms of revenue and 11% in terms profit compared to the non-relaxed SCUC solution. As for SCUC-SP had the dispatch solutions increased by 15% in terms of revenue and 26% in terms of profit compared to the non-relaxed SCUC solution. However, when comparing uplift payments, SCUC-FP had a 19% decrease. The lower uplift is due to the relaxations allowing cheaper generation to be dispatched at higher levels rather than being withheld due to line flow limits and capacity being withheld for reserves. The SCUC-SP solution had a 24% difference in terms of uplift payments.

With higher payments being allocated to generators in SCUC-FP and SCUC-SP solutions, consumers will have higher payments as well. The SCUC-FP solution required consumers to pay an additional 3% while the SCUC-SP solution required an increase of almost 11%. This increase is due to the higher settlements received by the generators. All of these settlements can be compared in Table 5.1 and Figure 5.7.

Increases in generator compensation result from market models choosing to relax all three constraints in the most economical manner based on penalty prices. Node/energy balance

constraint relaxations allow the market model to acquire artificial energy whenever the dual variable reaches the penalty price. Line relaxations allow cheaper generation that are behind congested lines resources to dispatch at higher levels. Finally, operating reserves are relaxations that allow cheaper generation to be dispatched at higher levels instead of having some of the capacity withheld for reserve, especially when the acquired reserve has no guarantee of making the system *N*-1 reliable.

Furthermore, the increase in compensation to generators (and the increase payments by the load) can be attributed to the higher overall LMPs found in the SCUC-FP and SCUC-SP solutions, which were approximately on average 26 and 27 $/MWh. The traditional SCUC had an average LMP of 25 $/MWh. This small increase led to higher settlements received for generators, but the objective remained fairly close and is due to the fact that a relaxed model should either be equal to or have a lower objective than a model without relaxations.

The final settlement, congestion rent, is the amount paid to financial transmission right (FTR) owners and is the difference between the amount paid by consumers (load payment) to producers (generator revenue). Market participants entered the market to hedge against price risk due to congestion that occurs in the system. However, the SCUC-FP and SCUC-SP witnessed a decrease in congestion rent by about 20% and 26%, respectively. The decrease in congestion rent is due to line flow being allowed to be relaxed and, therefore, when a relaxation occurs, the FMP is capped. Apparently, differences in LMPs between nodes that are connected by a transmission line are also limited in the SCUC-FP and SCUC-SP. Thus, these two solutions have decreased congestion rent.

To sum up, after solving traditional SCUC (without relaxations), the value of the dual variables was used to base the penalty prices chosen for two different penalty pricing schemes for relaxing the node balance, line flow thermal limit, and operating reserve constraints. With the node and reserve constraints, the rationale was followed that every generator should be able to dispatch – meaning that the penalty prices were greater than the highest generator cost to provide energy and operating reserve. The line flow limit relaxation penalty price was selected above the average observed non-zero FMP throughout the entire year.

The relaxation of any of these constraints means that decisions are pushed to the post-processing phase. With regard to the node balance constraint, the relaxation of this constraint means that artificial generation was acquired. Since the day-ahead market is based on a load forecast, there is no point in enforcing the node balance constraint strictly. Allowing the model to deviate even by a small amount provides the market software greater flexibility.

The relaxation of the line-flow constraint means that the line capacity has been violated. Market models today typically use a PTDF formulation to approximate line flow. These approximations can lead to infeasible market solutions and therefore constraint relaxation practice on line constraints is warranted. However, there is a post processing phase that must already occur to meet all operating requirements, most notably AC feasibility. A small

relaxation in the line flow constraint could mean that cheaper generation is awarded in the day-ahead market, which could lead to greater gains in market surplus.

In market models, operating reserve is acquired in an attempt to achieve *N*-1 reliability through the use of proxy reserve requirement policies. However, these policies cannot guarantee *N*-1 reliability even if an adequate quantity is acquired by the market. The location of the reserve is crucial. This locational aspect is not modeled because the post-contingency states must be explicitly modeled. Instead, operators will modify the proposed market solution to attain *N*-1 reliability in the post processing phase. Therefore, the relaxation of the operating reserve requirements is understandable. Even some ISOs have acknowledged without constraint relaxations, reserves cannot be priced [21].

ISOs and RTOs can use either penalty price schemes. It is likely more desirable to employ the stepwise penalty price scheme which allows market operators to have more control over the initial amount of relaxations and use the final relaxation step for price control. In any case, these relaxations can be handled in the post-processing phase that must occur anyway after the market is settled.

Table 5.1. Market settlements ($M).

Dispatch solution	Total cost	Load payment + uplift	Gen. revenue	Gen. profit + uplift	Congestion Rent
SCUC	502.11	1,371	1,201	719.09	149.97
SCUC-FP	499.94	1,413	1,277	798.88	120.06
SCUC-SP	501.03	1,517	1,380	906.48	111.70

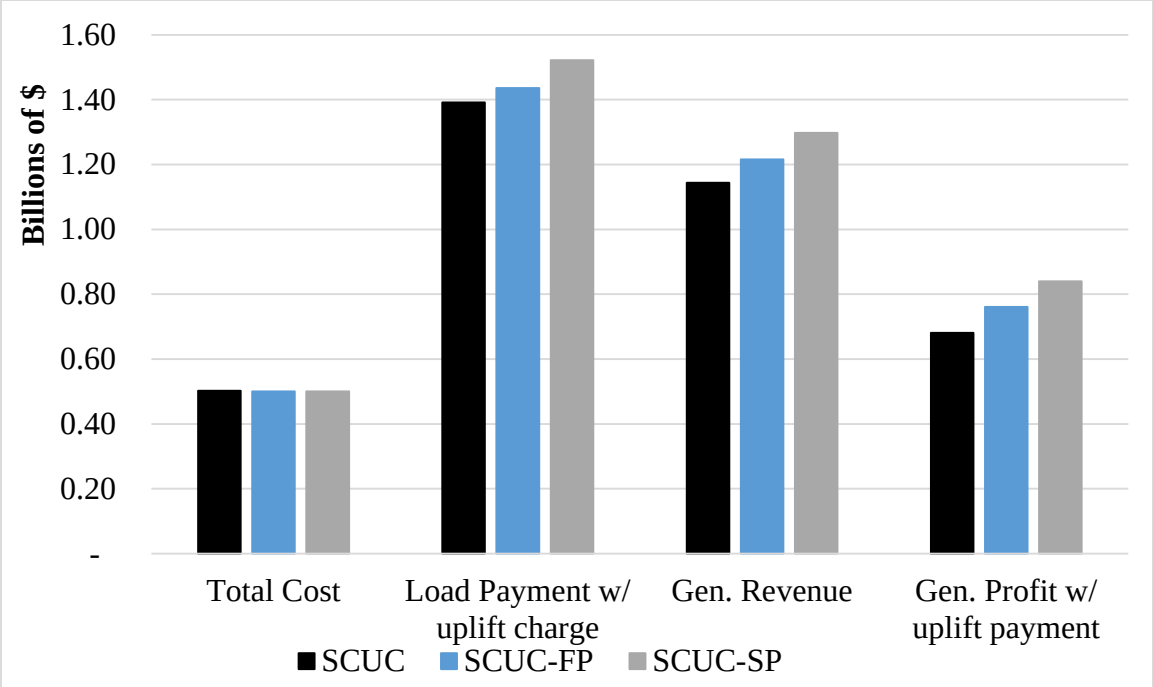

Figure 5.7. Various market settlements for RTS-96 test case over entire year.

5.6 Summary

ISOs and RTOs must not only manage the electric energy market, but must also account for all the complex operating and reliability requirements inherent in the power system. Market models employed by ISOs and RTOs today cannot fully capture all the complexities of the power system although they have improved algorithmic performance. Therefore, several modeled operating and reliability requirements are at best approximations. For example, complex generator operating requirements such as generator ramping constraints, although truly non-linear, are assumed to have linear ramping capability. Market models will also assume the more convenient linear DCOPF if a network topology is modeled. Additional complexity arises from the inaccuracy of load forecasts, which becomes more complex with the addition of distributed generation resources. Such approximated system operating conditions can cause the market model to be infeasible. Thus, market operators allow select constraints to be violated or relaxed for pre-determined penalty prices. The inclusion of constraint relaxations within the market model also limits the dual variable to the penalty price, giving the market operator a method of price control. Moreover, constraint relaxations can allow for gains in market surplus in the initial market solution, which are typically modified to achieve AC and *N*-1 feasibility by the process is given in [19]-[20].

Constraint relaxation practices and penalty prices are negotiated with market participants. In particular, penalty prices were originally a single fixed price penalty, but more recently ISOs and RTOs have adopted the use of stepwise penalty price schemes. Regardless, the

inclusion of either pricing scheme in the market model should not force the solution to deviate too far from a market without relaxations, if one existed. Furthermore, penalty prices should be chosen such that market participants are willing to enter the market. For example, in this report, penalty prices were chosen above the highest cost for generator energy production and reserve cost. Moreover, there is no point in choosing a penalty price to be so high such that there is no resulting price control. Again, these penalty prices must be negotiated with market participants.

Constraint relaxations do allow for gains in market surplus. Although, the model used in this report was a minimization problem, the total cost for the relaxed models was smaller than the traditional SCUC. Also notable, the market settlements for generators increased, especially generator profit, which is due to cheaper generators being dispatched at higher levels throughout the year, which resulted in the market clearing price being set by more expensive generators. Therefore, these generators were able to obtain higher profits.

The model used in this report was a minimization problem and as expected the total cost for the relaxed models was lower than the traditional SCUC. However, consumers had to pay more and generators received additional revenue in this test case. This was due to overall increases in LMPs in the relaxed market model solutions, but unlike the non-relaxed solution, the LMPs were not at such extremes. Recall that ISOs and RTOs included constraint relaxations as a form of price control in the market, which was originally uncapped due to only having bid-caps in place. Also, these extreme LMPs do not necessarily represent resource scarcity in the market as they can be a result of approximations within the market models, whose solutions must be adjusted anyway to meet operating and reliability standards. Therefore, the constraint relaxation practices are in place to limit prices.

When comparing the various market solutions, relaxations are included in the rationale that there is no point to strictly enforce approximated constraints. However, the operator and market participants desire a market solution that would not deviate too far from a market solution with relaxations. Otherwise, the operator will have to handle more issues in the post-processing phase. Some of these issues are handled through formal processes, e.g., a RUC or the informal process of out-of-market corrections. Furthermore, the operator can potentially aid the order of constraints that are relaxed through the penalty selection as well. If operators are more willing to have line relaxations than node relaxations, then the penalty for the lines should always be lower than the penalty to the nodes. These considerations as well as all of these constraint relaxation practices must be negotiated with stakeholders and participants in the electric energy market.

6. Penalty Price Determination for Thermal Constraint Relaxations

Electric power system operators must manage generation scheduling while considering complex operating requirements and strict physical restrictions in order to ensure reliable supply of electric energy. In market models employed by system operators, approximated system conditions are applied as constraints since exact modeling of every single physical characteristic is not possible even with advanced software and algorithmic performances. However, such approximations can cause model infeasibility; thus, some market models allow certain constraints to be relaxed with penalty prices to cope with model infeasibility, control shadow prices, and obtain possible gains in market surplus. In this chapter, the effect of thermal constraint relaxations including elevated temperatures and associated loss of tensile strength of overhead conductors will be presented. In addition, the systematic methodology to determine penalty prices for thermal constraint relaxations will be proposed along with numerical results.

6.1 Thermal Constraint Relaxations

Instead of strictly adhering to approximate constraints, market operators allow flexibility within optimization models by practicing constraint relaxations. Constraint relaxation treats certain constraints as soft constraints by adding slack variables and penalize them in the objective function. As discussed in Chapter 3, constraint relaxations provide several benefits including possible gains in market surplus, the ability to cope with model infeasibility, and a methodology to manage market prices. In this chapter, only thermal constraint relaxations will be discussed. Thermal constraint relaxation allows a line's flow to exceed its presumed thermal rating, based on a predefined penalty price. Such overloading of the transmission line only occurs when the benefits of the added transfer capability exceed the costs of relaxation captured by penalty costs.

Enabling thermal constraint relaxations limits the shadow prices, the flowgate marginal prices (FMP), of the relaxed constraints. Constraint relaxations obviously influence the FMPs but since the FMPs are also related to the LMPs (and Susceptance prices), the practice of constraint relaxations for thermal line ratings also influences market settlements on a much broader basis, including the financial transmission rights (FTR) market. Since the penalty prices influence the prices used within market settlements, it is important to ensure that the penalty prices are chosen to not cause market inefficiencies and to send inappropriate economic (price) signals to the market. Therefore, proper selection of penalty prices, based on the true cost of violating constraints, is key to practice constraint relaxations.

Intuitively, there is no variable cost, such as fuel costs for generators to generate electricity, to transport electric energy through the line; however, there is a huge investment cost as well as maintenance costs for transmission systems. Market participants who hold rights for physical transmission systems get paid by having such physical assets that enable transportation of electric energy, from different types of market, such as a financial transmission rights (FTRs) market. In such manner, transmission system owners may not

want to take any risk that may result in the loss or deterioration of their assets. This is one main reason why thermal ratings of transmission systems are typically determined conservatively so that transmission systems can be utilized as long as possible. The cost of thermal constraint relaxations can be considered as a risk exposure of a reduced service life that requires additional capital costs.

In order to investigate such risk exposure from thermal constraint relaxations, one needs to analyze a thermal dynamics of the overhead conductors as well as conductor degradation effects due to elevated temperatures. When more electric energy is transported through the line, the line temperature can be elevated. Since most conductors are metal, typically aluminum, elevated temperatures can cause an annealing effect on the aluminum strands that leads to a loss of conductor tensile strength. Such phenomenon is irreversible and accumulative [37]. Also, a transmission line should be replaced if it does not meet the minimum tensile strength requirements. Since line overflow due to thermal constraint relaxation can cause conductor degradations, it makes sense to determine the cost of the thermal constraint relaxation based on possible conductor degradation risks and its associated costs.

In this chapter, detailed effects of thermal constraint relaxations are presented. First, the thermal dynamics of the conductor for estimating the line temperature is introduced. With line temperature information in hand, the effect of high temperature on the conductors is investigated. In addition, the risk-based methodology to determine penalty prices for the thermal constraint relaxations is proposed. While such constraint relaxation practices are not new, limited work has been done to investigate the systematic methodology to determine penalty prices. The goal of this work is to determine penalty prices for thermal constraint relaxations for each line that captures the true cost of violating presumed thermal limits based on risk exposures. The model provides a more logical way to determine penalty prices instead of using arbitrary prices from historical data analysis or stakeholders' agreements, which may not consider the true cost of relaxations. Also, the proposed method provides different penalty prices for each line, which makes more sense because the benefits of relaxing lines may depend on the location of the assets and specific system conditions for each operating period.

The rest of the chapter is organized as follows; Chapter 6.2 discusses impacts of thermal constraint relaxations along with the IEEE standard models to estimate conductor temperature and degradation effects, which are used to capture the associated penalty prices of thermal constraint relaxations. Chapter 6.3 details a risk-based penalty price determination model. Chapter 6.4 gives the numerical results. Lastly, conclusions are presented in Chapter 6.4.

6.2 Thermal Dynamics of Overhead Conductors

Conductor temperature is an essential component of investigating the conductor degradation effect. A combination of heating and cooling energies contributes to the conductor temperature. The main sources of conductor heating are the line flow, radiation

from the sun, and reflection from the surroundings. At the same time, the ambient air temperature, wind speed, and radiation of heat from the conductor incurs cooling effects. These heating and cooling energies should be balanced all the times. A generic representation of the conductor thermal behavior is given in Figure 6.1 [38].

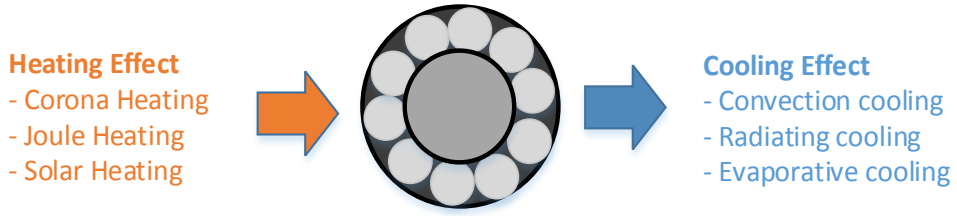

Figure 6.1. Generic representation of the conductor thermal behavior.

However, such quantities vary along the transmission line and are difficult to measure or predict precisely due to the inherent non-linearity of conductor thermal dynamics. IEEE and CIGRE working groups provide conductor temperature prediction models, which utilize the conductor thermal balance characteristic on a unit length of conductor [39]-[40]. This work adopts the IEEE standard model for calculating line temperatures, which also provide a methodology for calculating conductor temperature and thermal capacity. In the IEEE standard model, the heat balance equation in steady states is expressed as follows,

$$Q_c + Q_r = Q_s + I^2R(T_C) \tag{6.1}$$

where, Q_c is forced convection heat loss, Q_r is radiated heat loss, Q_s is solar heat gain, and $I^2R(T_C)$ is joule heating from the line flows at the line temperature T_C. The IEEE standard model ignores the corona heating effect, magnetic heating effect, and evaporative cooling effect, which have little impact on the thermal behavior of the conductor. In addition, this equation normally requires iterative calculations due to its inherent non-linearity, as shown in Figure 6.2.

Convection heat loss mainly depends on wind speed and direction. More winds directed perpendicular to the conductor gives a greater cooling effect. Solar heat gain is estimated based on how much solar energy is available while considering altitude and azimuth of the sun, as well as emissivity and absorptivity of conductor surfaces. Newly installed conductors typically have a lower emissivity and absorptivity whereas old conductors have higher values [37]. Therefore, even with fixed line flow, line temperature can vary based on ambient weather conditions.

There are other conductor temperature prediction models based on different assumptions and complexities. The CIGRE working group has published thermal behavior of overhead conductors in [40], which represents a more theoretically complete heat balance equation with more complexity. Schmidt *et al*. [41] examined the differences between both models in [39] and [40], as well as its impact on the line rating determination. Lastly, W. Z. Black *et al.* [42] proposed a simplified conductor temperature model with the linearized approximation of the radiation term.

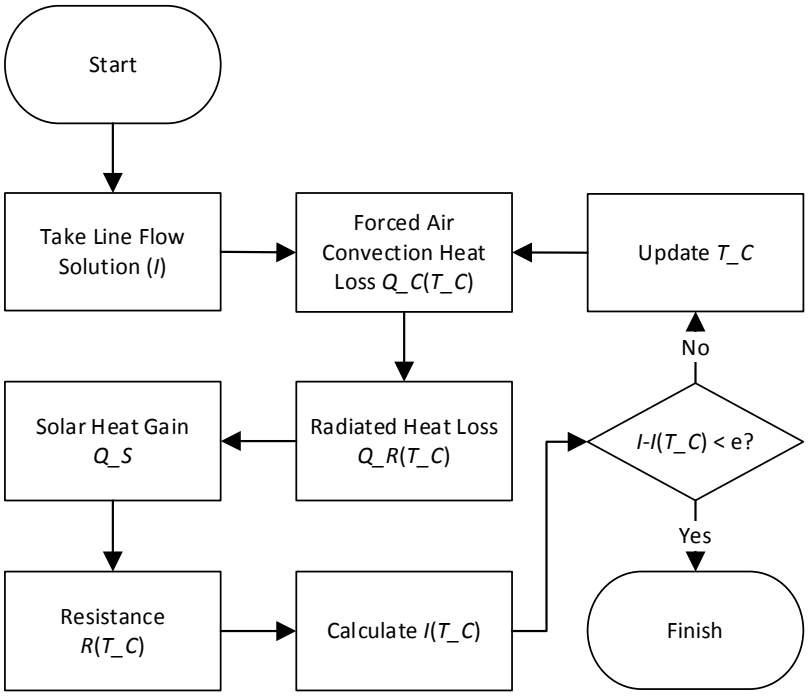

Figure 6.2. Flowchart for calculating conductor temperature.

6.3 Effect of High Temperature Operation on the Overhead Conductor

Material tensile strength of aluminum wires decreases with consecutive operations at elevated temperatures. In addition, the effects of elevated temperature operation on the aluminum conductor are irreversible and the damage experienced by the conductor are also cumulative. Such a loss of tensile strength of a conductor is caused by an annealing effect. Annealing is the metallurgical process whereby applied high temperature softens hardened metal, resulting in a loss of tensile strength. Predicting such loss requires a complex analysis of the metallurgical aspects of the conductor components as well as probabilistic characteristics of ambient factors that may influence the conductor temperature [43]. The key to predict the loss of tensile strength over the expected life of a conductor is to estimate the temperature exposures that may result in annealing. The projected remaining tensile strength of the conductor can be determined based on temperature exposure information.

This work adopts the IEEE standard model [44], which is based on the work by [45], to predict line degradation effect. The standard model calculates remaining tensile strength of the conductor for a given temperature exposure history. The conductor degradation predictor equations for high temperature operation are expressed as follows,

$$RS_{al} = (-0.24T_c + 134)^{-(0.001T_c - 0.095)\left(\frac{0.1}{d}\right)} \tag{6.2}$$

$$if\ (-0.24T_c + 134) > 100, use\ 100\ for\ this\ term \tag{6.3}$$

$$Deg_T = 100 - (RS_{al} * \left(\frac{STR_{al}}{STR_T}\right) + 109\left(\frac{STR_{st}}{STR_T}\right)) \quad (6.4)$$

where RS_{al} is the residual tensile strength of the aluminum strand with a diameter of d, Deg_T is the loss of tensile strength of the whole conductor, and $STR_{al}, STR_{st}, STR_T$ is the initial strength of aluminum strands, steel core, and the whole conductor, respectively. Note that this model is derived for an alloy aluminum conductor steel reinforced (ACSR) conductor.

In this model, line degradation effects mainly depend on the magnitude and duration of temperature exposures. Moreover, the number of aluminum strands and their diameter, the structure of a conductor, such as the number of aluminum layers and the portion of a steel core, are other key factors that influence line degradation effect. The higher number of aluminum strands, which also increases the relative portion of aluminum strands and decreases the portion of a steel core, will cause higher degradation effects for the same temperature exposures, since the impact of the annealing effect that causes loss of tensile strength of aluminum strands is higher and the supportive contribution of the steel core is relatively lower. Typically, steel cores will not anneal at temperatures incurred during steady state operation even for emergency operations of an ACSR conductor. Since ACSR derives about half of its strength from the steel core (depends on conductor size), the degradation effect of the aluminum strands only partially influences the overall conductor tensile strength. The factor 109 in the IEEE standard model accounts for this increased load carried by the steel core. In applying this model, the cumulative strength reduction for multiple exposures at the same conductor temperature can be obtained by simply adding up all the hours and calculating the residual strength. For multiple exposures at different conductor temperatures, all exposures should be expressed as an orderly time series of temperatures and converted to an equivalent duration at the highest temperature. Finally, they can be summed together to determine the cumulative loss of strength. This model may not provide an accurate result for short-term temperature effects.

There is a great deal of associated research regarding conductor loss of strength due to annealing effects. Morgan *et al.* [46] proposed that the percentage reduction in cross-sectional area during wire drawing has more effect on the loss of tensile strength than its diameter. There is no guarantee that a specific method will work perfectly in all cases. Therefore, it would be advisable to analyze different methodologies of predicting line degradation for given situations.

6.4 The Risk-based Penalty Price Determination Model

In this section, a proposed model to determine penalty prices for thermal constraint relaxations based on risk exposures for the line degradation will be introduced. The proposed method can determine penalty prices for each line. Since the benefits of thermal constraint relaxations are influenced by the location of the asset and system operating conditions, it would be more appropriate to set different penalty prices for each line based on expected thermal constraint relaxations and associated degradation risks.

6.4.1 Risk-based Conductor Degradation Model

The conductor degradation effect depends on line temperature exposures. By assuming that market models merely determine generation schedules and line flows, joule heating by line flow is only one variable in the conductor thermal dynamics model in (6.1) when the deterministic weather condition is taken. Reference [47] proposes a thermal constraint relaxation approach combined with the conductor degradation model within the transmission expansion planning, which investigates diverse ways to increase transmission system capacity while preserving right-of-ways. The work takes a renewable integration problem into consideration to evaluate the possible benefits of practicing thermal constraint relaxations in terms of conductor sizing in [48]. The above studies, however, mainly consider deterministic ambient weather conditions and the proposed methodology is not scalable. As mentioned, slightly different ambient weather condition can cause a higher variation of conductor temperatures even with the same line flows. Therefore, it is necessary to investigate a probabilistic approach to analyze conductor temperatures and associated degradation effects. In this paper, conductor degradation risk is quantified based on the expected degradation effect due to constraint relaxations. The risk quantifying is presented in [49].

Two main probabilistic weather conditions considered include ambient temperature and wind speed. The random behavior of air temperature and wind speed are modeled as a Normal and Weibull distribution, respectively in (6.5)-(6.6). The joint distribution of ambient weather condition z is the product of the distribution functions (6.5)-(6.6) as in (6.7) when the correlation between each other is ignored.

$$Pr(T_a|\mu,\sigma) = \frac{1}{\sqrt{2\pi\sigma^2}} e^{-(T_a-\mu)^2/2\sigma^2} \tag{6.5}$$

$$Pr(W_s|\gamma,\beta) = \frac{\gamma}{\beta} W_s^{\gamma-1} e^{-W_s{}^{\gamma}/\beta} \tag{6.6}$$

$$Pr(z) = Pr(T_a) * Pr(W_s) \tag{6.7}$$

Here, μ, σ, γ, and β are the scale and shape parameters, which can be estimated by point estimation for both distributions. Conductor degradation risk can be expressed based on the joint distribution of ambient weather condition and system operating conditions as follows,

$$Risk(X_k) = E_{z\in Z}\big(Im(Y(z)|X_k)\big) = \sum_{z\in Z} Pr(Y(z)|X_k) * Im(Y(z)|X_k) \tag{6.8}$$

where $E_{z\in Z}\big(Im(Y(z)|X_k)\big)$ is the expected conductor degradation impact of the operating condition X_k and the conductor temperature states $Y(z)$ within weather condition $z \in \{z_1, .., z_n\}$ for each line k.

Lastly, conductor degradation cost can be calculated by assuming the specific conductor tensile strength requirements. In this work, it is assumed that a conductor should be replaced when it reaches 10 % loss of tensile strength. Reconductoring costs are assumed by considering conductor material and labor costs; however, the out-of-service cost during

the reconductoring period is not considered. The expected degradation cost due to constraint relaxation can be obtained as follows,

$$Cost(X_k) = Risk(X_k) * C_k^{end}. \quad (6.9)$$

6.4.2 Risk-based Penalty Price Determination

In the proposed risk-based penalty price determination model, it is assumed that the generators' commitment schedules are predetermined and all the necessary adjustments have already been properly conducted. In addition, the model assumes that thermal constraint relaxation has been allowed in the real-time SCED. The flowchart of the proposed model to determine penalty prices for thermal constraint relaxations is presented in Figure 6.3. The SCED model is solved with thermal constraint relaxations using initial penalty prices and predetermined commitment schedules. The risk-based conductor degradation model provides the expected conductor degradation costs based on line flow information and probabilistic weather conditions. By comparing the estimated degradation cost from penalty prices in the SCED solution and the actual expected degradation cost, the model updates penalty prices such that the total system wide gap between estimated and expected cost can be decreased at each iteration until the gap falls into the presumed termination criterion. A sub-gradient method is employed to update penalty prices.

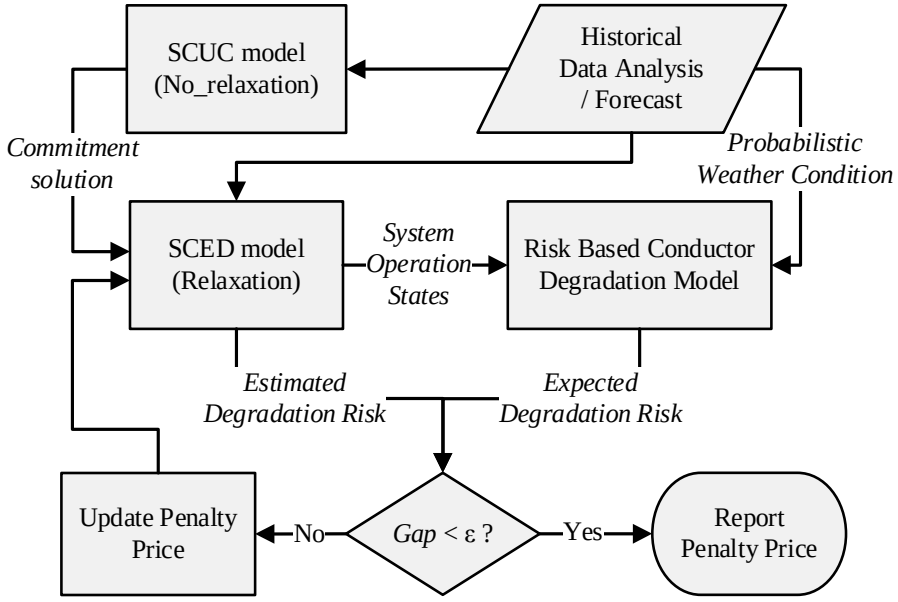

Figure 6.3. Flowchart of the risk-based penalty price determination model.

The proposed method anticipates system operating conditions and estimates thermal constraint relaxations over the presumed time period. The expected degradation effect is determined based on the specific time horizon. When considering a longer time period, the associated degradation effect may be increased since such phenomena are accumulative; however, it may not be appropriate forecast too much unless future system operating conditions can be forecast with high confidence. On the other hand, considering a very

short time period may not give proper degradation information since short-term overloading may not cause conductor degradation, even if there were an annealing effect and resultant loss of strength on the aluminum strands themselves, but the overall conductor may not be vulnerable to the degradation effect. Therefore, it is important to determine the appropriate time horizon to determine penalty prices. In this work, one year of operation has been chosen for the time period. In addition, the penalty price has been chosen such that accumulated penalty costs over the presumed period can be closer to the actual expected degradation cost insofar as possible. However, there is no guarantee that penalty prices determined by the proposed method will exactly capture the expected degradation cost in real operations. Nevertheless, the proposed method is a systematic approach to determine the true cost of thermal constraint relaxation on the off-line study. Also, it is always possible to adjust penalty prices based on system operation results analysis as well as conductor temperature or degradation information. Lastly, for the lines that are not congested, market operators can set the highest penalty prices for lines that has same conductor types in order to control FMPs as well as keep them operating within presumed line ratings.

6.5 Numerical Results

6.5.1 Simulation Premise

The simulation is performed on the modified IEEE 96-bus Reliability Test System (RTS), which is publicly available from [32]. The transmission capacity of the original system is redundant; therefore, system modifications need to be made to carry out further studies such that thermal constraint relaxations can be practiced. Four types of ACSR conductors include Raven, Penguin, Pelican, and Parakeet are selected based on the original line ratings. The Penguin conductor is used for de-rated lines that connects node 114-116, 214-216, and 314-316, respectively. Table 6.1 presents the electrical characteristics [50] and capital cost of these conductors [51]-[52]. Conductor rating is calculated based on the IEEE standard [44] such that Rate B is determined at the line flow that causes line temperature of 85 °C. Rate A is assumed to be 75 % of Rate B and Rate C is the line flow at 100 °C. The deterministic weather condition parameters from [44] are used for line rating determination as presented in Table 6.2. The probabilistic weather condition is obtained according to 5 years of historical data of Arizona State, US [53]. The mean and standard deviation of air temperature and wind speed are listed in Table 6.3. Testing is performed using the Java callable library of CPLEX 12.6 on an Intel® Xeon® 3.60 GHz CPU with 48GB memory. The risk-based penalty pricing model is terminated upon reaching a gap of 0.5 %.

Table 6.1. Conductor data for RTS-96.

	Raven	Penguin	Pelican	Parakeet
Structure	6/1	6/1	18/1	24/7
Rate A(MW)	160	247	433	483
Rate B(MW)	214	330	578	645
Rate C(MW)	241	370	667	744
Capital Cost (M$/mile)	0.84	0.87	0.91	0.94
End-of-service Cost(M$/mile)	0.29	0.30	0.32	0.34

Table 6.2. Deterministic weather conditions for determining line ratings.

Wind Speed	2 *ft*/*s*	Emissivity	0.5
Wind Angle	45 °	Absorptivity	0.5
Ambient Temperature	35 °C	Solar Time	12:00 PM
Elevation	150 *ft*	Atmosphere	Clear
Latitude	38.5 °	Line Direction	North-South

Table 6.3. Statistics of ambient weather conditions.

	Mean	Standard Deviation
Air Temperature	21.4	10.5
Wind Speed	6.3	4.5

6.5.2 Analysis Design

First, the SCUC model without constraint relaxation is solved for the entire year with Rate B as line ratings. Subsequently, generator commitment schedules are fed into the SCED model with and without constraint relaxations. For the SCED problem with relaxations, the line ratings are de-rated to Rate A, but thermal constraint relaxation is allowed for penalty prices. The purpose of such an analysis setting is to show the possible benefits of thermal constraint relaxations with a proper penalty price selection that captures the true cost of relaxations. For example, a line's steady-state capacity may be set at Rate B even though there are degradation risks when the line operates above Rate A. Therefore, it is possible to set the steady-state rating at Rate A, but still allow the line's flow to be relaxed based on the penalty prices that can capture the true cost of thermal overloading. Such practices do not reduce system reliability, but rather enhance the utilization flexibility of the transmission system.

6.5.3 Penalty Price Determination

In the modified test system, a total of three lines are congested. The proposed model finds penalty prices for these lines such that estimated degradation cost, the whole collected penalty cost over the year, is closer to the actual expected degradation cost as much as possible within the forecasted system operating conditions. Table 6.4 presents determined penalty prices for lines that are congested and associated expected degradation effects.

Table 6.4. Determined penalty prices and corresponding expected degradation effects.

Line Number	25	65	104
Conductor Type	Penguin	Penguin	Penguin
Location	114-116	214-216	314-316
Penalty Price ($/MWh)	0.66	12.18	8.45
Expected Degradation Effect (%)	0.004	0.091	0.063

The result shows that the relaxation benefit of line 25 is relatively smaller than the other two lines; therefore, fewer line relaxations are expected that lead to a lower degradation effect as well as lower penalty prices. The proposed model assumes that line relaxations are allowed. Penalty prices are determined based on this assumption and an attempt to collect appropriate amount of charges, from the overall market, in order to reimburse transmission system owners for the risk exposure and potential degradation impacts on the transmission lines. Hence, a lower penalty price infers that lower degradation effects are

expected (less compensation is needed) and it is not necessary to set a higher penalty price for that line (for the same relative overload). Even with such lower penalty prices, relaxations will not occur very frequently. If the relaxations do occur too frequently, then adjustment to the penalty prices would be needed to ensure there is not excessive overloading that can cause more degradation than anticipated by the determined penalty price. Figure 6.4 shows the convergence result of the proposed model.

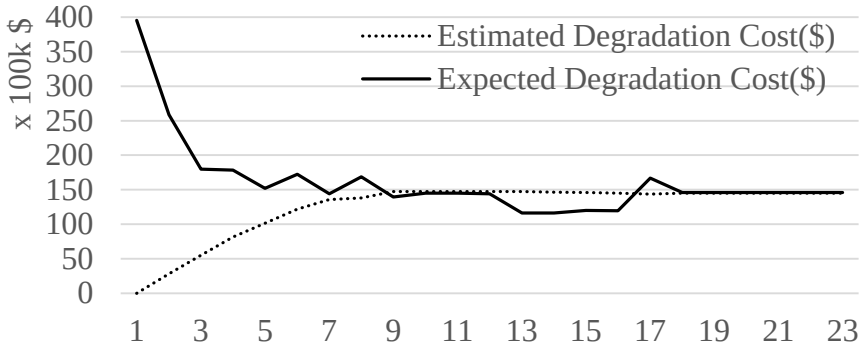

Figure 6.4. Convergence result for the penalty price determination.

6.5.4 Line Relaxations

Figure 6.5 presents a line flow histogram for the congested three lines. The results for non-relaxed cases show that even with exactly the same conductor type, congestion frequency is different based on the location of the line. In addition, when the lines are relaxed, one can see that relaxations do not always occur because the benefits of relaxations are not always greater than penalty prices. Line 24 is less congested in the non-relaxed case and its thermal rating is not violated as much in the relaxed case even when the penalty price for this line is relatively small.

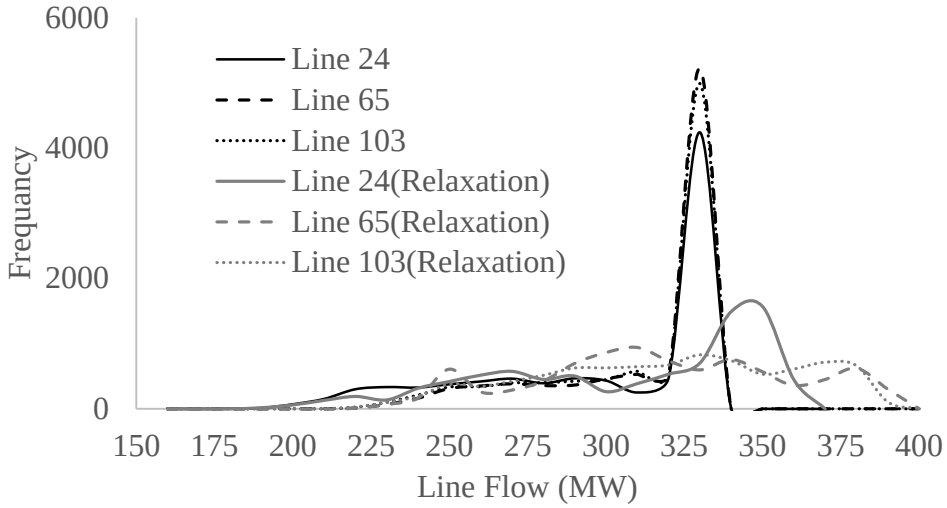

Figure 6.5. Line flow results for the congested lines with and without relaxation.

6.5.5 Market Settlements

When comparing market settlements, the constraint relaxation provides about 1.85 % of total system cost savings in comparison to the non-relaxed case over the entire year. This result is expected when constraint relaxations are employed. Other settlements also had deviations in the relaxed case compared to the non-relaxed case. One notable aspect is that generators were receiving higher revenue and profit through the entire year. Instead of having a few extreme prices, the constraint relaxation made it such that the overall payment to the generators, collectively, increased. For instance, some generators that were cheaper were not fully dispatch due to congestion and, hence, they were setting the price. With the constraint relaxation practices, the marginal units (on average) were generators with higher costs. With higher payments being allocated to generators in the relaxed case, consumer payments are reduced. Note that, while the overall system cost is lower, there is no guarantee that LMPs will decrease and there is no guarantee that the overall load payment will be lower. Nevertheless, in this case study, the average LMPs have decreased by 9 % in the relaxed case as well. Lastly, the congestion rent is significantly decreased in the relaxed case, which is the difference between the amount paid by consumers and generators' revenue. The congestion rent is used to fund the FTR market, where market participants purchases FTRs to hedge against price risk due to congestions. As mentioned, thermal constraint relaxation limits FMPs as well as LMP gaps between nodes that are connected by the transmission lines as presented in Table 6.5. Therefore, by limiting FMPs, congestion rent is limited as well. All of these settlements can be compared in Table 6.6 and Figure 6.6.

Table 6.5. Market prices comparison.

Line Number	25	65	104
LMP Gap (No Relaxation, Mean)	7.4	25.7	21.9
LMP Gap (Relaxation, Mean)	0.3	7.7	5.4
FMP (No Relaxation, Mean)	11.3	35.5	31.9
FMP Gap (Relaxation, Mean)	0.6	11.2	7.8

Table 6.6. Market settlements ($M).

Model	Total cost	Gen. revenue	Gen. profit	Gen. uplift	Load payment + uplift	Congestion Rent
No Relaxation	478.5	881.4	431.2	28.3	1,142.2	232.4
Relaxation	469.8	909.6	476.0	36.2	1,000.6	54.7

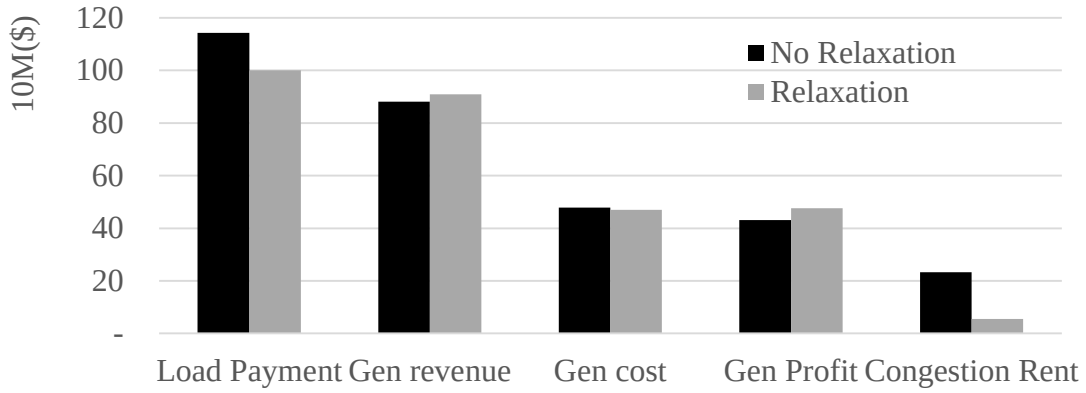

Figure 6.6. Market settlement results.

6.6 Summary

Power system operators must account for all the complex operating and reliability requirements inherent in the power systems. However, market models cannot fully capture all the complexities of the power system, although they have improved algorithmic performance. Thus, diverse approximated system conditions are employed as constraints in the market models, which can cause the market models to be infeasible. System operators employ constraint relaxation practices that allow certain constraints to be relaxed for predetermined penalty prices. Constraint relaxations also give operators a method of shadow price control and possible gains in market surplus. Therefore, proper selection of constraints that are to be relaxed and the determination of their penalty prices based on the true cost of violating specific constraints is key to implementing constraint relaxations.

In this chapter, a risk-based methodology to determine penalty prices for the thermal constraint relaxation is proposed. The proposed model can determine penalty prices for thermal constraint relaxations that captures the true cost of violating presumed thermal limits, based on the probabilistic line temperatures and associated line degradation risk exposures. Even when penalty prices for constraint relaxation practices are negotiable with market participants, the proposed model provides a more logical way to analyze the true cost of relaxing thermal constraints. Simulation results show that all market participants can achieve benefits by practicing thermal constraint relaxations with a proper selection of penalty prices.

7. Constraint Relaxations Impacts on Power System Performance

7.1 Introduction

Constraint relaxations, by definition, mean that certain security or operational constraints are allowed to be violated in the energy market models for a pre-determined penalty price. Some of these relaxations are physically unrealizable, such as the node balance constraint. Other relaxations, however, are physically achievable, such as branches thermal limits and, therefore, could appear in the AC real-time system as actual violations. Even physically unrealizable relaxations could appear in the real-time system as violations in other forms since these relaxations are a form of approximation. Therefore, in order to assess the true risk associated with allowing certain constraints to be relaxed, the impact of these relaxations on real-time system performance was investigated. Capturing the impact of constraint relaxations on real-time system performance provides operators with a better understanding on how relaxations in the energy market models are translated into physical violations. This information can be used not only to assess the criticality of constraint relaxations, but also as a basis for determining penalty prices more accurately. In this chapter power system performance criteria are presented and defined. The methodology of the analysis is discussed followed by the results. The last section summarizes this part of the work.

7.2 Power System Performance Definition

This section is devoted to defining the aspects of power system performance and discussing the relationship between them. Power system performance is defined by the following concepts:

- Reliability: NERC (North American Electric Reliability Council) defines power system reliability as: “the degree to which the performance of the elements of that system results in power being delivered to consumers within accepted standards and in the amount desired. The degree of reliability may be measured by the frequency, duration, and magnitude of adverse effects on consumer service” [54]. Hence, power system reliability can be regarded as the probability of satisfactory operation over an extended time period.
- Security: power system security is related to the robustness of the system following imminent disturbances (contingencies). NERC defines power system security as the degree of risk in the power system ability to withstand sudden disturbances such as short circuit faults or the loss of major components, without interruption of customer service. Security, therefore, depends on the system operating conditions as well as the probability of contingent events [55].
- Stability: power system stability can be defined as “the ability of an electric power system, for a given initial operating condition, to regain a state of operating equilibrium after being subjected to a physical disturbance, with most system variables bounded so that practically the entire system remains intact” [55]. Power

system stability depends on the severity and the physical nature of contingent events as well as the system operating conditions.

Power system performance aspects (reliability, security, and stability) are interrelated as all of them refer to system robustness and satisfactory operation. For instance, a power system cannot be considered reliable if it is insecure and it cannot be considered secure if it is unstable. Hence, reliability is the overall objective in power system planning and operation because it spans long period of time and comprises all other aspects. The distinction between power system security and stability is that security is more general, as it factors in the probability of contingent events. Power system security also counts for contingencies that are not classified as stability events, such as equipment failure or sabotage. Power system security also considers post-contingency operating conditions, such that a system could be stable following a contingency but insecure due to post-contingency overloads or voltage violations.

7.3 Voltage Stability

7.3.1 Overview

This section provides a brief overview of power system stability in general as it is the basic building block in assessing system security and reliability. For the purpose of this study, a detailed discussion on voltage stability is provided herein since test cases with constraint relaxations have significantly more voltage violations compared to non-relaxed cases. Power system stability can be classified into three main categories according to their physical nature [56]:

- Rotor angle stability: this type of stability is related to the ability to maintain or restore equilibrium between mechanical torque and electric torque in synchronous machines following a disturbance. Consequently, instability in this regard refers to growing deviation or oscillation of one machine with respect to other machines, resulting in loss of synchronism.
- Voltage stability: the ability of a power system to maintain steady and acceptable voltages at all buses in the system under normal operating conditions after being subjected to a disturbance.
- Frequency stability: refers to system ability to maintain or restore its frequency within an acceptable range following a major disturbance. Frequency stability is related to the equilibrium between generation and load throughout the system. Frequency instability usually appears as sustained frequency swings resulting is generation and/or load loss.

Disturbances could be large, such as major transmission faults, generating unit tripping, loss of major components or small, such as a gradual change in load. Voltage instability occurs when one bus or more in the system suffers from progressive and uncontrolled change in the voltage magnitude, usually in the form of voltage decrease. Voltage instability can cause prolonged periods of voltage depression conditions (brownout), or

even a voltage collapse and blackout, depending on the available reactive power and load dynamics. Although voltage instability is essentially a local phenomenon, voltage collapse, which is more complex than simple voltage instability and is usually the result of a sequence of events, is a condition that affects large areas of the system [57].

Rotor angle stability had been the primary aspect of stability studies for decades. However, recent events of abnormal voltage magnitudes and voltage collapse incidents in some large interconnected power systems have sparked an interest in the voltage stability phenomenon [58]-[59]. Rotor stability was believed to be responsible for voltage instability conditions. This case is true since a gradual loss of synchronism between two groups of machines as their rotor angles approach or exceed 180° would result in very low voltages at intermediate points in the network. However, this is not the case if the disturbance was close to load centers and the voltage depression was rather caused by reactive power deficiency and/or load dynamics. Therefore, voltage instability may occur when rotor stability is not an issue. Actually, sustained voltage instability conditions can cause rotor instability.

Several recent factors and operating conditions have also caused the voltage instability problem to become more prevalent, such as [60]-[61]:

- Power systems in general and specifically transmission lines tend to be operated under more stressed conditions. These stressed operating conditions are not only due to continuous and significant load growth, but also because of major changes and restructuring of energy markets, as well as unconventional practices such as constraint relaxations. Stressed transmission lines have less capability of delivering reactive power to demanding load centers because of the high reactive power losses. Transmission lines (especially long ones) with a relatively large voltage angle difference between sending and receiving ends also have limited capability of reactive power delivery.
- High rates of induction and single phase motor penetration, especially those used in air conditioning systems, heat pumps and refrigeration. These motors are known as low inertia machines. As a result they have fast response to disturbances and can decelerate or even stall rapidly. Voltage instability issues are directly affected by dynamic behavior of motors.
- Excessive reliance on shunt connected capacitor banks for reactive power compensation. In heavily shunt capacitor compensated systems, the voltage regulation tends to be poor. Another disadvantage for shunt capacitors is that the reactive power support they provide is directly proportional to the square of the voltage. Therefore, at low voltages when the reactive power support is most needed, the VAr output of the capacitor banks drops.
- High penetration of electronic loads which have significant discontinuous response to variations in voltage magnitude.
- The use of HVDC tie lines to transfer large amounts of electric power. The convertors associated with these lines consume significant amounts of reactive power.

7.3.2 Voltage Stability Classification

It is useful to classify voltage stability into subclasses in order to better understand system behavior under voltage instability conditions. Classification also helps choose the right analytical strategies depending on the nature of phenomenon of interest. Voltage stability is classified here according to the magnitude of the disturbance affecting the system into two subclasses:

- Small disturbance voltage stability: also called small-signal or steady-state voltage stability. This type of voltage stability is related to small and possibly gradual perturbations in the system, such as small changes in the load. Small-signal stability is determined by the characteristics of load and continuous and discrete controls at a specific instant of time. A criterion for this type of voltage stability is that at a given operating condition, for every bus in the system, the bus voltage magnitude increases as the injected reactive power at the same bus is increased. When analyzing small disturbance voltage stability, usually either midterm (10 seconds to few minutes) or long-term (few minutes to tens of minutes) studies are performed.
- Large disturbance voltage stability: also called transient voltage stability. Large disturbance here refers to major changes in operating conditions. These changes could be major faults on transmission lines, generating units tripping, transmission lines tripping, or other large disturbances. The transient voltage stability is determined by the load characteristics, continuous and discrete controls, as well as the protection systems. However, in order to capture the nonlinear dynamic interactions between the different system components and their effect on transient voltage stability, a dynamic time domain analysis should be performed. This type of analysis is referred to as short-term voltage stability analysis (0 to 10 seconds). A criterion for large disturbance voltage stability is that following a large disturbance and after the actions of system control devices, voltages at all buses reach acceptable steady state levels.

7.3.3 Voltage Stability Analysis

From the previous discussion, it is apparent that each type of voltage stability has its own characteristics and nature; therefore, each type has to be approached and analyzed using the appropriate analytical tool. In general, voltage stability problems are studied using two approaches [56], [61]:

- Static analysis
- Time domain dynamic analysis

Static analysis studies are used for steady state voltage stability problems initiated by small disturbances. The system dynamics affecting voltage stability in the event of small disturbances are usually quite slow and much of the problem can be effectively analyzed using the static approaches that examine the viability of a specific operating point of the

power system. Power flow is used for this type of study, where snapshots are captured from different system conditions at certain time instants. At each of these time frames, system dynamic equations are linearized, and time derivatives of the state variables are assumed to be zero, while state variables take their numerical values at that time instant. Therefore, the resultant system equations are simple algebraic equations that can be solved using power flow simulation. Static analysis can be performed faster than dynamic simulations and need fewer modeling details. However, with the presence of fast acting components such as motors, and solid state devices (such as HVDC convertors), the dynamic effect and the interactions between controllers and protection systems must be included in the voltage stability analysis to capture the actual behavior of the system.

Steady state static studies are not only useful in the determination of the voltage stability of a given operating condition, but they also provide information about the proximity of these conditions to voltage instability as well as voltage sensitivity. Static analysis has been solved by different approaches [56], [62]:

Q/V sensitivity analysis: The linearized region provided by power flow analysis around a given point is used to indicate the relation sensitivity between the voltage and reactive power. This sensitivity is described by the elements of the Jacobian matrix. The power equations (polar form) for any node *i* can be written as,

$$S_i = P_i + jQ_i = V_i I_i^* \tag{7.1}$$

where S_i, P_i, Q_i are the complex, real and reactive power injections at bus *i* respectively. The term V_i is the bus voltage, and I_i^* is the conjugate current injected at bus *i*.

Power flow equations (real form) of bus *i* with respect to the rest of the system are written as,

$$P_i = V_i \sum_{m=1}^{n} (G_{im} V_m cos\theta_{im} + B_{im} V_m sin\theta_{im}) \tag{7.2}$$

$$Q_i = V_i \sum_{m=1}^{n} (G_{im} V_m sin\theta_{im} - B_{im} V_m cos\theta_{im}) \tag{7.3}$$

where *G* and *B* are the real and imaginary parts of the admittance matrix, respectively. θ_{im} is the voltage angle difference between buses *i* and *m*. The Jacobian matrix is used to achieve the following linearized form,

$$\begin{bmatrix} \Delta P \\ \Delta Q \end{bmatrix} = \begin{bmatrix} J_{P\theta} & J_{PV} \\ J_{Q\theta} & J_{QV} \end{bmatrix} \begin{bmatrix} \Delta\theta \\ \Delta V \end{bmatrix} \tag{7.4}$$

where, $\Delta P, \Delta Q, \Delta\theta, \Delta V$ are the incremental changes is bus real power, reactive power injection, voltage angle and voltage magnitude, respectively. Although system stability is affected by real power, it is possible to keep *P* constant in order to evaluate the sensitivity only between the reactive power and voltage magnitude. Therefore, by setting $\Delta P = 0$,

$$\Delta Q = J_R \Delta V \tag{7.5}$$

where J_R is the reduced Jacobian matrix of the system and can be written as,

$$J_R = [J_{QV} - J_{Q\theta} J_{P\theta}^{-1} J_{PV}]. \quad (7.6)$$

The *Q/V* sensitivity at a bus represents the slope of the *Q/V* curve at a given operating point. A positive value for the sensitivity indicates stable conditions. The larger the sensitivity index, the closer the operating point is to instability. The value of infinity represents stability limit or the critical point. Negative values for sensitivity indicate unstable conditions, with very small negative values representing highly unstable conditions.

Q/V modal analysis: This analysis approach has the advantage of providing the mechanism of instability at the critical point. The eigenvalues and eigenvectors of the reduced Jacobian matrix are evaluated and used to indicate voltage stability. Positive eigenvalues represent stable voltage conditions, and the smaller the magnitude, the closer the relevant modal voltage is to being unstable. Compared to *Q/V* sensitivity analysis, *Q/V* modal analysis is more capable of identifying the critical voltage stability areas and elements that participate in each mode once the system reaches the critical voltage stability point; hence, *Q/V* modal analysis can describe the mechanism of voltage instability. *Q/V* sensitivity analysis is not able to identify individual voltage collapse modes; instead it only provides information regarding the combined effects of all modes of voltage-reactive power variations.

Q/V curve analysis: *Q/V* curves show the relationship between the reactive power support at a certain bus and the voltage of that same bus. For large power systems these curves are obtained by a series of power flow simulations. A fictitious synchronous condenser with unlimited reactive power capability is placed at the test bus and the voltage magnitude is varied through the simulation [63]. *Q/V* curves are useful in determining the amount of reactive power needed to be injected at a certain bus in order to obtain a desired voltage level. Therefore, these curves can be used for both voltage stability indication purposes and shunt compensation sizing. However, it should be noted that *Q/V* curves are only valid for steady state analysis [57]. It should also be noted that power flow equations tend to diverge around the voltage stability critical point; therefore, special techniques have to be used to overcome the divergence problem, such as continuation power flow.

Dynamic analysis provides the most accurate results for voltage stability phenomenon using time domain simulations which capture the real dynamic nature of the system without any approximations. Nonlinear dynamic simulation is, therefore, very useful and effective for short term voltage stability studies and fast voltage collapse situations following large disturbances. However, as a price for this accuracy, dynamic simulations are much more complicated than static studies since the overall system equations include first-order differential equations that have to be solved as well as the regular algebraic equations. Solving these equations requires significant computational capacity and is relatively time consuming. The accuracy of dynamic simulation results depends mainly on the models used; therefore, system components have to be modeled in detail and with high accuracy. The system set of differential equations can be expressed as follows,

$$\dot{x} = f(x, V) \quad (7.7)$$

and the set of algebraic equations as,

$$I(x, V) = Y_N V \tag{7.8}$$

where x: state vector of the system, V: bus voltage vector, current injection vector, Y_N: bus admittance matrix and (x_o, V_0) are the initial conditions.

Although no expression for time appears explicitly in the previous equations, Y_N is a function of both voltage and time since certain time varying components such as transformer tap changer, phase shift angle controls, and topology are included in it. Also, the relation between I and x can be a function of time. Numerical integration alongside power flow analysis is usually used to solve the nonlinear dynamic equations in the time domain.

7.4 Power System Performance Analysis and Results

In this section, a detailed description of the test cases used to conduct this work is provided. Also the analysis methodology used to investigate the impact of constraint relaxations on real-time system overall performance along with the results are presented.

7.4.1 Test Case Description

In order to capture the direct effect of constraint relaxations on system security and reliability as well as on related energy market aspects, the constraint relaxations process practiced by system operators was replicated using two test cases: the RTS-96 test case [32] and the PJM system. The RTS-96 test case was chosen for this part of the analysis because of the significant number of generators in this test case, which provide a suitable platform for studies related to this type of work such as security constrained unit commitment (SCUC), security constrained economic dispatch (SCED) and optimal power flow (AC OPF and PSCOPF). The RTS-96 test case is comprised of three identical areas where each area is connected to the other two areas (ring configuration). Table 7.1 shows the overall RTS-96 test case components.

Table 7.1. RTS-96 system components.

Component	Number
Areas	3
Buses	73
Generators	99
Shunts	3
Lines	104
Transformers	16
Load Aggregations	51
Max. Load (MW)	9405

The PJM test case is a large-scale real-life system. PJM provided hourly detailed power flow and dynamic data for one week in July 2013. The provided data includes PJM control

areas as well as the neighboring areas. Representing neighboring areas is required in this type of analysis in order to capture the power transfers between PJM control areas and other areas, as well as the dynamics of neighboring areas that could affect PJM control areas. PJM also provided their market data for that week, which was used in this work to obtain market solutions based on realistic and practical bidding data. Table 7.2 lists the overall components of PJM control areas as well as the neighboring areas. It should be noted here that the topology of the PJM test case changes from one time period to another.

Table 7.2 PJM system components (peak hour).

Component	PJM	Neighboring Areas
Areas	24	24
Buses	10150	5128
Generators	1682	1185
Shunts	810	786
Lines	8653	5899
Transformers	4201	1999
Load Aggregations	8101	3764
Max. Load (MW)	144340	134974

For each test case, market SCUC solutions were obtained and used as starting points to represent the AC real-time system. This process was conducted twice, once with no constraint relaxations, and another time allowing certain constraints to be relaxed. This approach facilitated the comparison process between the two different scenarios while ensuring high consistency between them. PSS/E ACOPF was used in order to attain a base-case AC feasible solution that is as close as possible to the market solution. Therefore, the same economic data and constraints used in the energy market models were used in ACOPF. Running ACOPF provided an accurate and consistent transition from the dispatch schedules generated by the DC market models to an AC feasible solution. Losses were distributed in an economic manner rather than being picked up by the slack bus and other controls, such as scheduled voltages, transformers tap settings, and switched shunts, were adjusted optimally.

The output of ACOPF is a base-case AC feasible system. However, this is not always the case because some cases needed out-of-market corrections to overcome AC infeasibility. Usually AC infeasibility is voltage related since voltage and reactive power are not represented in energy market models. In order to achieve AC feasibility with the least number of out-of-market corrections, a limited number of generators were turned on in areas that were causing infeasibility. It should be noted here that more out-of-market corrections were needed for cases with constrain relaxations. This can be explained by the lower number of committed generating units compared to cases with no constraint relaxations that resulted in less reactive power availability. In order to assess the impact of constraint relaxations on overall system performance, several static and time-domain studies were conducted, as will be presented in the following discussion.

7.4.2 Static Analysis and Results (RTS-96)

Since the goal here is to capture the impacts of constraint relaxations on real-time system performance, constraint relaxations that are physically realizable were allowed to appear as actual violations in the AC system. This approach also ensured that the cases with relaxed constraints have the least amount of out-of-market corrections and are as close as possible to market SCUC solutions. However, for cases that do not have constraint relaxations, PSS/E ACOPF and PSCOPF were both used to obtain AC feasible base-case and post-contingency solutions. This has resulted in feasible and *N*-1 secure cases that were used as benchmarks to compare with corresponding cases with relaxed constraints. Static analysis was used to investigate base-case and post-contingency line flows and bus voltage violations. Table 7.3 lists the market relaxations and their corresponding violations in the AC real-time system.

Table 7.3. RTS-96 AC line flow violations.

Time Period	Relaxed Line Number	DC Flow % (Market Solution)	AC Flow % (Real-time Solution)
7	65	110.3%	116.9%
	104	104.5%	108.2%
8	104	105.0%	111.0%
22	25	103.2%	105.1%
23	65	108.3%	115.8%
	104	105.4%	110.8%

From Table 7.3, it can be seen that all line flow relaxations in the market solution have appeared as actual flow violations in the AC real-time system. It can be also noticed that the AC violations are higher in magnitude than corresponding market relaxations. Discrepancy between DC and AC solutions is expected since the DC market solution is approximate. For instance, reactive power flow and thermal losses are not represented in the DC market model and, therefore, line flows are most likely to be higher in the AC system. However, this is not always the case. In large scale complicated cases, the relationship between DC and AC line flows cannot be deduced intuitively as will be shown in PJM test case.

Table 7.4 shows the number of voltage violations in the relaxed cases shown in Table 7.3. A bus voltage is considered in violation if it falls outside the tolerance range of 0.95 – 1.05 p.u. It also shows the number of committed generators for the relaxed cases and the corresponding non-relaxed cases. The number of additional generators needed to make the non-relaxed market solution feasible and *N*-1 secure is also displayed; hence, no voltage violations are present.

From Table 7.4 it can be seen that the cases (time periods) with more relaxations (7 and 23) tend to have more voltage violations compared to cases with fewer relaxations. It can also be noticed that relaxed cases usually have fewer number of committed generators

compared to cases with no relaxations, which explains voltage violations due to reactive power deficiency. It should be noted here that all voltage violations listed in Table 7.4 are low voltage violations.

Table 7.4. RTS-96 voltage violations and out-of-market corrections.

Time Period	Relaxed		No Relaxations	
	Committed Generators	Voltage Violations	Committed Generators (Market)	Added Generators (out-of-market)
7	56	6	58	4
8	64	5	65	1
22	63	2	63	0
23	55	6	59	1

From the results in Table 7.3 and Table 7.4, it is apparent that cases with relaxed constraints sustained both line flow and bus voltage violations in the base-case. The next and final step in RTS-96 static analysis is to investigate the impact of constraint relaxations on post-contingency line flow and bus voltage violations. The post-contingency operating conditions were determined by running a full-blown *N*-1 contingency analysis. Post-contingency analysis was conducted for cases with constraint relaxations and for their corresponding non-relaxed cases. Table 7.5 summarizes the post-contingency results.

Table 7.5. RTS-96 post-contingency violations.

Time Period	Relaxed		
	Voltage Violations	Line Flow Violations	Unsolved Contingencies
7	62	13	9
8	14	9	5
22	26	7	1
23	22	8	15

For post-contingency analysis, the bus voltage tolerance range is 0.90 – 1.10 p.u. Also, line emergency thermal limits (Rate-C) were used. As can be seen in Table 7.5 there are a significant number of post-contingency violations and therefore the relaxed cases are not secure without out-of-market corrections. Unsolved contingencies indicate that the power flow for some contingencies was not successfully solved, usually because of reactive power mismatches. Consequently, there were additional violations that were not reported due to those unsolved contingencies. Additionally, special attention was given to the relaxed lines, i.e., the lines with AC line flow violations in the base-case, since those lines were already overloaded. Table 7.6 shows the post-contingency power flow on those relaxed lines.

Table 7.6 shows that the relaxed lines were vulnerable to high flow violations following certain contingencies. Similar to Table 7.5, emergency thermal limits are used in Table 7.6,

which also lists the flows on the same lines for cases with no relaxations. As expected, there were no post-contingency violations for those cases since they were *N*-1 secured.

Table 7.6. RTS-96 post-contingency relaxed lines flows.

Time Period	Relaxed Line Number	Post-contingency AC Flow %	
		Relaxed	No Relaxation
7	65	103.0%	98.7%
	104	115.6%	96.8%
8	104	116.6%	94.5%
22	25	109.5%	100%
23	65	103.2%	99.3%
	104	118.0%	99.9%

7.4.3 Dynamic Analysis and Results (PJM)

Following the RTS-96 test case static analysis, the dynamic behavior of the relaxed cases was investigated and compared to corresponding cases with no relaxations. The original RTS-96 dynamic data only consisted of classical machine models. Therefore, realistic and detailed dynamic data was created and used for this analysis. The detailed dynamic data included synchronous machine models, exciter models and governor models. Each generator size and type were considered throughout this dynamic modeling process. Time periods 8 and 23 were chosen for this analysis since the post-contingency line flow violations were the highest in those time periods as shown in Table 7.6. The sequence of contingent events was started by placing a three-phase fault at one terminal of the line that corresponds to the contingency causing the relaxed lines to be overloaded. After 5 cycles the fault was cleared and the first line was tripped. After one second, the overloaded relaxed line is tripped. This sequence of events represents an *N*-1-1 contingency. The same process was repeated for the non-relaxed cases and rotor angles of the most affected generators were plotted and compared. Figure 7.1 and Figure 7.2 show the relative rotor angle plots for the relaxed and non-relaxed cases, respectively, for time period 8.

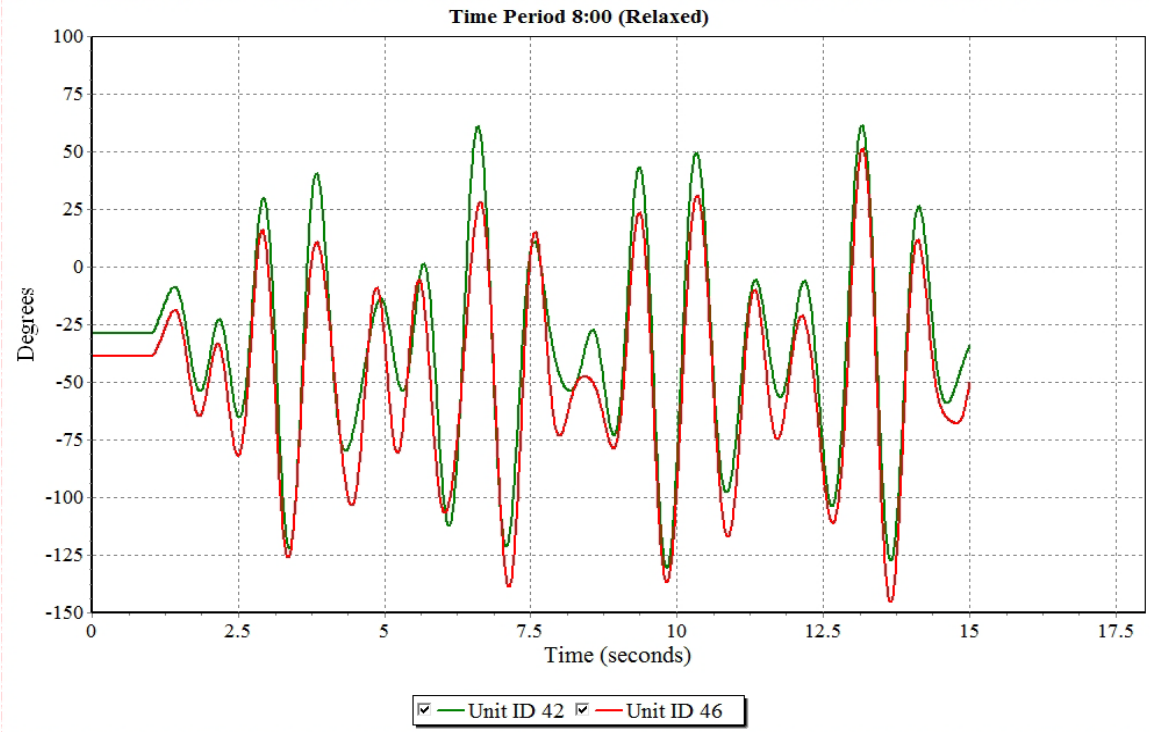

Figure 7.1. RTS-96 rotor angles – time period 8 (relaxed).

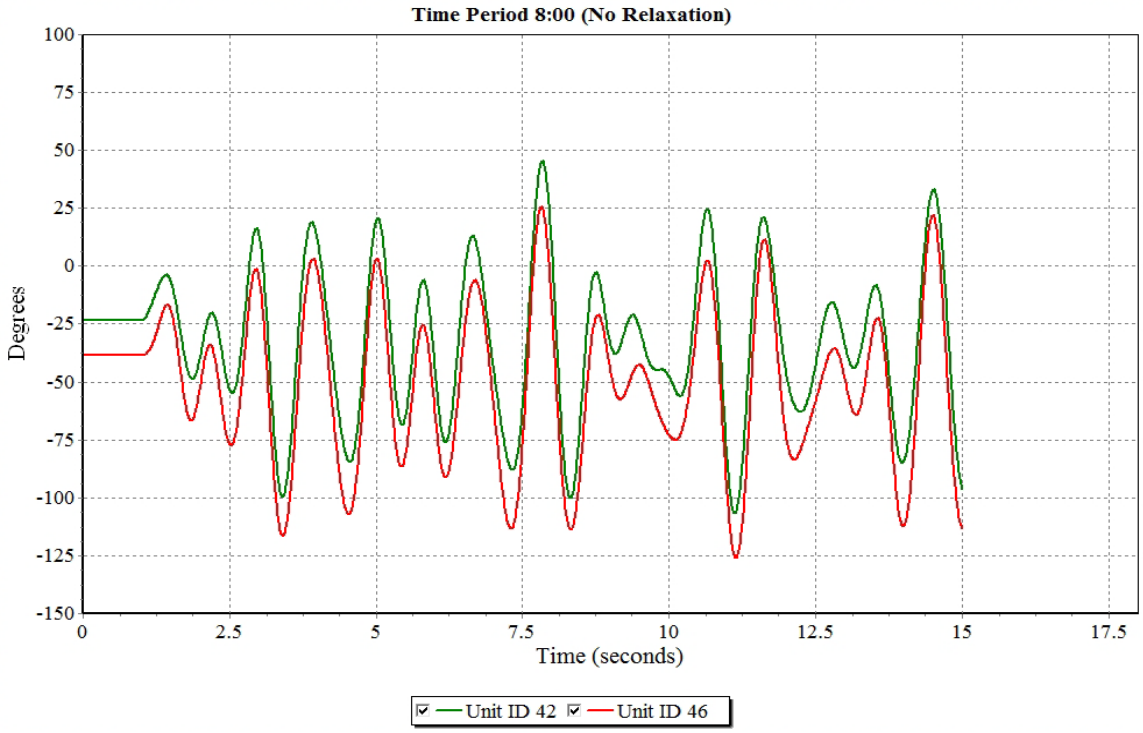

Figure 7.2. RTS-96 rotor angles – time period 8 (no relaxations).

Figure 7.1 and Figure 7.2 show the relative rotor angle plots for generating units 42 and 46, which were most affected by the imposed contingency. Despite the sustained oscillations in both cases which indicate poor damping, it can be noticed that the oscillations in the relaxed case have higher magnitudes compared to the non-relaxed case. Although both cases are considered stable, the higher oscillations imply that the relaxed case is more prone to stability problems. The same analysis was conducted for time period 23; rotor angle plots are shown in Figure 7.3 and Figure 7.4 for the relaxed and non-relaxed cases respectively.

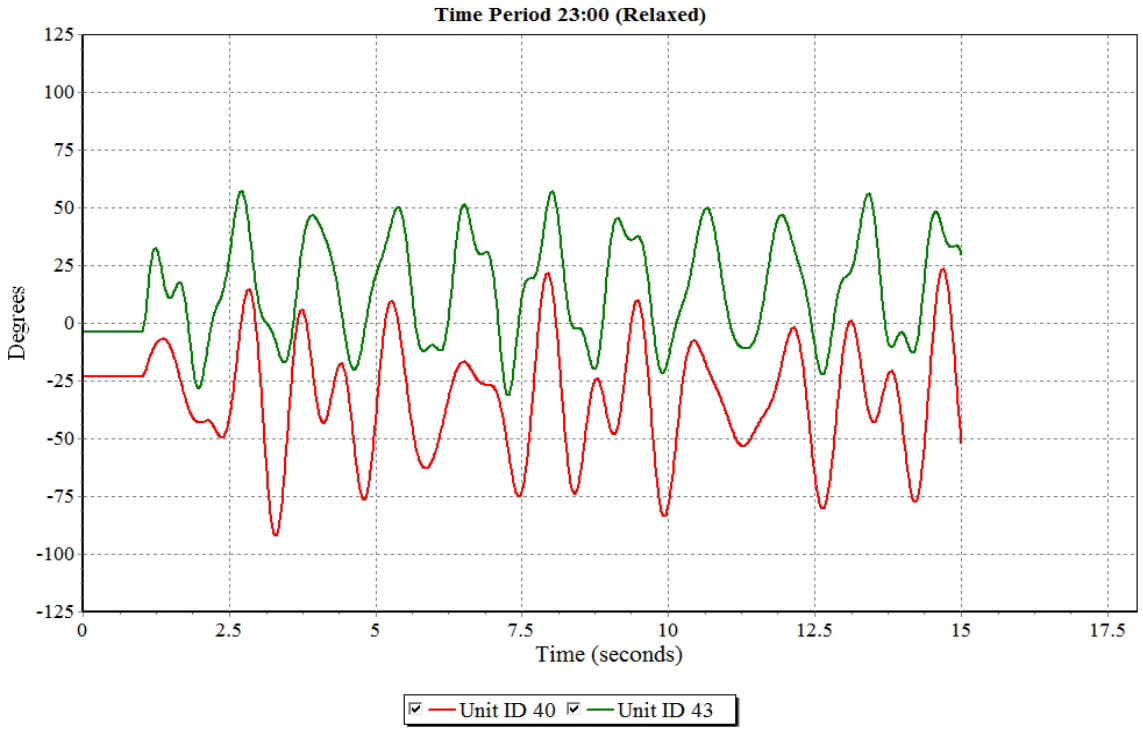

Figure 7.3. RTS-96 rotor angels – time period 23 (relaxed).

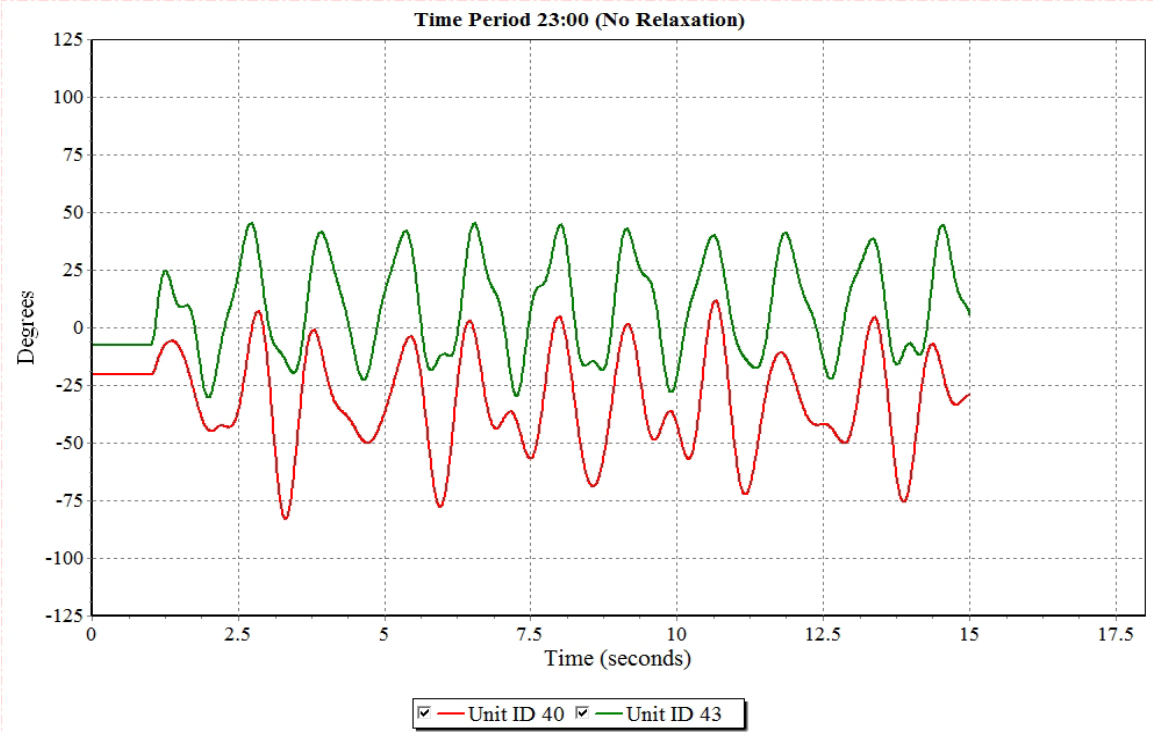

Figure 7.4. RTS-96 rotor angles – time period 23 (no relaxations).

Figure 7.3 and Figure 7.4 show the relative rotor angle plots for generating units 40 and 43 were most affected by the imposed contingency. Similar to time period 8, higher oscillations were observed in the relaxed case compared to the non-relaxed case for time period 23. The higher oscillations are not an exclusive result of relaxations from the proposed market solution. Out-of-market corrections that directly affect operating conditions also have an impact on the dynamic behavior of the cases under study.

It was also desired to investigate the dynamic voltage profiles of the relaxed cases following a large disturbance. A full *N*-1 contingency analysis was conducted for the relaxed cases in order to identify the contingencies causing the most severe post-contingency voltage violations. Table 7.7 shows the contingencies resulting in the most severe voltage violations along with the post-contingency voltage and affected buses.

Table 7.7. RTS-96 post-contingency voltage violations.

Time Period	Contingency ID	Lowest Voltage Bus ID	Voltage p.u.	Voltage Base kV
7	57	207	0.74	138
23	103	307	0.77	138

For each time period listed in Table 7.7, time-domain dynamic analysis was conducted to investigate the dynamic post-contingency voltage profiles. A three-phase fault was placed at one terminal of the lines corresponding to the contingencies shown in Table 7.7. After 5

cycles, the fault was cleared and the line\ was tripped, resulting in the post-contingency low voltage violations shown. The analysis was conducted for the cases with no relaxations as well in order to demonstrate the differences between the two scenarios. Figure 7.5 and Figure 7.6 show the voltage plots for the relaxed and non-relaxed cases respectively for time period 7.

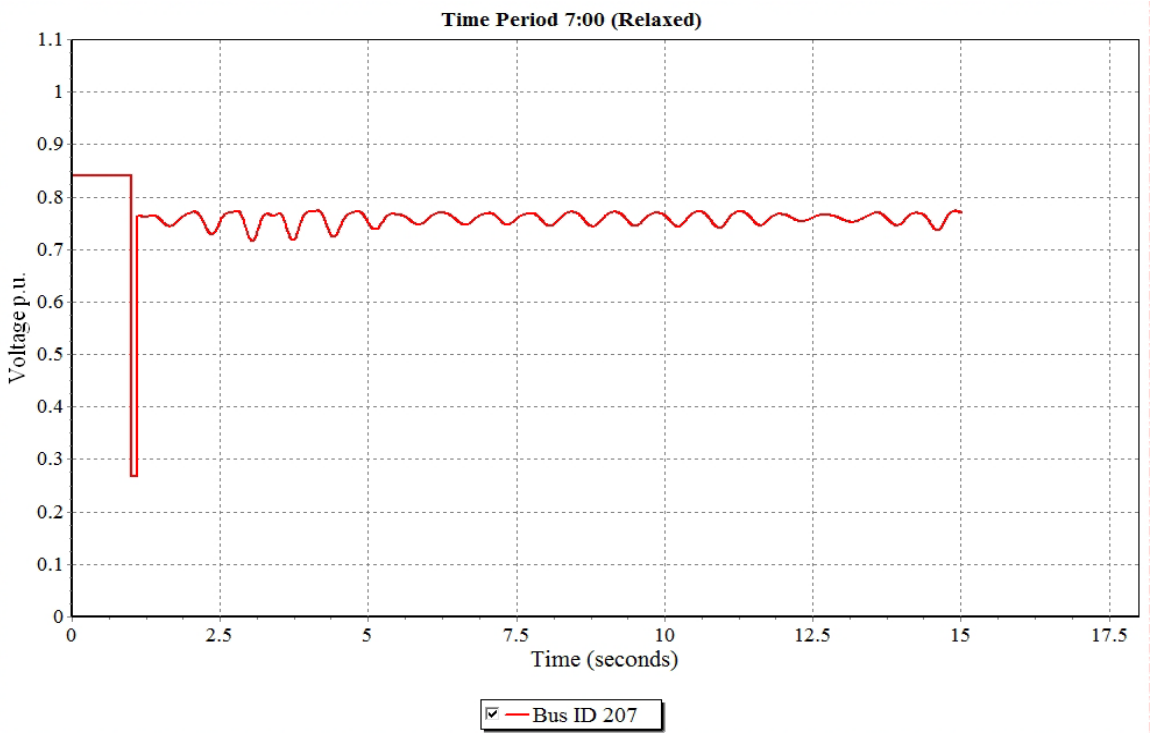

Figure 7.5. Bus ID 207 voltage profile – time period 7 (relaxed).

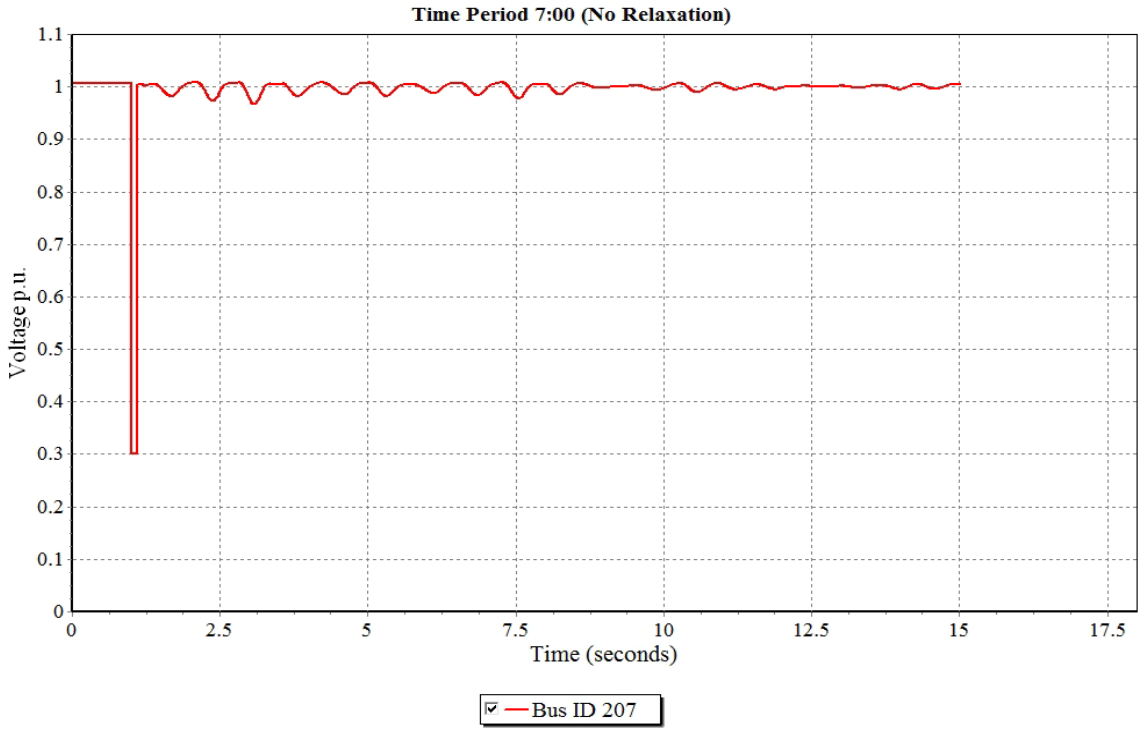

Figure 7.6. Bus ID 207 voltage profile – time period 7 (no relaxation).

Figure 7.5 and Figure 7.6 show a significant difference in voltage magnitude between the relaxed and non-relaxed cases. It can be noticed that bus ID 207 had a base-case low voltage violation in the relaxed case and it sustained an even lower voltage following the imposed contingency. On the other hand, there were no voltage violations in the non-relaxed case since it was *N*-1 secured. Figure 7.7 and Figure 7.8 show the voltage plots for the relaxed and non-relaxed cases, respectively, for time period 23.

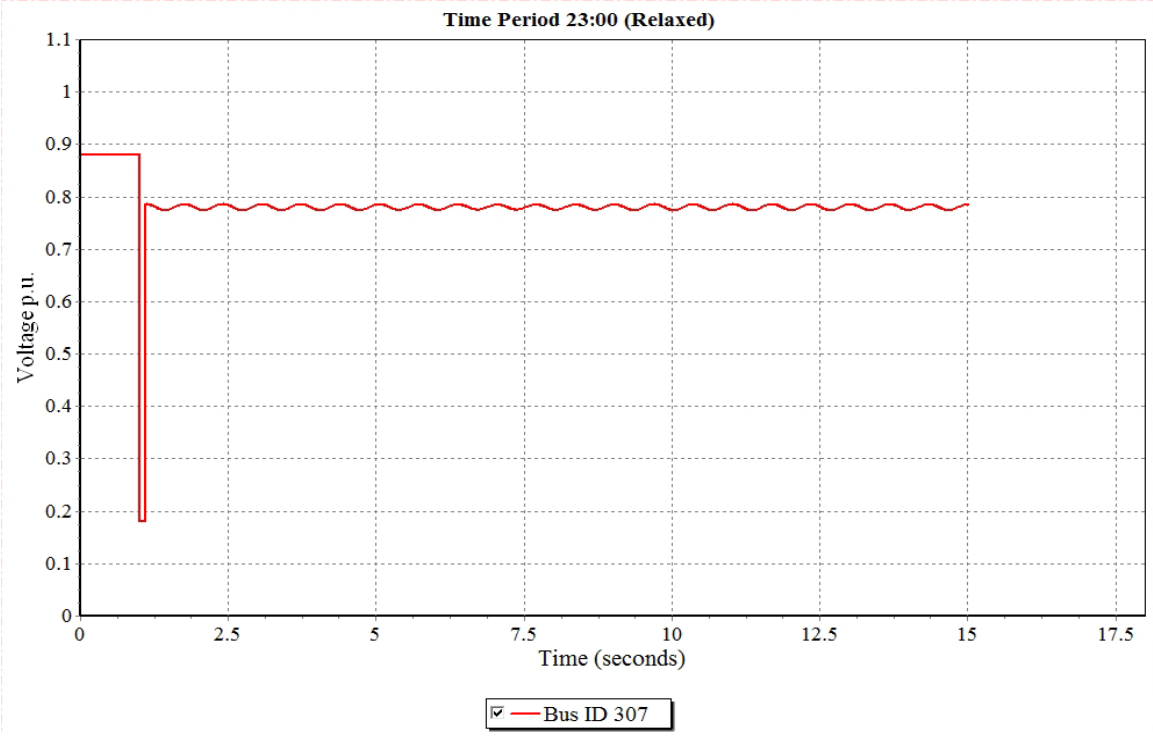

Figure 7.7. Bus ID 307 voltage profile – time period 23 (relaxed).

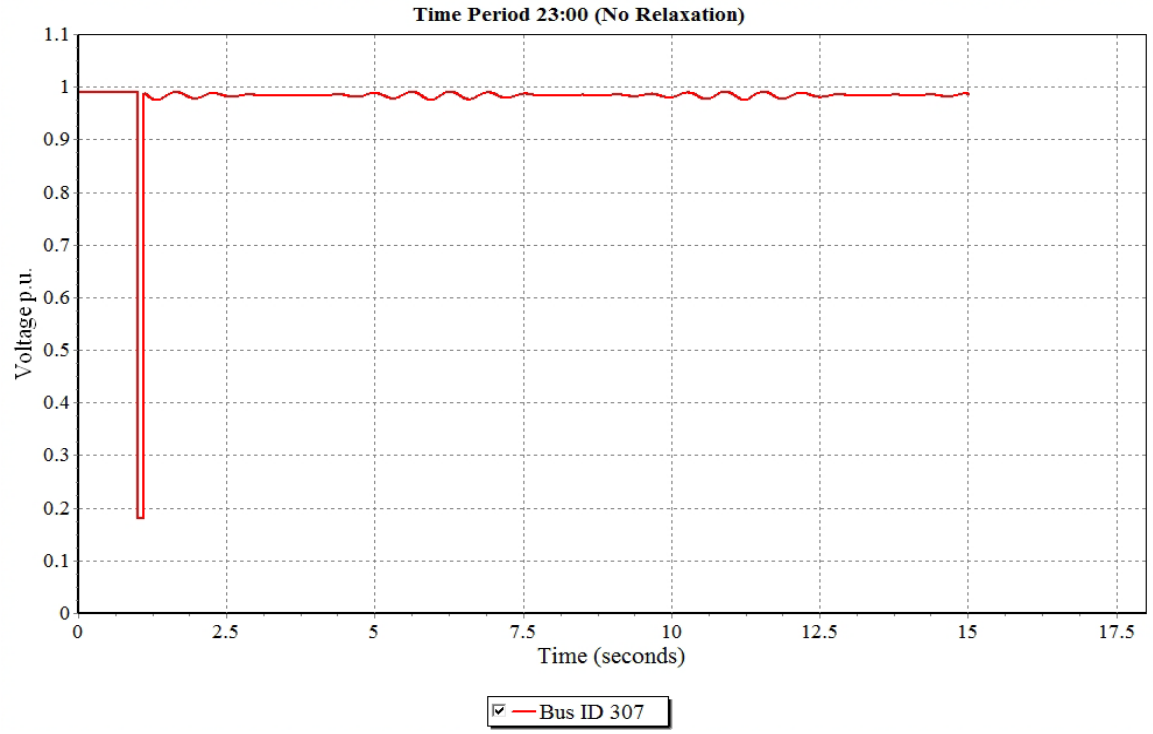

Figure 7.8. Bus ID 307 voltage profile – time period 23 (no relaxation).

Similar to time period 7, Figure 7.7 shows that the relaxed case for time period 23 had a sustained depressed voltage profile following the imposed contingency with base-case low voltage violation as well. On the other hand, Figure 7.8 shows normal base-case and post-contingency voltage magnitudes for the non-relaxed case. The voltage plots presented in Figure 7.5-Figure 7.8 indicate reactive power deficiency in the relaxed cases compared to cases with no relaxations for both time periods. This difference in reactive power availability is due to the larger number of committed generators in the non-relaxed cases as a result of the market solution as well as the out-of-market corrections as shown in Table 7.4.

7.4.4 Static Analysis and Results (PJM)

PJM test case performance was investigated in a similar manner to RTS-96. However, due to the size and complexity of PJM test case and the lack of specialized commercial tools, only two time periods (hours) were investigated. An off-peak and on-peak time periods were chosen to represent light and heavy load conditions respectively. Relaxed market SCUC solutions for those two time periods along with their corresponding non-relaxed cases were used as starting points to achieve an AC feasible solution. However, for PJM test case out-of-market corrections were required for all cases (relaxed and non-relaxed) as a first step to obtain a successful power flow. Intensive out-of-market corrections using PSS/E ACOPF and PSCOPF were conducted on the non-relaxed cases to achieve AC feasibility and *N*-1 security. On the other hand, limited out-of-market corrections were applied to the relaxed cases in order to sustain the line relaxations in the real-time system and keep the final solution as close as possible to the market solution. Table 7.8 lists the market relaxations and their corresponding violations in the AC real-time system.

From Table 7.7, it can be seen that not all AC line flow violations were originated from the market solution as constraint relaxations and, equally, not all line relaxations in the market solution were realized as actual AC line flow violations in the real-time system. This discrepancy between market solution and actual AC solution is expected since the DC market models contain several of approximations, which include neglecting thermal losses and reactive power. For large scale systems such as the PJM test case, these approximations effect is more evident compared to smaller test cases like RTS-96. However, it can be noticed that the AC violations that were not originated from the market models have relatively small magnitudes compared to the lines that were relaxed in the market solution. It can also be noticed that line relaxations in the market models most likely do appear as AC flow violations in real-time.

Table 7.9 shows the number of voltage violations in the relaxed cases shown in Table 7.8. A bus voltage is considered in violation if it falls outside the tolerance range of 0.90 – 1.10 p.u. It also shows the number of committed generators for the relaxed cases and the corresponding non-relaxed cases. The number of additional generators needed to make the non-relaxed market solution feasible and *N*-1 secure is also displayed; hence, no voltage violations are present.

Table 7.8. PJM AC line flow violations.

Time Period	Line Number	DC Flow % (Market Solution)	AC Flow % (Real-time Solution)
Off-peak	878	159%	140%
	1464	252%	252%
	4605	106%	97%
	4649	102%	96%
	5020	103%	96%
	9048	No Relaxation	101%
	9049	No Relaxation	101%
	10519	117%	130%
	11115	109%	110%
	11255	129%	102%
On-peak	190	101%	92%
	878	210%	187%
	1464	148%	87%
	1703	101%	107%
	3460	No Relaxation	106%
	5020	No Relaxation	101%
	5590	No Relaxation	102%
	6470	107%	99%
	7318	No Relaxation	105%
	7557	108%	101%
	9965	105%	104%
	10519	118%	143%
	11001	101%	106%
	11049	No Relaxation	106%
	11111	No Relaxation	106%
	11255	109%	109%

Table 7.9. PJM voltage violations and out-of-market corrections.

Time Period	Relaxed			No Relaxations	
	Committed Generators (Market)	Added Generators	Voltage Violations	Committed Generators (Market)	Added Generators
Off-peak	1395	17	60	1445	63
On-peak	1837	26	52	1935	84

As shown in Table 7.9, 17 and 26 out-of-market generators had to be turned on in the relaxed off-peak and peak time periods, respectively, to attain a base-case AC feasible

solution. Base-case voltage violations were found in both relaxed time periods. It should be noted here that most of the voltage violations in the off-peak case are high voltage violations. A greater number of generators had to be turned on in the non-relaxed off-peak and peak time periods (63 and 84 generators respectively) to attain AC feasible and *N*-1 secure cases. Similar to the RTS-96 test case, the PJM relaxed solutions had fewer committed generators compared to their corresponding non-relaxed cases.

For *N*-1 contingency analysis, line flow violations, voltage violations and unsolved contingencies were reported in the relaxed cases. Table 7.10 presents the post-contingency flows on the lines that had originally base-case flow violations.

Table 7.10. PJM post-contingency relaxed lines flows.

Time Period	Relaxed Line Number	Post-contingency AC Flow %	
		Relaxed	No Relaxation
Off-peak	878	175%	100%
	1464	315%	98%
	10519	285%	100%
	11115	97%	38%
	11255	120%	42%
On-peak	878	234%	100%
	1703	102%	73%
	7557	104%	87%
	9965	86%	84%
	10519	380%	100%
	11001	115%	22%
	11255	140%	60%

As can be seen from Table 7.10, relaxed lines had significant post-contingency flow violations. Table 7.10 also shows that there were no post-contingency flow violations in the non-relaxed cases, as they were *N*-1 secure. Therefore, relaxed lines with AC flow violations were more vulnerable to excessive post-contingency flow violations. It should be noted here that the *N*-1 analysis included lines that have a voltage base of 138 kV and above. Moreover, post-contingency thermal ratings (Rate-C) were used to conduct the post-contingency analysis.

In order to assess the reactive power sufficiency and availability, *Q/V* analysis was conducted. *Q/V* analysis provides an informative tool to compare reactive power availability between relaxed and non-relaxed cases and can also be used as a tool to estimate the reactive power injection needed in order to obtain a local desired voltage level. Therefore *Q/V* curves can be used for both voltage stability indication purposes, and shunt compensation sizing. A 13.8 kV bus that is directly connected to the 138 kV level through a transformer was chosen to conduct this analysis. This bus was chosen because it suffered from a significantly depressed voltage magnitude (around 0.82 p.u.). The PSS/E *Q/V* analysis tool placed a fictitious synchronous condenser with unlimited reactive power

capability at the test bus, and the voltage magnitude was varied from 0.9 p.u. to 1.1 p.u. in 0.02 p.u. steps. This process was applied to base-case as well as to *N*-1 post-contingency. The same analysis was conducted for cases with no relaxations. Figure 7.9 and Figure 7.10 show the base-case *Q/V* curves for relaxed and non-relaxed cases, respectively.

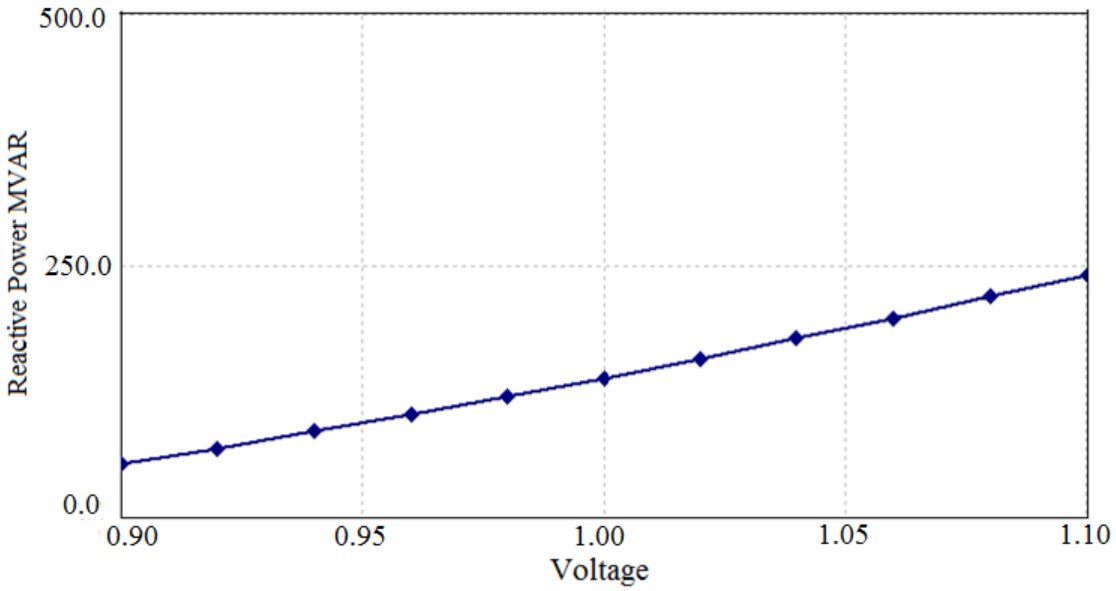

Figure 7.9. Base-case *Q/V* curve (relaxed).

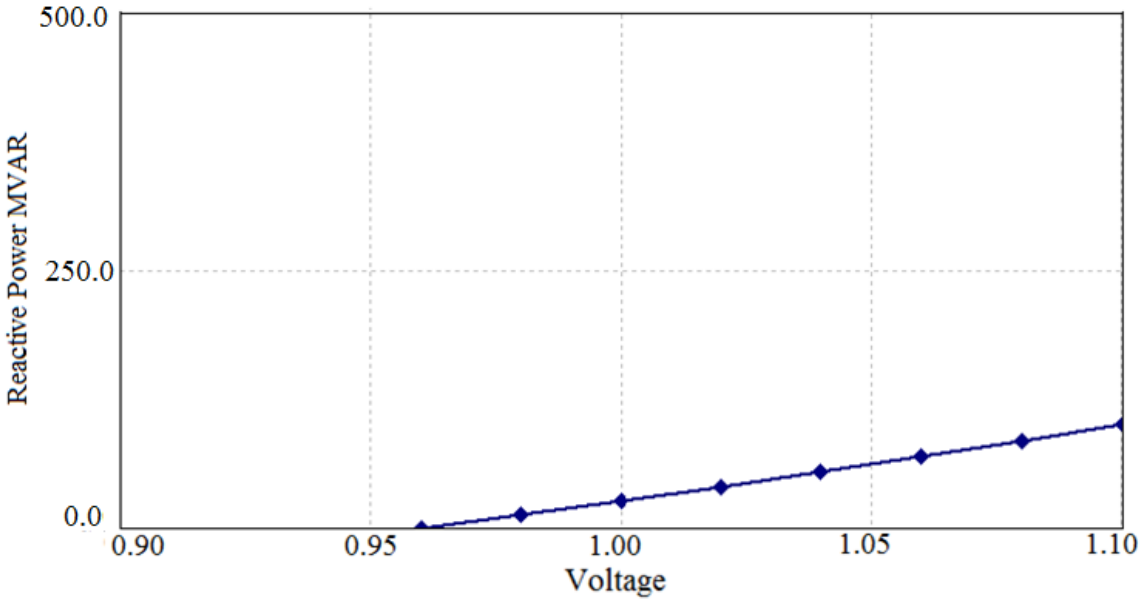

Figure 7.10. Base-case *Q/V* curve (no relaxation).

As can be seen from Figure 7.9 and Figure 7.10, more reactive power was needed in the relaxed case to obtain the various voltage magnitudes at the test bus. Figure 7.9 shows that

around 138 MVAR were needed to obtain a 1.0 p.u. voltage in the relaxed case while in Figure 7.10, only 26 MVAR were needed to obtain the same voltage level in the case with no relaxations. This result clearly implies less reactive power availability in the relaxed case compared to the case with no relaxations, which makes the relaxed case more prone to voltage stability issues. Figure 7.11 and Figure 7.12 extend the *Q/V* analysis to post-contingency in order to investigate the effect of reactive power availability on post-contingency operating conditions.

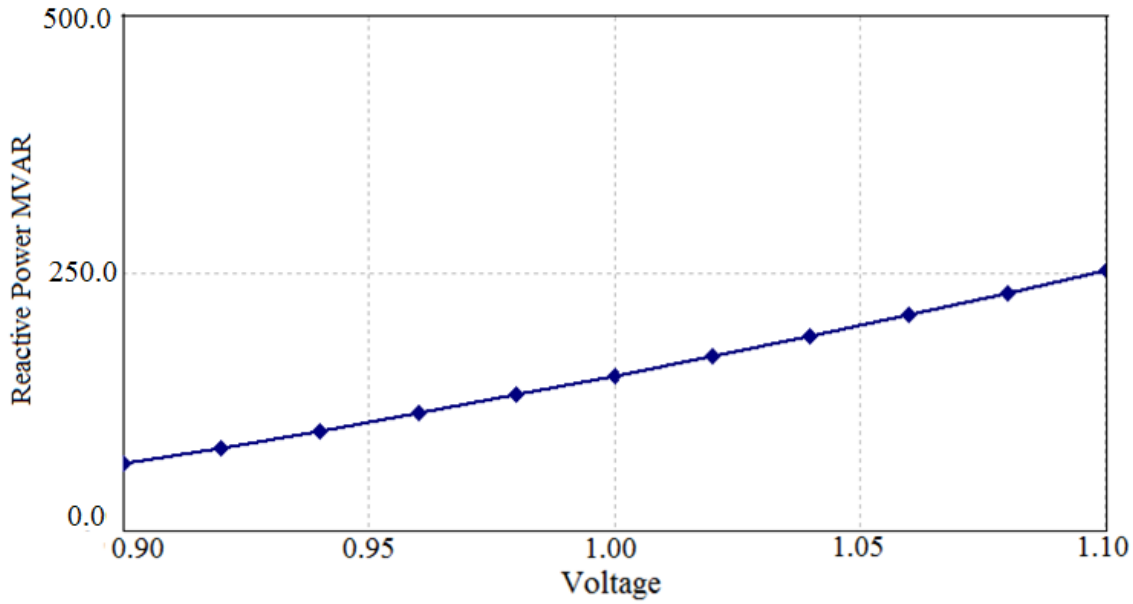

Figure 7.11. Post-contingency *Q/V* curve (relaxed).

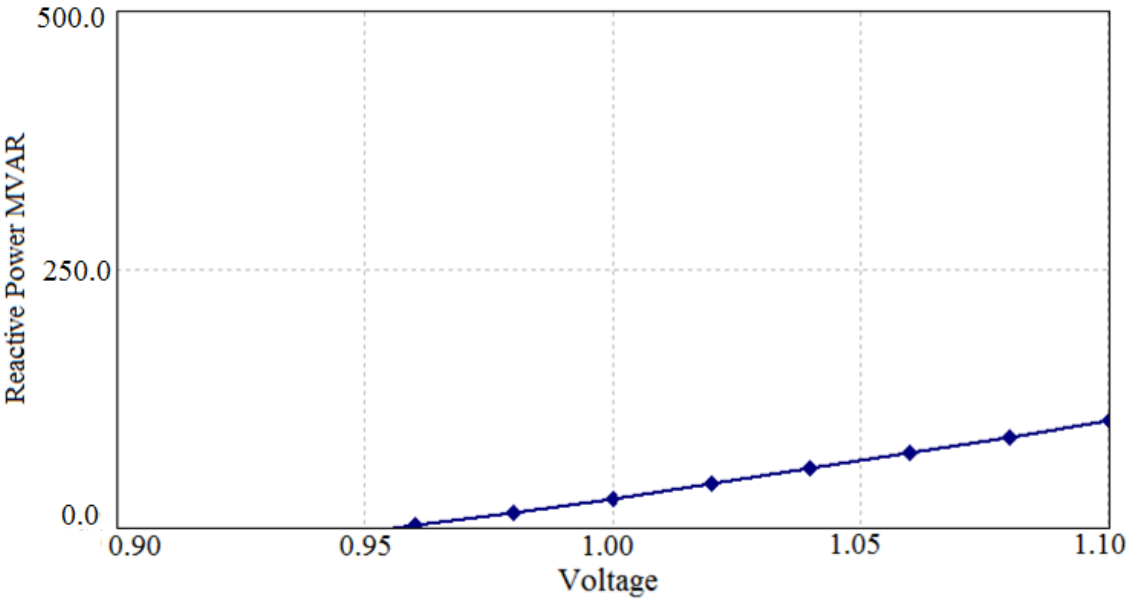

Figure 7.12. Post-contingency *Q/V* curve (no relaxation).

Similar to the base-case *Q/V* curves, more reactive power was needed following a contingency to obtain the various voltage magnitudes at the test bus; as a result, 150 MVAR were needed to obtain a 1.0 p.u. voltage level following a certain contingency in the relaxed case, while only 28 MVAR were needed in the non-relaxed case. The main reason behind the reactive power deficiency in the relaxed case compared to the non-relaxed one is the difference in the number of committed generators. The non-relaxed case had more generators because more generators were originally committed in the market solution compared to relaxed solution. Moreover, additional generators were turned on in the non-relaxed case as out-of-market corrections to attain an AC feasible and *N*-1 secure operating conditions.

7.4.5 Dynamic Analysis and Results (PJM)

The test case provided by PJM included detailed dynamic model data that was used to investigate the dynamic behavior of the PJM test case. Similar to the static analysis presented here, dynamic analysis was conducted on the relaxed cases and the corresponding cases with no relaxations in order to show the impact of relaxations on system dynamics. Rotor angle stability following a large disturbance was first checked. A full *N*-1 contingency analysis was conducted for the relaxed peak time period (on-peak hour) and the contingencies were ranked according to their severity and impact on the relaxed lines. The peak time period was chosen to conduct this type of analysis since it has more stressed operating conditions and is more likely to witness stability problems. The three most severe contingencies that appear in Table 7.10 were chosen for this analysis, as shown in Table 7.11.

Table 7.11. PJM post-contingency flow highest violations.

Contingency No.	Relaxed Line Affected	Voltage Base kV	Post-Contingency Flow %
710	878	230	234%
4592	10519	500	380%
5006	11255	138	140%

It should be noted here that the contingencies shown in Table 7.11 are all single line loss events. A sequence of contingent events was initiated in order to exploit those contingencies and examine the system dynamic post-contingency response. A three-phase fault was first placed at one terminal of the lines corresponding to the contingencies shown in Table 7.11. After 5 cycles the fault was cleared and the line was tripped resulting in the post-contingency flows shown in Table 7.11. After 1 second the relaxed line with the excessive post-contingency flow was tripped. Therefore, this series of events can be considered an *N*-1-1 contingency. The same contingencies were also applied to the cases with no relaxations and results were compared. Figure 7.13 and Figure 7.14 show the rotor

angle plots for the most affected generators for the relaxed and non-relaxed, respectively, following contingency 710 (Table 7.11).

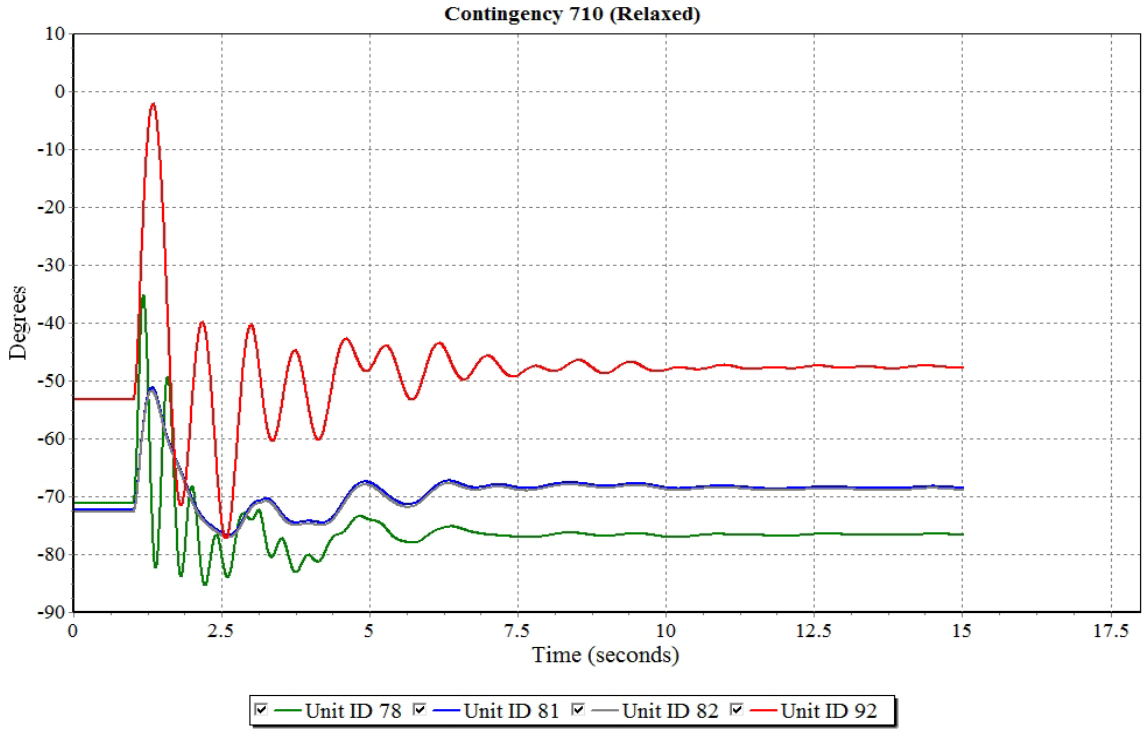

Figure 7.13. Rotor angles following contingency 710 (relaxed).

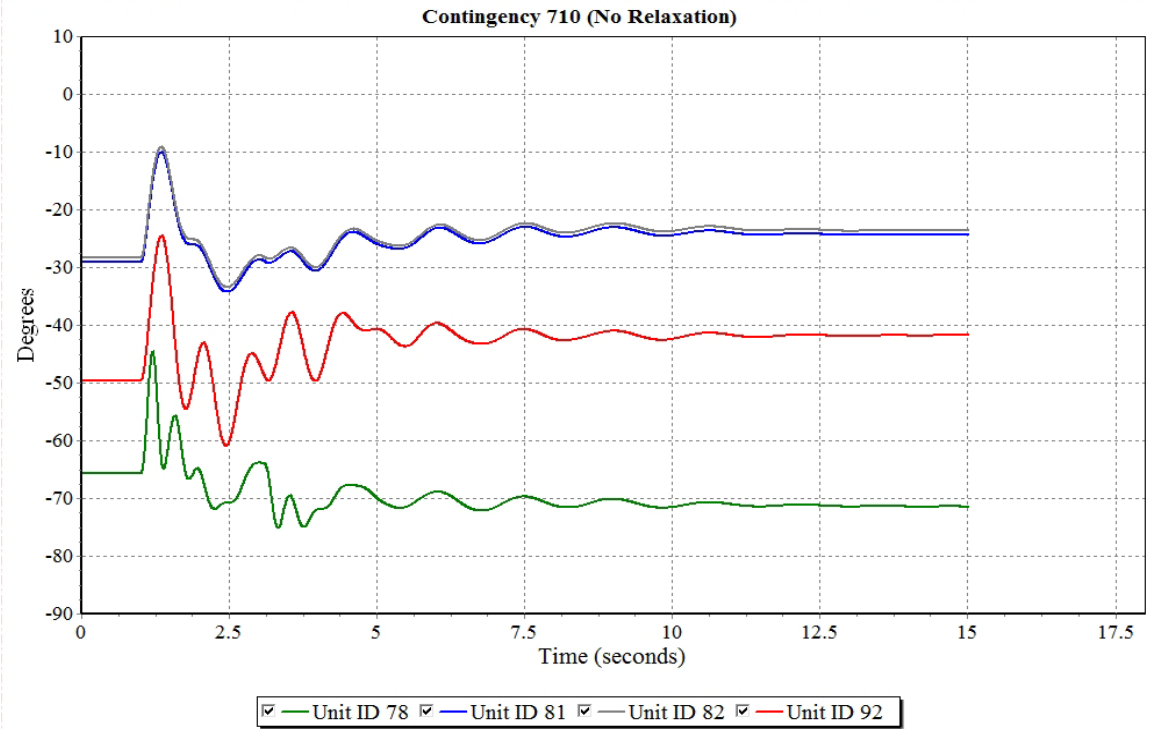

Figure 7.14. Rotor angles following contingency 710 (no relaxation).

Figure 7.13 and Figure 7.14 show that the system is stable following the sequence of contingent events for relaxed and non-relaxed cases. However, it can be seen that the oscillations for rotor angles in the relaxed case are higher compared to the non-relaxed case. Moreover, the settling time is larger for the relaxed case. This indicates that although both systems are stable, the relaxed case is closer to its stability margins and is more likely to suffer from stability related problems. Figure 7.15–Figure 7.18 show the same analysis for contingencies 4592 and 5006.

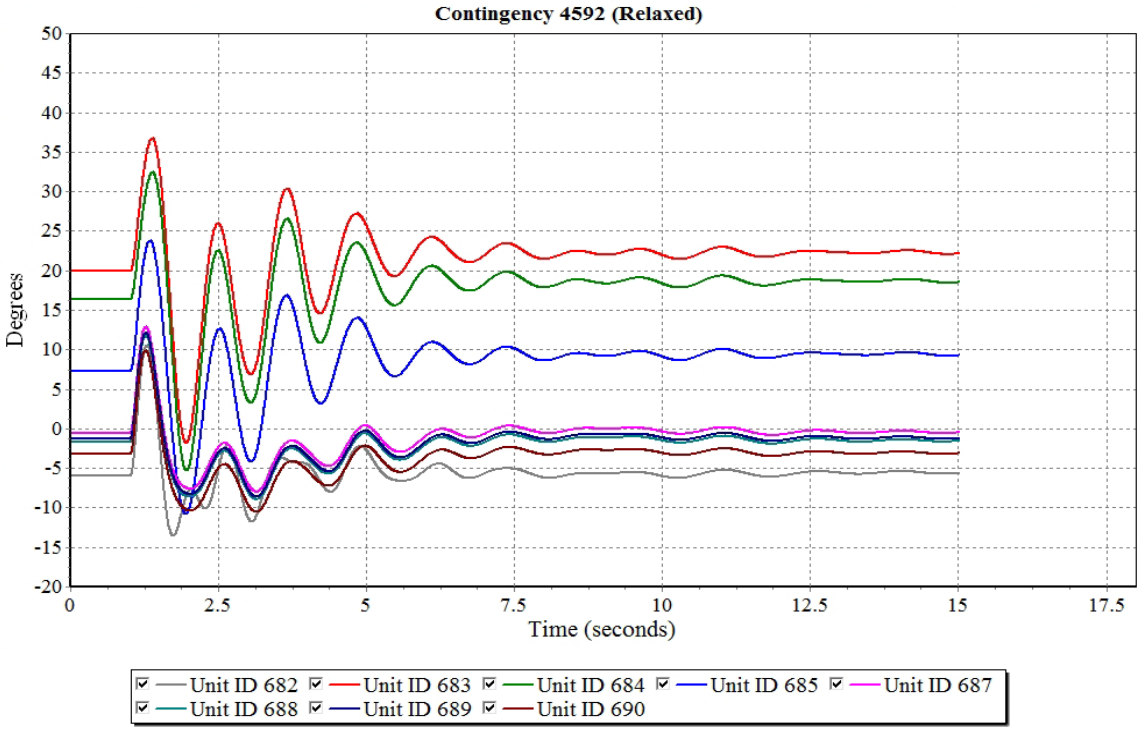

Figure 7.15. Rotor angels following contingency 4592 (relaxed).

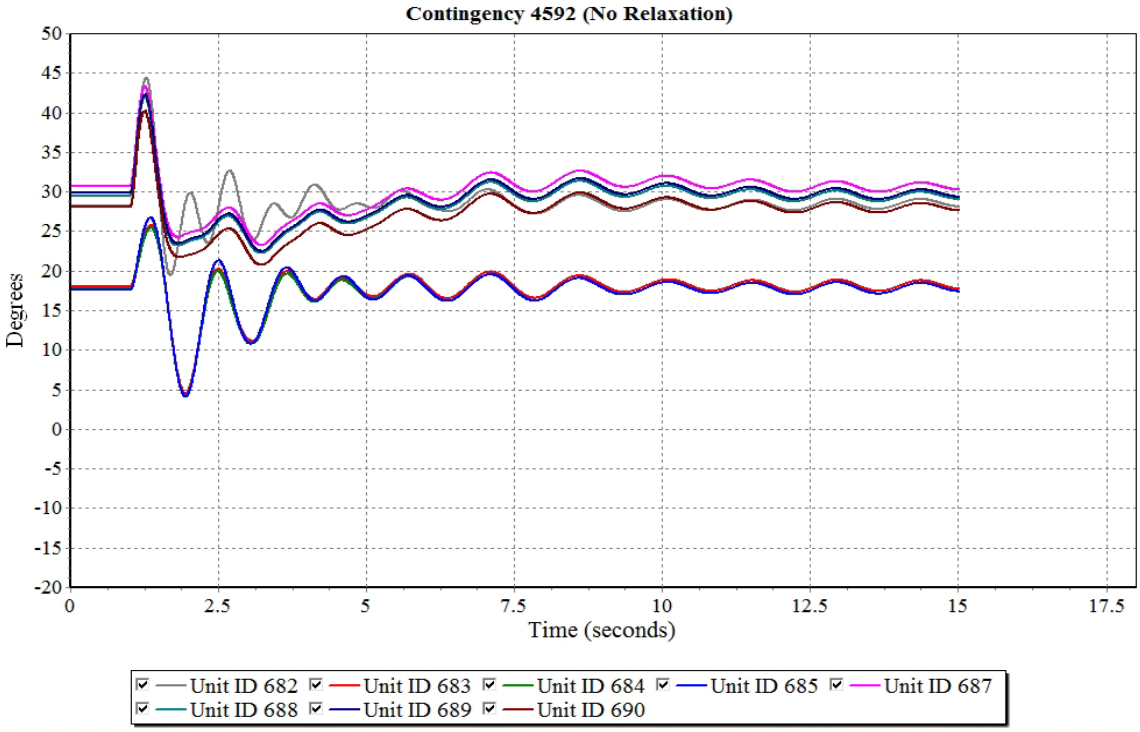

Figure 7.16. Rotor angles following contingency 4592 (no relaxation).

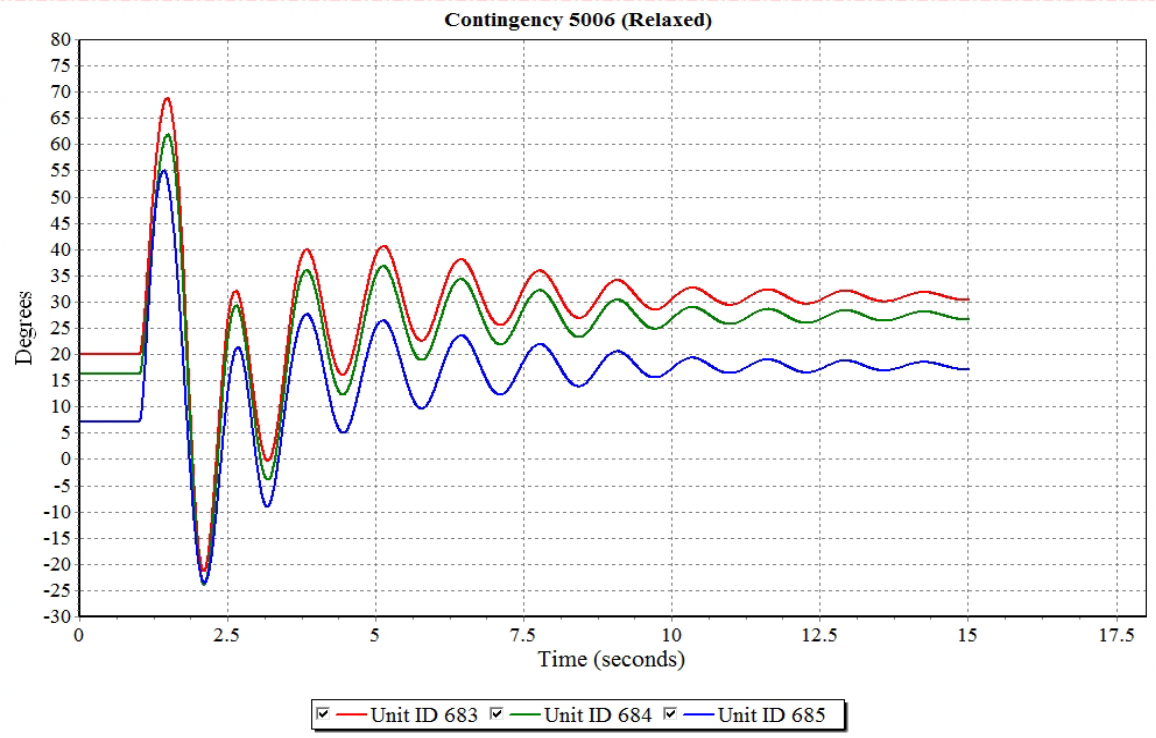

Figure 7.17. Rotor angles following contingency 5006 (relaxed).

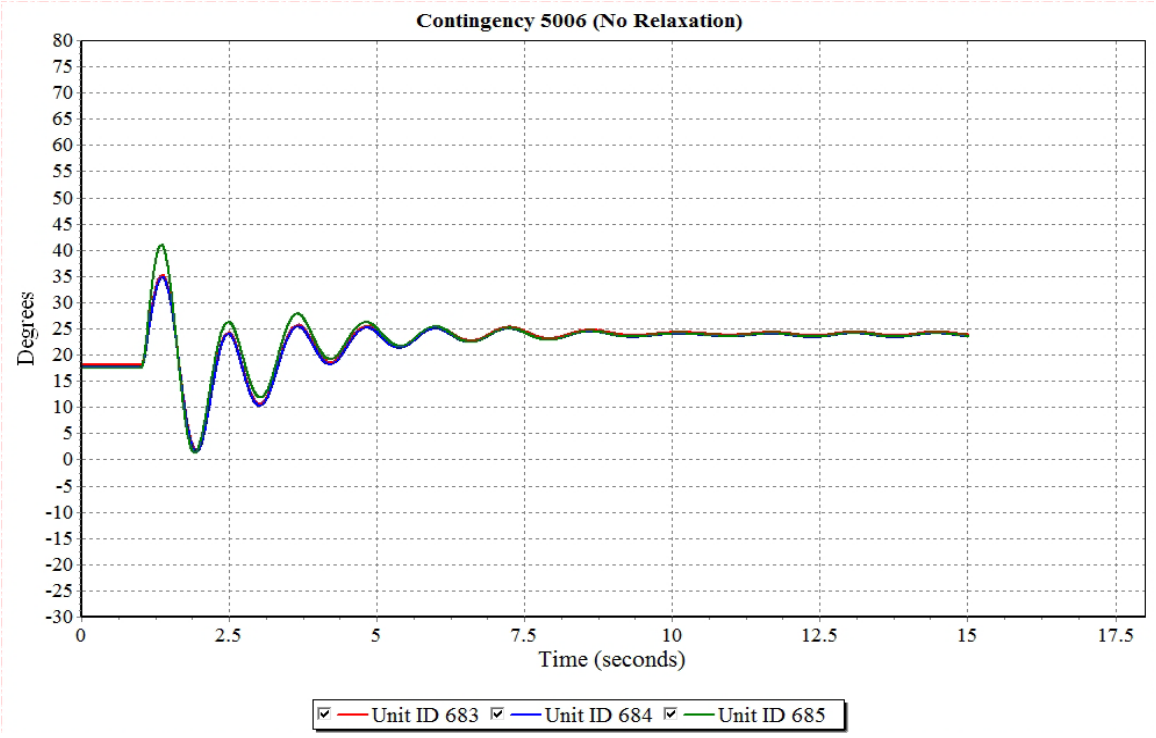

Figure 7.18. Rotor angles following contingency 5006 (no relaxation).

The same dynamic response observed in contingency 710 was repeated in the other two contingencies. It can be seen from Figure 7.15 – Figure 7.18 that the magnitude of the oscillations and settling time were higher for relaxed cases compared to cases with no relaxations. However, this dynamic response is not an exclusive result of constraint relaxations. The particular operating conditions of the test cases are what determine the difference in post-contingency dynamic behavior between relaxed and non-relaxed cases. Moreover, out-of-market corrections affect operating conditions and, therefore, will also affect the post-contingency dynamic behavior.

A similar analysis was conducted to assess the dynamic post-contingency voltages. A full *N*-1 contingency analysis was conducted for the same relaxed peak time period (on-peak hour) and the contingencies that caused post-contingency low voltages were ranked according to their severity. The three most severe contingencies are listed in Table 7.12.

Table 7.12. PJM post-contingency lowest voltages.

Contingency No.	Lowest Voltage Bus ID	Voltage p.u.	Voltage Base kV
2427	546	0.82	138
5471	436	0.83	138
1941	1166	0.87	138

For each contingency listed in Table 7.12, time-domain dynamic analysis was conducted to investigate the dynamic post-contingency voltage profiles. A three-phase fault was placed at one terminal of the lines corresponding to the contingencies shown in Table 7.12. After 5 cycles, the fault was cleared and the line was tripped, resulting in the post-contingency low voltage violations shown. The analysis was conducted for the case with no relaxations as well in order to point out the differences between the two scenarios. Figure 7.19 and Figure 7.20 show the voltage plots of the most affected buses corresponding to contingency 2427 for the relaxed and non-relaxed cases, respectively.

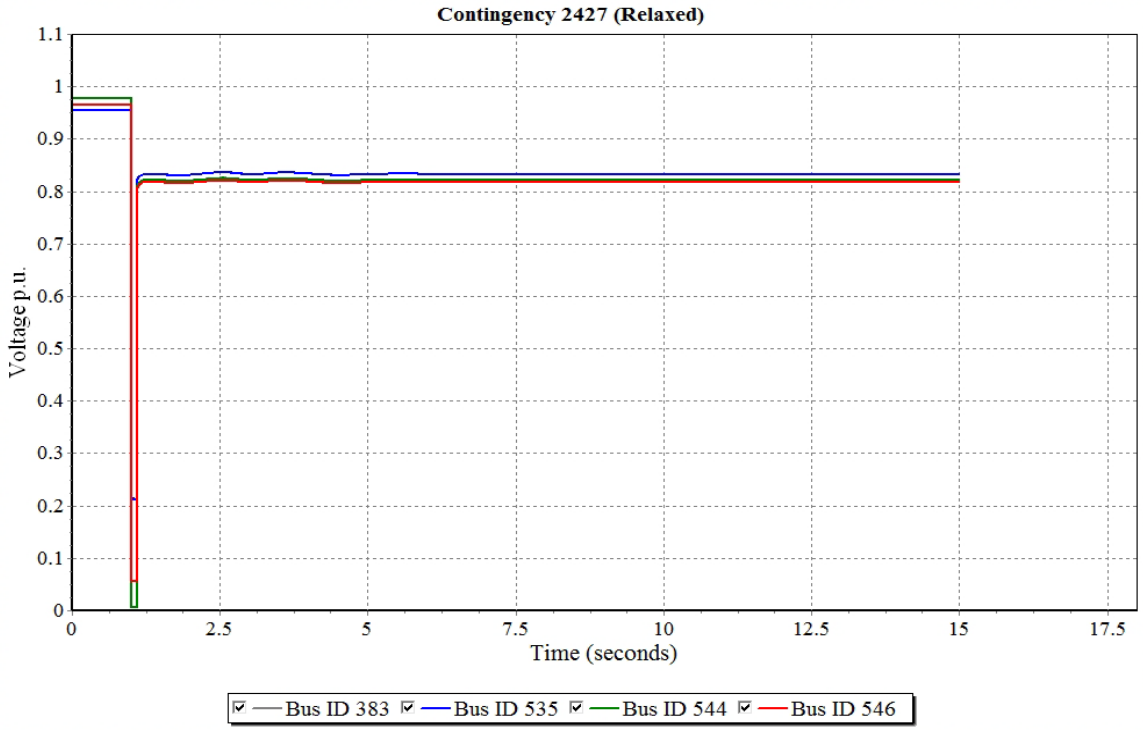

Figure 7.19. Voltage profiles following contingency 2427 (relaxed).

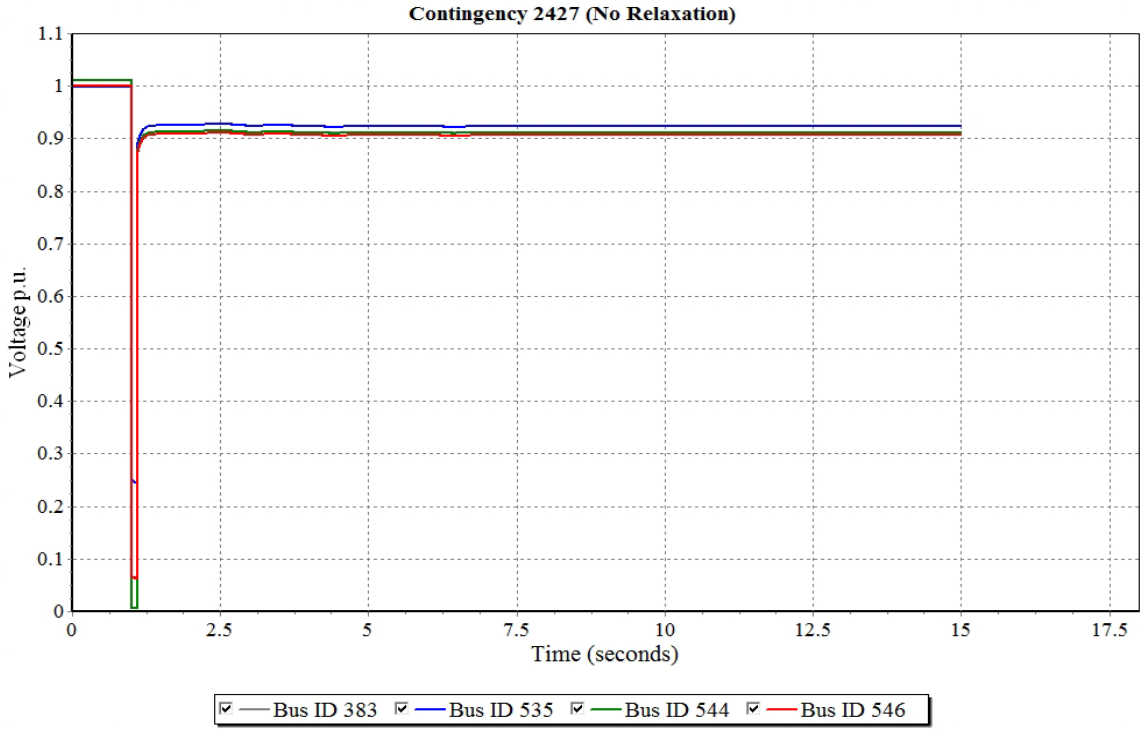

Figure 7.20. Voltage profiles following contingency 2427 (no relaxation).

Figure 7.19 indicates post-contingency voltage violation as the voltage is 0.82 p.u. as shown in Table 7.12 as well. On the other hand, Figure 7.20 shows that the voltage for the same bus following the same contingency in the non-relaxed case is approximately 0.9 p.u. This result is expected since the non-relaxed case is *N*-1 secure. The same analysis was conducted for the other two contingencies listed in Table 7.12. Figure 7.21-Figure 7.24 show the corresponding voltage plots for relaxed and non-relaxed cases.

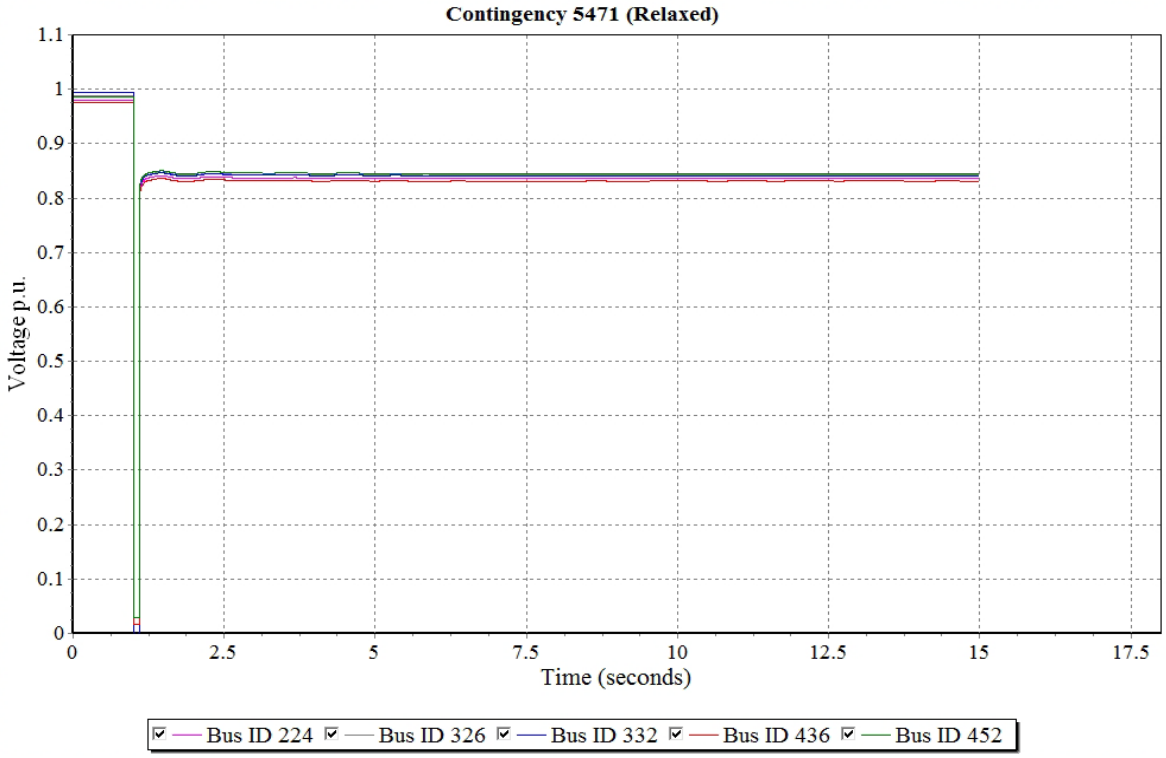

Figure 7.21 Voltage profiles following contingency 5471 (relaxed).

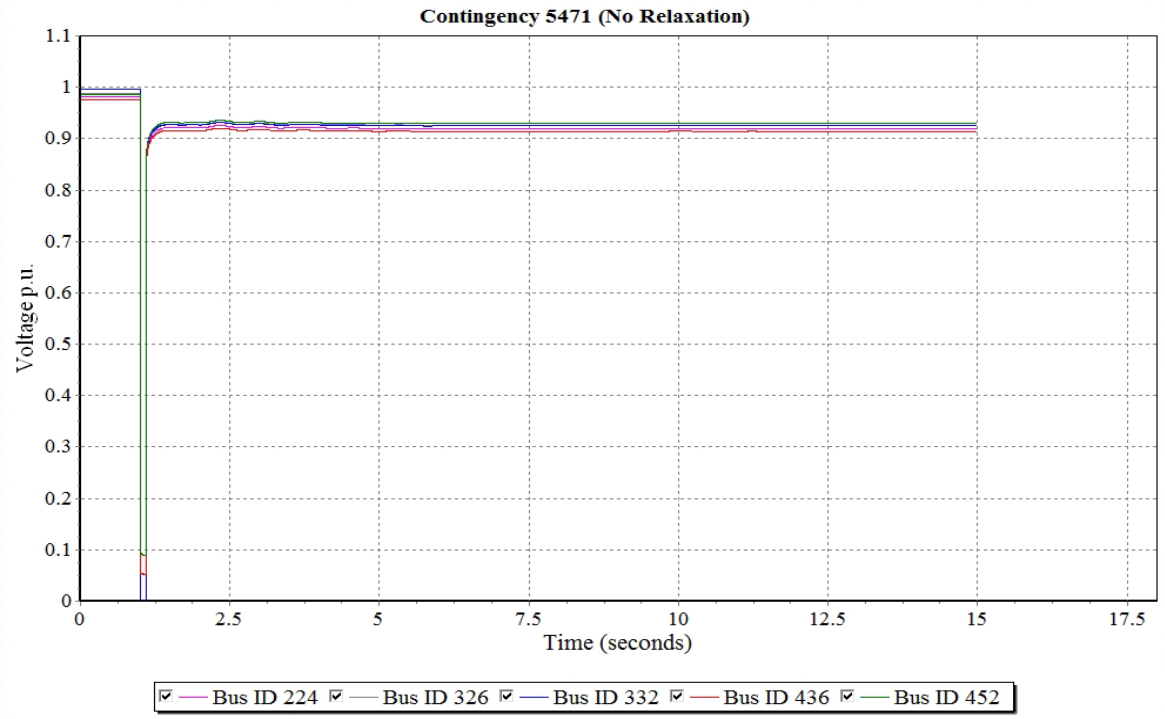

Figure 7.22 Voltage profiles following contingency 5471 (no relaxation).

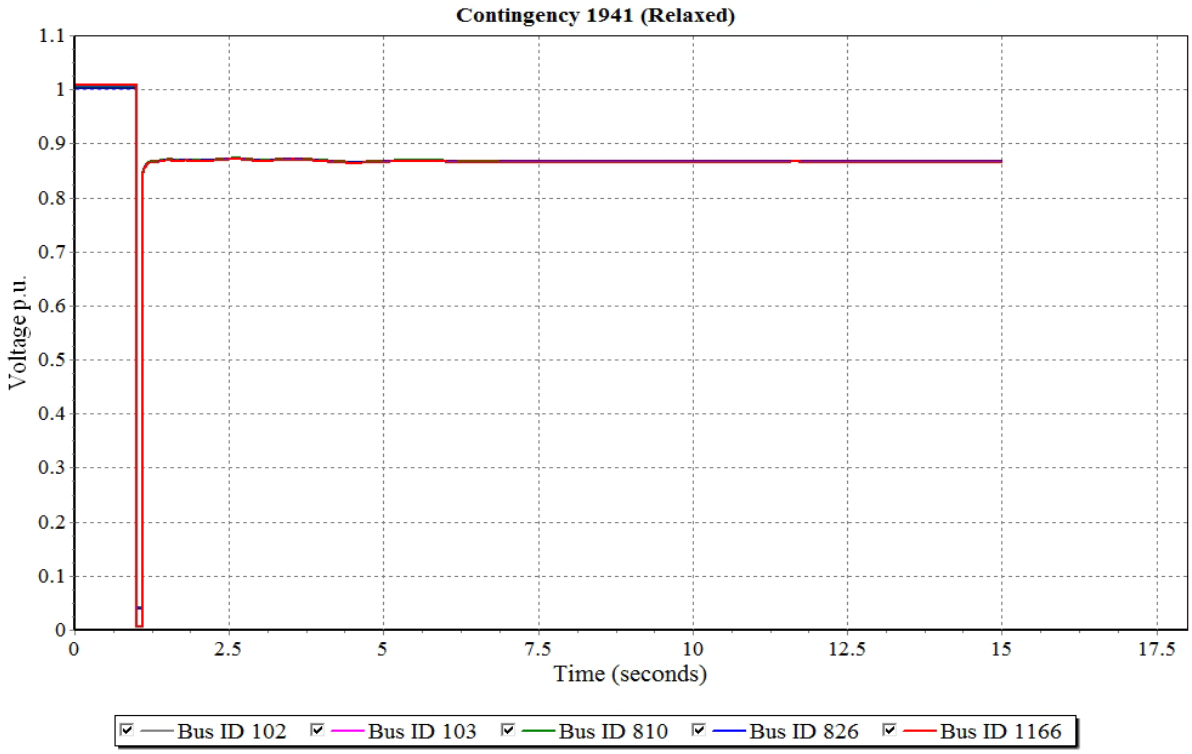

Figure 7.23 Voltage profiles following contingency 1941 (relaxed).

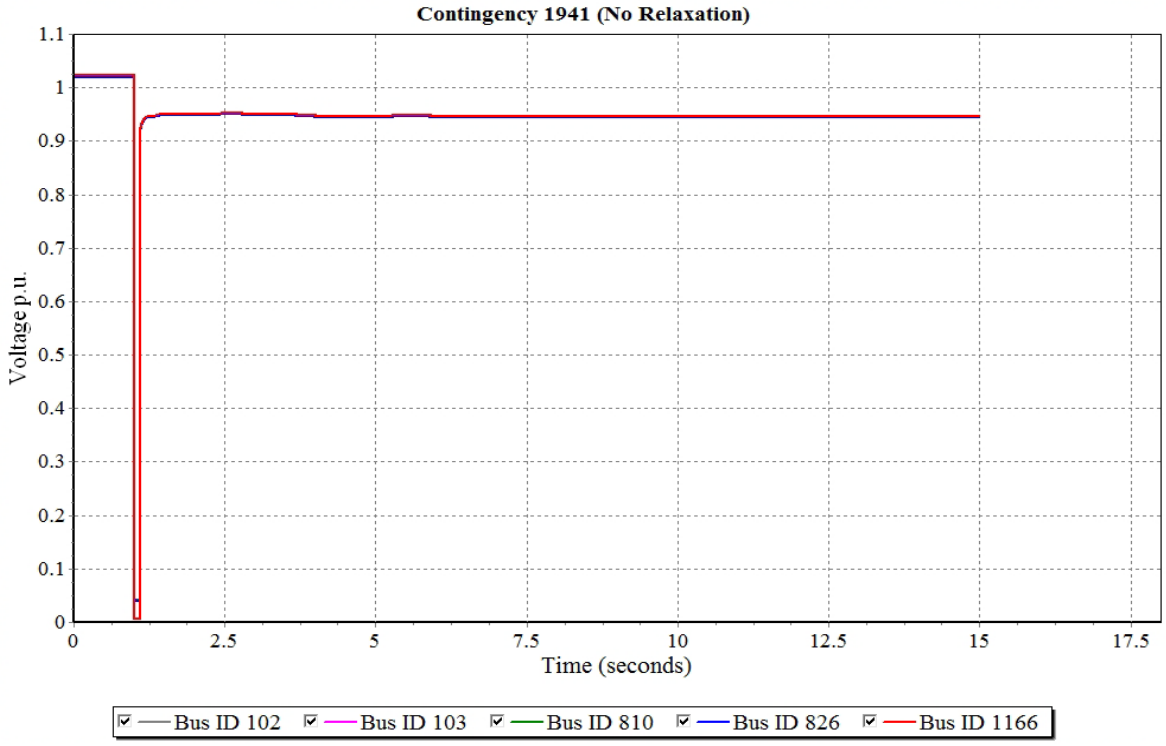

Figure 7.24 Voltage profiles following contingency 1941 (no relaxation).

Figure 7.21-Figure 7.24 show that in the relaxed cases the voltage sustained depressed values (less than 0.9 p.u.) following certain severe contingencies. On the other hand, there were no post-contingency steady state voltage violations in the non-relaxed cases as the final voltage value was higher than 0.9 p.u. for all tested contingencies. The provided PJM dynamic models data does not include load models; thus, the voltage recovers instantaneously following the fault clearance. The depressed voltage magnitudes in the relaxed cases compared to the cases with no relaxations imply reactive power deficiency in those cases. The dynamic voltage analysis conducted here confirms the *Q/V* analysis results shown in the static analysis part. Reactive power deficiency in the relaxed case can be directly related to the relatively smaller number of committed generators compared to non-relaxed cases. Moreover, the non-relaxed cases were subject to intensive out-of-market corrections that resulted in increasing the number of committed generators.

7.5 Summary

In this work, assessing the impacts of market constraint relaxations on real-time system performance was desired. Capturing the impacts of constraint relaxations on a real-time system provides operators with the needed information to accurately assess the risk associated with various constraint relaxations and, therefore, it enables decision makers to determine penalty prices accordingly. Moreover, this analysis also provides better understanding on the correlation between DC market models and AC real-time systems and the analysis shows how relaxations in market models propagate to real-time systems.

In this work, two test cases were used to replicate operator practices related to constraint relaxations. The first test case was the RTS-96 system that was used to demonstrate the constraint relaxations mechanism and the methodology of analysis on a relatively small and simple system. The second test case was a real-life large-scale system that represented PJM control areas and their neighboring areas. PJM also provided the corresponding economic and dynamic data.

Static steady state and dynamic time-domain analysis were conducted for both test cases twice, once for cases with relaxed constraints and again for non-relaxed cases. This approach has provided a systematic and consistent approach to demonstrate the impact relaxations on a real-time system. SCUC market solutions were used as starting points to achieve AC feasible solutions. ACOPF was used as the first step to achieve base-case feasible solutions. However, it was found that in some cases, some out-of-market corrections were needed to achieve AC feasibility. Out-of-market corrections mainly consist of committing additional generators for voltage support purposes and/or lines overloading alleviation. It was noticed that more out-of-market corrections were needed for relaxed cases, which can be explained by the commitment of fewer generators in the relaxed cases in market solutions. It was also noticed that more out-of-market corrections were needed in the PJM test case compared to the RTS-96 case. This can be explained by the effect of the approximations inherent in market models and this become more evident in large-scale systems. It was also desired to attain *N*-1 security for the non-relaxed cases in order to be used as benchmarks for the corresponding relaxed cases. Attaining *N*-1 security required additional out-of-market corrections using PSS/E PSCOPF tool.

Static analysis of both test cases revealed that line relaxations in market models have a high tendency of appearing as AC line flow violations in real-time systems. In the RTS-96 test case, all base-case AC flow violations were originated from the market solution as line relaxations. However, in the PJM test case, most of the market solution relaxations appeared as AC flow violations alongside line flow violations that did not come from market models, which can be explained due to the various approximations used in market models. However, flow violations that were not originated from the market solutions had relatively lower values. Static analysis has also revealed reactive power deficiency in relaxed cases that was translated into wide-spread voltage violations. Relaxed cases sustained reactive power deficiency because fewer generators were committed in those cases in the original market solutions as well as in the out-of-market corrections compared to non-relaxed cases. *Q/V* analysis was also conducted for the PJM test cases to confirm the reactive power problem and it was found that significantly greater amount of reactive power was needed to regulate the voltage in relaxed cases. Static post-contingency analysis was also conducted and relaxed lines flows were monitored. It was noticed that relaxed lines were more likely to violate their thermal emergency limits following certain critical contingencies since they were already overloaded in base-case.

Dynamic time-domain analysis was also conducted to investigate the dynamic performance of relaxed cases compared to cases with no relaxation. Using *N*-1 analysis, the most severe contingencies were identified and ranked. A sequence of events representing *N*-1-1 contingencies was used to investigate the dynamic response of overloading and tripping

relaxed lines. Relative rotor angles of the most affected generators were plotted and compared. Rotor angle stability analysis revealed higher oscillations in relaxed cases with prolonged settling time compared to non-relaxed cases. This observation was more evident in the PJM test case, as it represents a large-scale system with realistic dynamic models. Although all tested contingencies were stable, higher oscillations indicate narrower stability margins and, therefore, higher vulnerability to stability related problems. Dynamic post-contingency voltage profiles were also investigated for both test cases. Similar to stability studies, contingencies causing the most severe voltage violations were identified and ranked using *N*-1 analysis. Dynamic voltage analysis confirmed the static analysis results related to reactive power deficiency. It was noticed that relaxed cases sustained base-case and post-contingency depressed voltage levels compared to non-relaxed cases. Again, this is explained due to the fewer committed generators in the relaxed case.

8. Conclusions and Future Work

8.1 Conclusions

Market management systems, employed by ISOs and RTOs, employ unit commitment and are mixed integer linear programs. Even though the software and algorithmic performance have been improved, market models cannot fully capture all the complexities inherent in operating the complex power system. For example, there are various approximations within market models: the linear DCOPF rather than the more accurate ACOPF, linear ramping constraints, and proxy reserve requirements are used in market models instead of explicitly modeling all contingencies. Additional complexities come from load uncertainty and, more recently, variable generation. Due to the approximations and inaccuracies that are inherent in electric energy market models, at times the market itself leads to infeasible solutions. To guarantee feasibility, ISOs and RTOs allow select constraints to be violated or relaxed in their market models, a practice known as constraint relaxation. To incorporate a constraint relaxation within a market model, the ISO or RTO adds a slack variable to a constraint in the market model. The slack variable is then added to the objective function multiplied by a pre-determined penalty price.

In this report, issues with constraint relaxation practices have been investigated, including a review of the use of this practice by various ISOs and RTOs. Subsequently, a proposed model with key constraint relaxations was presented. The model was solved with and without relaxations utilizing a standard IEEE test case and a 15,000 bus test case based on proprietary PJM data. Both proposed market solutions were adjusted to attain AC and *N*-1 feasibility. All solutions were compared with regard to their market outcomes. Market solutions with constraint relaxations typically needed more out-of-market corrections to reach an AC and *N*-1 feasible solution. However, this was not always the case and was demonstrated with one of the test cases used. Most of the results from this analysis were typical.

This report included a penalty price analysis as well. Penalty prices greatly affect the frequency of constraint relaxations. Penalty prices and constraint relaxation practices are negotiated with market participants. Originally, constraint relaxation practices utilized only a single fixed price penalty scheme, but today some ISOs and RTOs utilize stepwise penalty price curves. ISOs and RTOs can examine the dual variables of proposed constraints to be relaxed and choose the penalty price based on these dual variables. However, caution should be taken because operators should not choose a price such that a market participant is not willing to enter the market. Again, these penalty prices and schemes must be negotiated with market participants.

Additionally, the report investigated the issue of determining penalty prices with regard to line relaxations and their thermal ratings. The work included investigations on the effect these relaxations had associated with the loss of tensile strength to overhead conductors. The risk of loss of tensile strength is used as a basis for a systematic methodology to determine the penalty price for thermal limit line relaxations.

Finally, the effect of constraint relaxation practices on power system performance, including system reliability, security, and stability, is examined. Static and dynamic studies were performed on dispatch solutions with and without constraint relaxations. Static analysis demonstrated that line relaxations have a high probability of appearing in real time, if not corrected by the operator earlier. As for the dynamic time domain testing, these results revealed that although contingencies for both dispatch solutions with and without relaxations are stable, the dispatch solution with relaxations have narrower stability margins. Therefore, these dispatch solutions with relaxations were more vulnerable to stability related problems. Stability results are system dependent and are directly related to the system operating conditions, as well as the nature of the contingency event.

The potential effects of constraint relaxation practices were investigated in this report. Constraint relaxation practices are necessary for electric energy markets. In summary, this report demonstrates that,

- The approximations within market models can lead to infeasibilities. However, the use of constraint relaxations aid the market model in finding feasible solutions fast.
- Price caps are directly ensured through the use of constraint relaxations.
- The proposed market solution, with constraint relaxation, typically committed fewer generators. Thus, most of the out-of-market corrections made to the proposed market solution were due to limited reactive power support.
- Typically constraint relaxations associated with line thermal limits appeared in real-time as line flow violations, unless corrected for in the post-processing phase.
- Different penalty price schemes can be utilized by ISOs. The functional form of the constraint relaxation and penalty prices are negotiated with market participants, but should still serve the purposes of the market. This report investigated a more systematic way to generate penalty prices for specific constraint relaxation applications and suggests that similar methodologies be considered in practice. More accurate penalty prices should be determined based on the overall impact on market surplus while considering the risk associated to system reliability and security.
- ISOs can determine, for themselves, the penalty price for violating line thermal limits based on the risk associated with line degradation.
- When constraint relaxations were allowed in real-time operations, higher post-contingency rotor angle oscillations with longer settling times were observed. Although these oscillations did not cause system instability, the results implied that the system had narrower stability margins. This study was conducted on the PJM system with actual system data.

The inclusion of constraint relaxations within market models is a necessary practice for ISOs and RTOs. This report has aided in the investigation of the impact of constraint relaxation practices. However, ISOs and RTOs should establish more transparent policies regarding these practices, along with the steps taken to remove violations from market

solutions. Furthermore, penalty prices can still be negotiated with market participants, but a more realistic approach would incorporate the overall impact on market surplus while considering the risk associated to system reliability and security.

8.2 Future Work

This report examined the impacts of the constraint relaxation practices when relaxed constraints were mainly corrected by the system operator prior to real-time operations (i.e., the violation reported by the market model is not allowed to exist within the actual operation of the system). Future work will focus on situations in which relaxations occurring within market models are allowed to propagate into real-time operations (i.e., pre-contingency and post-contingency system violations actually occur during system operations) and the associated impacts on reliability and stability. Such situations have been confirmed by multiple ISO/RTOs [21]; for instance, real-time SCED models employ constraint relaxations and the dispatch solution is implemented directly. While such violations can occur, they are flagged and reported to the operator based on the next state estimation and real-time contingency analysis cycle. It is frequently thought that such a practice does not follow NERC's reliability standards; on the contrary, constraint relaxation practices described in this report are both consistent with NERC's standards as well as approved by FERC.

Today, system operators enable constraint relaxation by allowing the constraint to be violated for a set penalty, i.e., price, which is the same as placing a limit on the shadow price (dual variable) of the constraint. Constraint relaxations that occur within dispatch models, such as security constrained unit commitment (SCUC), are generally corrected by the system operator before the actual real-time dispatch. That is, a required operating limit (for instance, an IROL) may be violated within a mathematical model but, with the operator's out-of-market correction (e.g., turning on additional generation), the IROL is still enforced during actual operations. However, based on confirmation from industry advisors from PSERC Project M-29, these relaxations can and do occur in real-time. For example, a transmission thermal rating may be violated during actual operations due to a constraint relaxation that occurs within a market model, such as a security constrained economic dispatch tool (SCED). During real-time operations, if the SCED solution includes relaxations of the constraints, then that solution is implemented since instructions are sent to the generators. Note that, however, these relaxations are subsequently caught by the next cycle of the real-time contingency analysis (RTCA) tool in the energy management system (EMS).

The extension of the PSERC Project M-29 specifically focuses on the situations when these relaxations occur in real-time operations. The goal is to answer prior requests from the industry to analyze the impacts of constraint violations that propagate into actual operations and to examine very specific situations when these relaxations occur. Analysis will include reliability analysis, stability analysis, risk-based analysis, as well as market economic analysis. There are four main key takeaway points from this work:

- Real-time constraint relaxations occur. For example, a line's flow can exceed its SOL or IROL limit due to the modeling of constraint relaxations within security constrained economic dispatch.
- No prior work has analyzed the risk associated with these occurrences.
- A risk-based OPF seems more appropriate
- PSERC industry members have requested additional work in the following areas and this project will focus completely on requests and concerns from the industry advisors: a) risk assessment of real-time violations in comparison to a risk-based OPF framework; b) analysis of the system stability when such relaxations occur; c) systematic ways to derive penalty prices for the relaxations and the form of the reserve demand curves as opposed to creation of these policies based solely on stakeholder negotiations.

The main outcome for the next phase of the project will be a technical report along with decision support tools for decision makers that will provide a holistic investigation and analysis on the impacts of current constraint relaxation practices along with tools to further assess such impacts. This report will also include an investigation and analysis on alternative market practices. Furthermore, additional deliverables for this project include: a) semi-annual progress reports provided to the industry advisor, b) posters and presentations at the IAB meetings, c) dissemination of the results through publications and presentations at conferences and postings on the project website, and d) a final report.

References

[1] NERC Criteria for Reliability Coordinator Actions to Operate Within IROLs, NERC Standard IRO-009-1, Feb. 2014.

[2] NERC Criteria for Reliability Coordinator Actions to Operate Within IROLs, NERC Standard IRO-008-1, Feb. 2014.

[3] WECC, "Real-time tools guideline," Western Electricity Coordinating Council, Jan. 2013. [Online]. Available: https://www.wecc.biz/Reliability/Real-time%20Tools%20Guideline.pdf.

[4] PSS/E 33.5, "Program operational manual," Siemens, Oct. 2013.

[5] O. Akinbode, "EEE 590 Reading and conference final report," School of Electrical, Computer, and Energy Engineering, Arizona State University, 2012.

[6] PJM, "Penalty factors and maximum prices," PJM Interconnection, 2009. [Online]. Available: http://www.pjm.com/~/media/%20committees-groups/working-groups/spwg/20100108/20100108-item-03-penalty-factors-and-max-prices.ashx.

[7] FERC, "Recent ISO software enhancements and future software and modeling plans," Federal Energy Regulatory Commission – Office of Energy Policy and Innovation, 2011, [Online]. Available: https://www.ferc.gov/industries/electric/indus-act/rto/rto-iso-soft-2011.pdf.

[8] M. Tahanan, W. Ackooji, A. Frangioni, and F. Lacalandra, "Large-scale unit commitment under uncertainty: a literature survey," University of Pisa Department of Computer Science. [Online]. Available: http://compass2.di.unipi.it/TR/Files/TR-14-01.pdf.gz.

[9] A. Casto, "Overview of MISO day-ahead markets," Midwest ISO Day-Ahead Market Administration, Nov. 2007. [Online]. Available: http://www.atcllc.com/oasis/Customer_Notices/NCM_MISO_DayAhead111507.pdf.

[10] A. Papalexopoulos, "Theoretical and practical considerations in implementing and using a reliability unit commitment (RUC) in restructured electricity markets," *IEEE PES General Meeting*, pp. 1-2, Montreal, Canada, 2006.

[11] G. L. LaBove, R. B. Hytowitz, and K. W. Hedman, "Market implications of reliability unit commitment formulations for day-ahead scheduling," *IEEE PES General Meeting*, pp. 1-5, Washington, DC, USA, Jul. 2014.

[12] A. D. Papalexopoulos and P. E. Andrianesis, "Market design for the simultaneous optimization of the day-ahead market and the reliability unit commitment applications," *2013 IREP Symposium*, pp. 1-8, Crete, Greece, Aug. 2013.

[13] ERCOT, "ERCOT nodal protocols – section 4: day-ahead operations," Electric Reliability Council of Texas, March 2014. [Online]. Available: http://www.ercot.com/content/mktrules/nprotocols/current/04-030114_Nodal.doc.

[14] CAISO, "Parameter tuning for uneconomic adjustments in the MRTU market optimizations," Dept. Market and Product Development, May 6, 2008. [Online]. Available: http://www.caiso.com/1fbf/1fbfe3a2498e0.pdf.

[15] CAISO, "Price inconsistency market enhancements – revised straw proposal," [Online]. Available: http://www.caiso.com/Documents/RevisedStrawProposal-PriceInconsistencyMarketEnhancements.pdf.

[16] CAISO, "Update to CAISO draft final proposal on uneconomic adjustment policy and parameter values," Dept. Market and Product Development, Oct. 29, 2008, [Online]. Available: http://www.caiso.com/Documents/RevisedDraftFinalProposalUpdate-UneconomicAdjustmentPolicyandParameterValues29-Oct-2008.pdf.

[17] CAISO, "2012 annual report on market issues and performance," California ISO, Apr. 2013. [Online]. Available: http://www.caiso.com/Documents/2012AnnualReport-MarketIssue-Performance.pdf.

[18] MISO, "MISO completes largest-ever power grid integration," Midcontinent ISO, December 2013. [Online]. Available: https://www.misoenergy.org/AboutUs/MediaCenter/PressReleases/Pages/MISOCOMPLETESLARGEST-EVERPOWERGRIDINTEGRATION.aspx.

[19] Y. Al-Abdullah, M. Abdi-Khorsand, and K. W. Hedman, "Analyzing the impacts of out-of-market corrections," *2013 IREP Symposium*, pp. 1-10, Crete, Greece, Aug. 2013.

[20] Y. M. Al-Abdullah, M. Abdi-Khorsand, and K. W. Hedman, "The role of out-of-market corrections in day-ahead scheduling," *IEEE Transactions on Power Systems*, accepted for publication.

[21] K. W. Hedman and V. Vittal, "Constraint relaxations: analyzing the impacts on system reliability, dynamics, and markets (M-29)," Power Systems Engineering Research Center: Industry Advisor Conference Calls, Sep. 17, 2013 and Apr. 10, 2014.

[22] MISO, "2011 state of the market report for MISO electricity markets," Potomac Economics – Independent Market Monitor for MISO, June 2012. [Online]. Available: http://www.potomaceconomics.com/uploads/midwest_reports/2011_SOM_Report.pdf.

[23] MISO, "Constraint relaxation update," MISO Market Subcommittee, May 2012. [Online]. Available: https://www.misoenergy.org/Library/Repository/Meeting%20Material/Stakeholder/MSC/2012/20120501/20120501%20MSC%20Item%2004a%20Constraint%20Relaxation.pdf.

[24] MISO, "2010 State of the market report for MISO electricity markets," Potomac Economics – Independent Market Monitor for MISO, June 2011. [Online]. Available:

http://www.potomaceconomics.com/uploads/midwest_reports/2010_State_of_the_Market_Report_Final.pdf.

[25] MISO, "Schedule 28A demand curves for transmission constraints version 1.0.0," Midcontinent ISO, [Online]. Available: https://www.misoenergy.org/Library/Repository/Meeting%20Material/Stakeholder/MSC/2013/20130806/20130806%20MSC%20Item%2004a%20Schedule%2028A%20TCDC.pdf.

[26] ERCOT, "ERCOT business practice – setting the shadow price caps and power balance penalties in security constrained economic dispatch," Electric Reliability Council of Texas, [Online]. Available: http://www.ercot.com/content/meetings/tac/keydocs/2010/1104/05._ercot_buspract_shadow_price_caps_pwr_bal_pen_v0_21.doc.

[27] ERCOT, "ERCOT nodal protocols – section 6: adjustment period and real-time operations," Electric Reliability Council of Texas, March 2014. [Online]. Available: http://www.ercot.com/content/mktrules/nprotocols/current/06-030114_Nodal.doc.

[28] NYISO "Day-ahead scheduling manual," New York ISO, February 2013. [Online]. Available: http://www.nyiso.com/public/webdocs/markets_operations/documents/Manuals_and_Guides/Manuals/Operations/dayahd_schd_mnl.pdf.

[29] NYISO, "Ancillary services manual," New York ISO, December 2013. [Online]. Available: http://www.nyiso.com/public/webdocs/markets_operations/documents/Manuals_and_Guides/Manuals/Operations/ancserv.pdf.

[30] A. George, "ISO New England – consumer liaison group meeting," ISO New England, Sept. 2014. [Online]. Available: http://www.iso-ne.com/static-assets/documents/2014/09/george_clg_9_24_14.pdf.

[31] W. Coste, "Interregional economic study update," ISO New England, Sept. 2010. [Online]. Available: http://www.iso-ne.com/committees/comm_wkgrps/prtcpnts_comm/pac/mtrls/2010/sep212010/interregional_eco_study.pdf.

[32] University of Washington, "Power system test case archive," Dept. of Elect. Eng., 2007. [Online]. Available: http://www.ee.washington.edu/research/pstca/.

[33] CAISO, "Spinning reserve and non-spinning reserve," California Independent System Operator, Jan. 2006. [Online]. Available: http://www.caiso.com/docs/2003/09/08/2003090815135425649.pdf.

[34] K. W. Hedman, M. C. Ferris, R. P. O'Neill, E. B. Fisher, and S. S. Oren, "Co-optimization of generation unit commitment and transmission switching with N-1 reliability," *IEEE Transactions on Power Systems*, vol. 25, no. 2, pp. 1052-1063, May 2010.

[35] PJM, "Reserves - scheduling, reporting, and loading," PJM Interconnection, June 2013, [Online]. Available: https://pjm.adobeconnect.com/_a16103949/p5fd94w2vhd/.

[36] T. Zheng and E. Litvinov, "Ex-post pricing in the co-optimized energy and reserve market," *IEEE Transactions on Power Systems*, vol. 21, no. 4, pp. 1528-1538, Nov. 2006.

[37] Aluminum Electrical Conductor Handbook, 2nd ed. Washington, DC: The Aluminum Association, 1982.

[38] S. Uski-Joutsenvuo and R. Pasonen, "Maximising power line transmission capability by employing dynamic line ratings-technical survey and applicability in Finland," *VTT Technical Research Centre*, Finland, Tech. Rep. VTT-R-01604-13, Feb. 2013.

[39] IEEE Standard for Calculating the Current-Temperature of Bare Overhead Conductors, *IEEE Standard 738-2006*, Jan. 2006.

[40] R. Stephen, D. Douglas, and M. Gaudry, "Thermal behavior of conductors," *CIGRE ELECTRA*, No. 144, Oct. 1992.

[41] N. P. Schmidt, "Comparison between IEEE and CIGRE ampacity standards," *IEEE Transactions on Power Delivery*, vol. 14, no. 4, pp. 1155-1159, Oct. 1999.

[42] W. Z. Black and R. L. Rehberg, "Simplified model for steady state and real-time ampacity of overhead conductors," *IEEE Transactions on Power Apparatus and Systems*, vol. PAS-104, no. 10, pp. 2942-2953, Oct. 1985.

[43] PJM Overhead Conductor Ad Hoc Committee, "Bare overhead transmission conductor rating," [Online]. Available: http://www.pjm.com/~/media/planning/design-engineering/maac-standards/bare-overhead-transmission-conductor-ratings.ashx.

[44] IEEE Guide for Determining the Effects of High-Temperature Operation on Conductors, Connectors, and Accessories, *IEEE Standard 1283-2013*, Aug. 2013.

[45] J. R. Harvey, "Effect of elevated temperature operation on the strength of aluminum conductors," *IEEE Transactions on Power Apparatus and Systems*, vol. PAS-91, no. 5, pp. 1769-1772, Sept. 1972.

[46] V. T. Morgan, "The loss of tensile strength of hard-drawn conductors by annealing in service," *IEEE Transactions on Power Apparatus and Systems*, vol. PAS-98, no. 3, pp. 700-709, May 1979.

[47] J. Kwon and K. W. Hedman, "A transmission expansion planning model considering conductor thermal dynamics and HTLS conductors," *IET Generation, Transmission, and Distribution*, submitted for publication.

[48] J. Kwon and K. W. Hedman, "A transmission expansion planning model for wind integration with conductor sizing," working paper.

[49] H. Wan, J. D. McCalley, and V. Vittal, "Increasing thermal rating by risk analysis," *IEEE Transactions on Power Systems*, vol. 14, no. 3, Aug. 1999.

[50] Southwire Company, "ACSR," [Online]. Available: http://www.southwire.com/products/ACSR.htm.

[51] General Cable, "Bare aluminum conductor," [Online]. Available: http://www.stabiloy.com/nr/rdonlyres/d83c028b-0d2a-4680-84e7-bc9b44e7129b/0/pbare.pdf.

[52] Commerce Commission New Zealand, "Bunnythorpe-Haywards A and B lines conductor replacement investment proposal - options and costing report," [Online]. Available: http://www.comcom.govt.nz/regulated-industries/electricity/electricity-transmission/.

[53] University of Arizona, "Arizona meteorological network weather data," [Online]. Available: http://ag.arizona.edu/azmet/.

[54] NERC Reliability Assessment Guidebook, Version 3.1 (August 2012) [Online]. Available: http://www.nerc.com/files/Reliability%20Assessment%20Guidebook%203%201%20Final.pdf.

[55] P. Kundur, V. Ajjarapu, V. Vittal, *et al*., "Definition and classification of power system stability," *IEEE Transactions on Power Systems*, pp. 1387 – 1401, 2004.

[56] C. Taylor, "Power system voltage stability," MC Graw Hill, New York, 1994.

[57] P. Kundur, "Power system stability and control," McGraw Hill, New York, 1994.

[58] T. Yong, M. Shiying and Z. Wuzhi, "Mechanism research of short-term large-disturbance voltage stability," *International Conference on Power System Technology*, pp. 1-5, 2006.

[59] P. Li, B. Zhang, C. Wang, J. Shu, M. You, Y. Wang, Z. Bo, and A. Klimek, "Time-domain simulation investigates short-term voltage stability with dynamic loads," *Asia-Pacific Power and Energy Engineering Conference*, pp. 1-5, 2009.

[60] J. Diaz de Leon II, and C. Taylor, "Understanding and solving short-term voltage stability problems," *IEEE Power Engineering Society Summer Meeting*, vol. 2, pp. 745 – 752, 2002.

[61] C. Sharma, and M. Ganness, "Determination of power system voltage stability using modal analysis," *International Conference on Power Engineering, Energy and Electrical Drives*, pp. 381 – 387, 2007.

[62] M.Hasani and M.Parniani, "Method of combined static and dynamic analysis of voltage collapse in voltage stability assessment," *IEEE Transmission and Distribution Conference and Exhibition: Asia and Pacific*, pp. 1-6, 2005.

[63] T. Cutsem, and C. Vournas, "Voltage stability of electric power systems," Kluwer Academic Publishers, 1998.

Intentionally Blank

Part II

Risk-Based Constraint Relaxation for Security Constrained Economic Dispatch

Xian Guo
James McCalley

Iowa State University

For information about this project, contact

James McCalley
Iowa State University
Electrical and Computer Engineering Department
1115 Coover
Ames, IA 50011
Phone: 515 294-4844
Fax: 515 294-4263
Email: jdm@iastate.edu

Power Systems Engineering Research Center

The Power Systems Engineering Research Center (PSERC) is a multi-university Center conducting research on challenges facing the electric power industry and educating the next generation of power engineers. More information about PSERC can be found at the Center's website: http://www.pserc.org.

For additional information, contact:

Power Systems Engineering Research Center
Arizona State University
527 Engineering Research Center
Tempe, Arizona 85287-5706
Phone: 480-965-1643
Fax: 480-965-0745

Notice Concerning Copyright Material

Table of Contents

List of Figures

List of Tables

Nomenclature

Indices and sets

l	The l th circuit/line/branch
k	The k th post-contingency condition
CR	Candidate lines that can be used for constraint relaxation
NCR	Lines that are not allowable for constraint relaxation
CCS	The set of critical contingencies
$COCS$	The set of critical overloaded circuit

Parameters

N	Number of buses
NG	Number of generators
NC	Number of contingencies
NL	Number of lines
D_i	Nodal loads at bus i
$Limit_l^0$	Transmission thermal limit of line l at normal state
$Limit_l^k$	Transmission thermal limit of line l at post-contingency state k
Pr^k	Occurrence probability of contingency k

Variables

c_i	Generation bid price at bus i
P_i	Generation output level at bus i
GSF_{l-i}^0	Generation shift factor to line l from bus i at normal state
GSF_{l-i}^k	Generation shift factor to line l from bus i at post-contingency state k
h_l^k	Power flow on line l at post-contingency state k
Sev_l^k	Overload severity of circuit l at post-contingency k
$Loss$	Transmission loss for the entire network

Terms

SCED	Security constrained economic dispatch
OPF	Optimal power flow
ED	Economic dispatch
ISO	Independent system operator
IMM	Independent Market Monitor
RCPF	Reserve constraint penalty factors
LMP	Locational marginal prices
CR	Constraint relaxation
LTE	Long time emergency rating
STE	Short time emergency rating
DAL	Drastic Action Limit
RBSA	Risk-based security assessment
RBCR	Risk-based constraint relaxation
RA	Resource adequacy/ Risk assessment
PR	Percentage of rating
RUC	Residual unit commitment
MVL	Default marginal value
TCDC	Demand curve for transmission constraint
IFM	Integrated Forward Market
ATR	Adaptive transmission ratings

1. Introduction

1.1 Research premise

Security constrained economic dispatch (SCED) has been widely used in power system electricity markets, to derive dispatch decisions and the corresponding market solutions for real-time operation. The objective is to minimize production costs while satisfying demand as well as the system security requirements. The system security requirements include both those under normal (no contingency) conditions and those under post-contingency conditions (NERC's class B contingencies, otherwise known as, 'N-1' contingencies). The SCED also enforces other constraints such as minimum and maximum MW output for generators, as well as regulation and contingency reserve requirements.

The SCED is a linear program and is therefore a convex programming problem. If a solution is obtained by the optimization engine, it is certain that the solution is indeed optimal. However, there is no guarantee that the optimization engine will be able to identify a solution, because the problem may be infeasible. If the problem is infeasible, then the problem's constraints are such that there is no solution which can satisfy all of them. The occurrence of this situation is problematic because it means that market has failed for that particular condition, an unacceptable outcome.

The approach to handling infeasible problems is to relax one or more constraints. The most common constraints to relax are those associated with line flow limits. The enabling reason why constraint relaxation for line flow limits can be considered is that it is possible to allow flows on lines in excess of their modeled limit, since thermal limits generally have margin due to the fact that they are set under conservative conditions. The deterrent to relaxing line flow limits is that it exposes the power system to increased risk.

As long as the constraint is a post-contingency constraint, the additional risk depends on the occurrence of a contingency, and therefore the additional risk is relatively small. If the constraint is associated with normal (no contingency) conditions, then the additional risk may be significant. As a result, we view these two situations as fundamentally different due to the level of additional risk introduced by relaxing the constraint. We view constraint relaxation as a viable strategy for handling SCED infeasibilities when post-contingency constraints need to be relaxed. We view that use of constraint relaxations for SCED infeasibilities when normal constraints need to be relaxed may not be a viable strategy.

In this report, we develop, describe, and illustrate our suggested approach to handling SCED infeasibilities so that additional risk is minimized or reduced. Our focus is on the case where the constraint relaxation is applied to a post-contingency constraint, because we believe that this case is by far the most frequent, motivating over 90% of all SCED infeasibilities. Although we will outline a procedure for handling constraint relaxations as applied to normal constraints, we will more fully address this less frequent (but more problematic) situation in a follow-on project.

1.2 Report organization

This report includes seven chapters:

- Chapter 2 describes the background of risk-based constraint relaxation, including the concept of unmanageable constraints in SCED and application of constraint relaxation in handling infeasibility of SCED;
- Chapter 3 provides a literature review on the application of constraint relaxation with SCED, covering both academic perspectives and industry practices; in particular, it summarizes and formulates the industry-based constraint relaxation approach and describes the methods of penalty price selection among various ISOs;
- Chapter 4 formulates the approach of risk-based constraint relaxation, based on the introduction of risk indices and risk limits;
- Chapter 5 compares the industry-based constraint relaxation and the risk-based constraint relaxation approach in terms of formulation, implementation, and results, paying particular attention to the effects on LMPs;
- Chapter 6 illustrates the risk-based constraint relaxation approach;
- Chapter 7 summarizes the work, draws conclusions, and indicates future work.

2. Background

Security constrained economic dispatch (SCED) has been widely used in both operation and electricity market. However, so-called 'unmanageable constraints[1]and the resulting SCED infeasibility may occur under certain operation conditions. In this chapter, we provide necessary background associated with this problem.

2.1 Security constrained economic dispatch

The priority objective of modern electricity grids is that generation supply must meet power demand. However, there exists uncertain factors in objects of both generation and demand: 1) demand vary greatly over the time period of a day, a week or a year; 2) the costs, ramping performance are different among various generation type; 3) the introduction of renewable energy, such as wind power and solar energy. Thus, the conventional optimal power flow (OPF), or economic dispatch (ED) cannot satisfy the requirements of reliable power supply. In addition, the network security constraints at both steady-state and contingency situation must be considered at the same time. Especially, affected by the occurrence of probability, NERC's class B contingency, that it to say, 'N-1' contingency should be included in real-time dispatch, when constructing SCED. The solution of SCED will provide dispatch decisions for real-time operation, given actual load and system status, such that the reliability is maintained and the production costs are minimized.

SCED is widely used by independent system operators (ISOs) as the application within real-time electricity markets for identifying generator dispatch and related locational marginal prices (LMPs) on which market settlement is based. SCED must satisfy constraints on generators (e.g., MW output and reserve requirements) as well as constraints on circuit thermal limits under both normal and 'N-1' contingency conditions.

2.2 Unmanageable constraints and infeasibility in SCED

In SCED model, under some operating conditions, the thermal limits and generation output limits cannot be simultaneously satisfied, and as a result, the SCED is unable to provide a dispatch decision.

The industry has coined the term 'unmanageable constraint,' where a branch loading cannot be decreased below its thermal limit on a five-minute basis. This is a significant issue in congestion management. According to the Independent Market Monitor (IMM) market status report of MISO in 2007, about 25% of binding constraints cannot be managed on a five-minute basis[1]. In addition, the investigation of operation condition in MISO shows that the primary reasons for unmanageable constraints are: 1) generation inflexibility, i.e., limited re-dispatch capability is available and 2) selection of modeling parameters causes the market software to not re-dispatch resources that have small effects on the

[1] Unmanageable cases refers to the situation that a branch loading cannot be decreased below its thermal limit on a five-minute basis, and the corresponding constraints limiting the branch loading is called "unmanageable constraints". If such unmanageable cases can result in infeasibility in SCED, it will be called "infeasible cases".

transmission constraints. However, the occurrence of unmanageable constraints does not necessarily mean that the system is in violation of NERC requirements, considering that such overflows can be reduced within 30 minutes, which meets the reliability requirements.

Unmanageable cases include infeasible cases, which are generally due to an inability to resolve a transmission constraint violation. This is caused by insufficient control capability because of constraints related to ramping rate, regulation reserve and capacity.

This report focuses on infeasible cases.

2.3 Application of constraint relaxation in handling infeasibility of SCED

The general approach for handling such infeasibilities is to employ constraint relaxation (CR), where one or more constraints are relaxed to a level sufficient to obtain a feasible solution, thus avoiding the infeasibility. In electricity markets, this is a reasonable approach because emergency thermal rates of conductors are chosen with some margin so that they can withstand slightly higher loadings for a limited time[2]; for example, the actual loading could reach 110% of the long term emergency (LTE) rating if the time duration of the overload is short enough. This feature provides the foundation for the application of CR in obtaining an operating solution (and thus a market solution) for SCED problems that would otherwise be infeasible.

There are four categories of actions for constraint relaxation. (1) Accept a relaxed constraint ‘as is’ because it does not cause much risk of damage to the circuit or of additional outage to the system. This action can be used to relax constraints imposed by contingency conditions; we are cautious regarding using this approach to relax constraints imposed by normal conditions. (2) Accept a relaxed constraint because it will be possible to take a corrective action to relieve the constraint if the contingency occurs. This action can be used only for constraints imposed by contingency conditions. (3) Use monitoring equipment that reduces uncertainty associated with sagging and annealing of the circuit. This is essentially category (1), with the requirement that the investment in monitoring equipment has been made. This approach is very attractive for circuits that experience frequent constraint violations under normal conditions. (4) Utilize load curtailment. In this report, we focus on category (1), emphasizing its application for relaxation of post-contingency constraints.

2.4 Summary

This chapter provides background for the project. It introduces the concept of unmanageable constraints, unmanageable cases and infeasible cases, and points out that the focus of this report is infeasibility in SCED. In addition, it also describes the reason why the approach of constraint relaxation can play an important role in handling infeasibility of SCED. Thus, this chapter lays the foundation of the remaining report.

3. State of the art in handling SCED infeasibilities

In order to address the issue of constraint relaxation in solving infeasible SCED problem, related research has been conducted, and based on this, valuable practice has been carried out in industry, especially in ISOs. We summarize these research and practice in this chapter.

3.1 Overview

3.1.1 Constraint relaxation of SCED in academic area

CR is not unfamiliar in the general optimization literature where it refers to omitting specific constraints or changing the bound (upper bound, lower bound or both), so as to expand the feasible region. According to the literature [3-7], methods implementing CR for optimization problems involving economic dispatch include direct method, hierarchical dual revised simplex method, an analytical algorithm, and a minimum violation method - referred in this paper as the industry model. These approaches are summarized in what follows.

1. Direct method

Stott and Hobson present a method for constraint relaxation, where they increase all branch limits by a certain level and resolve the LP problem [3], repeating this procedure until a feasible solution is attained. This method is quite straightforward, but it tends to over-relax, i.e., it relaxes more constraints than are necessary; in addition, it does not account for the effects on system-level security.

2. The hierarchical dual revised simplex method

Based on the sparse dual revised simplex method, which is tailored to benefit from sparsity in economic dispatch formulations [4], Irving and Sterling [5] present a hierarchical method for constraint relaxation with economic dispatch. In an infeasible case, the 'softest' branch constraint is selected to be relaxed for each iteration, evaluated by the sensitivity to correct the violation condition. This approach guarantees that the violation only affects the relevant constraints because for each iteration, only the soft constraints which have control sensitivity sufficient to alleviate violations in the overloaded line (called eligible soft constraints), are chosen to be relaxed; however, the LP iterations for relaxation will increase significantly.

3. Analytical algorithm [6]

This method is an extension of method 2; it implements a 'sensitivity-weighted sharing' strategy for situations where the sensitivity of eligible soft constraints are not equal. A specific weighting function is designed for each eligible soft constraint, and the constraint with higher sensitivity is relaxed, attached with higher relaxation value. This relaxation procedure does not require additional iterations or memory.

4. A minimum-violation method

This method is proposed in reference [7], where the objective function is the minimum deviation to achieve a feasible solution. In this method, the transmission lines, whose thermal ratings can be relaxed, are considered as candidate constraints for relaxation; then a slack variable is imposed in each candidate constraint, and a corresponding penalty cost for each violation (a function of the corresponding slack variable) is added to the objective function. For this method, the introduction of slack variables increase the computational burden, although not significantly so. This method has been widely applied in the industry, as described in section 3.1.2.

In method 1, method 2 and method 3, there is no consideration of system-level security[2] in relaxing the constraint, and there is no explicit criteria to choose the relaxation level. Method 4 does consider system-level security, at least indirectly, in that it minimizes the amount of violation costs. However, in method 4, the selection of penalty price is subjective; if too low, the line may be over-relaxed, but if too high, the constraint may result in LMP spikes.

3.1.2 Constraint relaxation of SCED in industry

The ISOs in the U.S., responsible for operating their electricity markets, have made significant efforts in addressing infeasible SCEDs. In this subsection, we describe the specific implementations in five of the ISOs, with particular focus on the nuances of each ISO's implementation.

1. Constraint relaxation in California ISO (CAISO)[8]

When the market optimization attempts to satisfy the objective of balancing supply and demand, considering the transmission constraints, there are times when the transmission limits cannot be satisfied under the current market software and calculation procedure. That is to say, economic bid alone cannot yield a complete and feasible solution, i.e. there exists some violations in constraints. Thus, uneconomic adjustments policy are implemented by market software to allow constraint relaxations in transmission flow limits.

'Uneconomic adjustments' refers to constraint relaxation in overloading transmission lines, in which slack variables representing the level of constraint relaxation and the corresponding penalty price resorts to the required priority hierarchy[3], which is irrelevant to costs and only intended as an optimization tool in CAISO. That is the reason that such a policy is called 'uneconomic adjustments'. The value of penalty price is artificially extreme, completely beyond the range of bid floor and bid cap, to guarantee that economic bids are relied on first to reach the market solution. In addition, the penalty prices of different priority are significantly far apart from each other, to ensure that adjustment of higher priority is in effect before that of the lower priority. As mentioned above, the extreme value of penalty price tend to result in LMP spike, thus it is not appropriate to determine LMP. Currently, two market runs are applied in market structure of CAISO, to achieve

[2] System-level security reflects the expectation of the sum, over all 'N-1' contingencies, of normalized flows on post-contingency heavily loaded circuits. We quantify system-level security using risk, which will be described in Section 4.2.1.

[3] Priority hierarchy represents the priority of constraint relaxation among soft constraints.

operationally sound and economically reasonable solutions: a scheduling run includes extreme penalty price to determine schedule plans for generators and ancillary service; a pricing run which determines reasonable LMP price for energy and market marginal price for ancillary service. Especially, the penalty price is huge in the scheduling run, to ensure the priority of constraint relaxations. However, the penalty price in the pricing run is not extreme value; they are set according to multiple of bid cap or bid floor, and can reflect the costs of violating flow limits. The price for a transmission slack variable is set to 3 times the bid cap in 2008. Thus, for those constraints without constraint relaxations, the LMP prices calculated from the scheduling run and pricing run have no differences; for those constraints with constraint relaxations, the above two LMPs are different.

2. Constraint relaxation in MISO [9]-[10]

In the implementation of constraint relaxation by MISO, when the constraint exceeds its binding limit, the SCED is unable to determine the shadow price for the energy that is flowing through the constrained circuit. Historically, MISO has applied three approaches to address this condition.

Prior to February 1, 2012, when a transmission constraint violates, a constraint relaxation algorithm would attempt to relax the constraint limit, considering the available resources. The price of relaxation is set according to the marginal price of the available resources. However, such a method could not reflect the severity of the exceedance level. For instance, if there is no resources available for constraint relaxation, the shadow price would be zero, which is obviously not appropriate.

In order to solve the above problems, beginning in 2012, the other two approaches are applied in practice, one is default marginal value limit (MVL) and the other is demand curve for transmission constraint (TCDC). These two methods are described in Section 3.2.2.

3. Constraint relaxation in ERCOT [11]-[12]

Constraint relaxation in ERCOT is concentrated on transmission network and power balance constraint managements, thus shadow price caps have been established by ERCOT Board. In which, 1) the effect of the shadow price cap for transmission network constraints is to limit the cost calculated by SCED optimization to resolve an additional MW of congestion on a transmission network constraint to the designated maximum Shadow Price for that transmission network constraint; 2) The effect of the shadow price cap for the power balance constraint is to limit the cost calculated by the SCED optimization when power balance constraint is violated.

(1) The SCED optimization model based on constraint relaxation

a. Objective function:

Minimize {Cost of dispatching generation + Penalty for violating power balance constraint + Penalty for violating transmission constraints}, or

Minimize {sum of (offer price * MW dispatched) + sum (Penalty * power balance violation MW amount) + sum (Penalty *Transmission constraint violation MW amount)}

b. Constraints:

- *Power Balance Constraint :*

Sum (Base Point) + under gen slack – over gen slack = generation to be dispatched

- *Transmission Constraints:*

Sum(Shift Factor * Base Point) – violation slack ≤ limit

- *Dispatch Limits*

Lower Dispatch Limits ≤ Base Point ≤ Higher Dispatch Limits

c. LMP at each electrical bus:

$$LMP_{bus,t} = SP_{demand,t} - \sum_{c} GSF_{bus,c,t} \cdot SP_{c,t}$$

Where, $SP_{demand,t}$= Power Balance Penalty (if a Power Balance violation exists) at time interval 't';
$GSF_{bus,c,t}$= Generation Shift Factor impact of the bus 'bus' on constraint 'c' at time interval 't';
$SP_{c,t}$= Shadow price of constraint 'c' at time interval 't' (capped at Max Shadow Price for this constraint).

(2) Situations with insufficient reserve

During scarcity if a transmission constraint is violated then transmission constraint and power balance constraint will interact with each other to determine whether to move up or move down a resource with positive *SF* to the violated constraints if there are no other resources available.

1) Cost of moving up the Resource = Shift Factor * Transmission Constraint Penalty + Offer cost;
2) Cost of moving down the Resource = Power Balance Penalty.

If 1) > 2), the resource will be moved down for resolving constraints;
If 1) < 2), then the resource will be moved up for meeting power balance.

4. Constraint relaxation in Other ISOs

(1) Reserve constraint penalty factors (RCPF) in ISO-NE [13]

When there is constraint violations in transmission line flow, more reserve requirements are addressed, in order to relax the constraints, thus to have a feasible solution. RCPF in the real-time market is to limit the cost that the model may incur to meet the reserve demand, and determine the market behavior under tight operating conditions. Once the reserve is in shortage, the unit whose marginal cost is lower than RCPF will be backed down to provide the reserve instead of the energy. Thus opportunity costs are generated.

At first, the local RCPF is set as $50/MWh, but according to the real-time operation practice, this value is not high enough to schedule all the available resources, so the value is changed to $250/MWh in January 1, 2010. This value can meet the reserve requirements for real-time market operation.

(2) Reserve penalty factors in PJM [14]

When energy and reserve prices are allowed to fall in the wake of some emergency actions, such as voltage reduction or manual load dump actions, the wrong price signal would be sent to market participants, for the demand of additional resources. PJM proposes to apply reserve penalty factors to avoid such a problem. Similar to those approved for the NY-ISO and ISO-NE, price caps for both synchronized and non-synchronized reserves are developed. If there is a shortage of primary reserve, the reserve price would be $850/MWh. Furthermore, if the shortage is within the synchronized reserves, the price is $1700/MWh.

PJM states that the reserve penalty price must be set high enough, to make use of all the physical available resources. What's more, the price for regulation service at five-minute intervals has been set, and emergency resources are allowed to set price.

5. Summary of industry approaches

According to the literature review, the industry has rich practice in constraint relaxation for the real-time market based on SCED. The constraints that could be relaxed include power balance, transmission line limits and reserve market constraints.

Overall, the general idea is to introduce slack variables where the constraints are violated. Then add the penalty costs for the slack variable in the objective function. Thus, the infeasible SCED are guaranteed to be optimal. But the challenge is that how to define the penalty price and whether the reserve resources are sufficient for regulation. As discussed above, the ISOs introduce many reasonable approaches to set the penalty price.

The motivation of our work is that we perceive two distinct weaknesses in the existing industry-based method for performing constraint relaxation for infeasible SCED problems. The first is that it requires a penalty price of flow violations, exogenously selected, which has significant influence on the resulting LMPs. The second is that constraint relaxation necessarily results in increased exposure to adverse consequences of contingencies, characterized as system risk, yet this increased exposure is not quantified and therefore not used in deciding which constraint to relax or how much. To this end, we investigate the benefits of using a risk metric, as discussed in Section 3.1.3, for constraint relaxation. We believe risk-based constraint relaxation is effective in addressing infeasible SCED problems.

3.1.3 Risk-based optimal power flow

Risk assessment (RA) has been widely used in other industries such as nuclear, aerospace, oil, food, public health, information technology and financial engineering. Although risk assessment for thermal overload –related security assessment has been used in a variety of power system engineering applications, its use for purposes of security assessment is relatively new, with the first publication on this topic occurring in 2003 [15,26] and a number of others occurring thereafter [16-26].

According to the IEEE standard, risk can be calculated as the product of the probability a contingency occurs multiplied by the consequence of that contingency. In real world, both the probability and the consequence of an event occurrence are difficult to quantify.

Risk is a measure of uncertainties, which could be applied in addressing the increasing uncertainty factors in current power system, such as the integration of various generation resources (wind power and solar energy) and humans behavior in using electricity (such as demand response), and also the allocation of smart grid. This is a major motivation of proposing risk-based approach in economic dispatch and system operation.

Risk-based approach is an emerging new direction and has already been used in related research on power system. Literature [17] and [18] implement risk metrics in obtaining better schemes of power system planning; while literature [19] and [20] describe the application of risk in power system maintenance. We notice that most of the previous work refers to risk-based security assessment (RBSA). Until then, research on the application of risk-based approach for real-time operation is rare and none for handling infeasibility in SCED problem. Literature [21] and [22] proposed the frameworks of risk-based approach application for power grid, but did not provide details on how to realize it. A risk-limiting dispatch under smart-grid environment was proposed in literature[23]. Although it has provided models taking into account the stochastic nature of renewable sources and the demand response, it is difficult to extend the model in real-world large-scale power systems.

Literature [24] and [25] have done significant work on risk-based optimal power flow, especially risk-based SCED and congestion management. It answers the following question appropriately,

- How to embed risk and the benefits of its use into the real-time operation software of today's ISO-based power system while maintaining it to be mathematically rigorous and computationally tractable, without decreasing the system's overall security level.

The introduction of the parameters motivates the coordination between system risk and thermal limits, we would get the trade-off between economy and security by conducting risk-based SCED. We can also improve economy and security at the same time. These study and achievements have paved the way for implementing risk metric in handling infeasibility of SCED.

3.2 Formulation of industry-based constraint relaxation

As mentioned in Section 3.1, constraint relaxation with penalty price has been implemented in solving infeasible SCED in industry. This subsection summarizes and formulates the industry-based CR method. In addition, the selection of penalty price is described in detail.

3.2.1 Formulation

A slack variable $\propto_l^k$ is added into a designated soft constraint (usually a transmission thermal limit), and the corresponding penalty cost is introduced in the objective function. The formulation is as follows, denoted as CR-F1.

$$Min \sum_{i=1}^{NG} c_i \times P_i + \sum_{k=1}^{NC} \sum_{l=1, l \in CR}^{NL} Penalty_l^k \times \alpha_l^k \tag{3-1}$$

subject to:

$$\sum_{i=1}^{N} P_i - \sum_{i=1}^{N} D_i - Loss = 0 \tag{3-2}$$

$$P_i^{\min} \le P_i \le P_i^{\max} \tag{3-3}$$

$$\sum_{i=1}^{N} GSF_{l-i}^{0}(P_i - D_i) \le Limit_l^0, \quad for\ l \in \{all\ \ lines\} \tag{3-4}$$

$$\begin{cases} h_l^k = \sum_{i=1}^{N} GSF_{l-i}^{k}(P_i - D_i), \\ for\ l \in \{all\ \ lines\}\ k \in \{contingency\ set\} \end{cases} \tag{3-5}$$

$$\begin{cases} h_l^k - \alpha_l^k \le Limit_l^k,\ (\alpha_l^k \ge 0) \\ for\ l \in CR, k \in \{contingency\ \ set\} \end{cases} \tag{3-6}$$

$$\begin{cases} h_l^k \le Limit_l^k, \\ for\ l \in NCR, k \in \{contingency\ set\} \end{cases} \tag{3-7}$$

where (3-1) is the objective function, including production costs and penalty costs, (3-2) is the power balance constraint, (3-3) are the generation output constraints, (3-4) are the transmission thermal constraints under the normal (no contingency) state, (3-5) are the post-contingency circuit flows (here, we only consider 'N-1' contingency), and (3-6)~(3-7) are the corresponding post-contingency thermal constraints. Equation (3-6) represents the soft constraints for the optimization problem, i.e., those constraints that are considered to be relaxable under the allowed range of thermal ratings. Equation (3-7) is the hard thermal limit constraints that have been identified as unrelaxable constraints . Such unrelaxable constraints may exist for two reasons: 1) high loadings may damage the circuit, e.g., an older transformer is known to be gassing; 2) outage of the circuit causes extreme consequences, e.g., studies indicate a particular transmission line will create very severe voltage problems if it sags and outages. The first kind of unrelaxable constraint are manually entered into constraint relaxation applications; the latter kind are identified through a pre-screen.

As mentioned in the Section 3.1, the industry model does not monitor or control system-level security, and the selection of the penalty price value is heuristic, which has been a significant challenge.

3.2.2 Determination of penalty price

ISOs set penalty prices as constants, with respect to voltage level, violation severity and reserve availability. The values vary according to the specific condition and individual ISO. Here, we describes the selection of penalty price in CAISO, MISO and ERCOT. The values of penalty price in other ISOs have already been mentioned in Section 3.1.2.

1. Penalty price in CAISO [8]

Based on the ongoing testing, CAISO has proposed recommended values for Integrated Forward Market (IFM), residual unit commitment (RUC) and real-time market. Here, we address some important parameters in real-time market, according to different subjects. Penalty values are negatively valued for supply reduction and positively valued for demand reduction.

Group1: Energy balance/Load curtailment and Self-Scheduled exports utilizing non-RA (resource adequacy) capacity
The penalty price for scheduling (or pricing) run is $6500/MW (or $500/MW). In the scheduling run, it is essential to produce supply matching demand plus losses. Using the energy bid cap as the parameter in the pricing run, the energy price will rise to at least the energy bid cap to reflect the energy supply shortage. Since Self-Scheduled exports supported by Non-RA capacity receive the same priority as the CAISO demand forecast, the same priority is used for exports.

Group 2: Transmission constraints: branch, corridor, nomogram (base case and contingency analysis)
The penalty price for scheduling (or pricing) run is $5000/MW (or $500/MW). In the scheduling run, the guideline applied to transmission constraints is that an Economic Bid should be accepted if it is priced at the bid cap and is at least 10% more effective in relieving a transmission constraint. In the pricing run, a single penalty price segment is modeled at the Energy Bid cap. This is consistent with the pricing parameter value for energy balance relaxation under a global energy supply shortage.

2. Penalty price in MISO [9][10]

Beginning February 1, 2012, considering that insufficient shadow price is generated by the constraint relaxation algorithm with available resources, as well as the reliability costs of violating the constraints is understated. MISO adopts MVL value for the shadow price when a constraint exceeds its binding limit, as recommended by IMM. Since MVL is the maximum amount that the market is willing to spend to manage the constraint, the price transparency is increased, and will inspire the market participants to reduce the transmission line flow.

Currently, MISO applies default MVL based on transmission voltage, shown as Table 3-1. Group 1 is applied in the regular operation status; while Group 2 is implemented for transmission constraints that cannot be managed by the established MVL for the voltage in Group 1.

Table 3-1 MVL values of MISO

Group 1	Group 2
• $3,000 for Interconnection Reliability Operating Limit (IROL) constraints • $2,000 for System Operating Limit (SOL) constraints, $V \geq 161\text{kV}$ • $1,000 for SOL constraints with voltage $100\text{kV}\sim161\text{kV}$ • $500 for SOL constraints, $V \leq 100\text{kV}$	• Constraints with $V \leq 138\text{kV}$ have been determined to be significantly impacted by regional flows, and these constraints use a $2,000 default MVL

Applying MVL has so many advantages, but significant price spikes have occurred in the operation practice, which is caused by insufficient ramping capability over a five-minute dispatch period. However, these exceedances usually have no detrimental reliability impact. In order to solve such a problem, TCDC is proposed to add a second, lower MVL value for overloaded flow between 100% and 102% of the binding limit. That is to say, when the overloaded flows are between 100% and 102%, TCDC is applicable, while the original MVL value is still maintained, when it exceeds 102%.

TCDC shall be used by the Transmission Provider to limit the cost of the re-dispatch incurred to manage a constraint and to determine the shadow price for transmission constraints when the flow over a constraint cannot be managed within the binding limit in a dispatch interval. TCDCs shall be used in both day-ahead and real-time energy and operating reserve markets. Table 3-2 indicates the demand curve for Group 1 and Group 2 correspondingly.

Table 3-2 Demand curve for transmission constraints (unit: $/MWh)

Group 1		$\leq 100\text{kV}$	$100\sim161\text{kV}$	$\geq 161\text{kV}$
Binding constraint exceeding percentage	$\geq 2\%$	500	1000	2000
	$< 2\%$	400	700	1000
Group 2		$\leq 100\text{kV}$	$100\sim161\text{kV}$	$\geq 161\text{kV}$
Binding constraint exceeding percentage	$\geq 2\%$	1000	2000	3000
	$< 2\%$	700	1000	2000

3. Penalty price in ERCOT [11],[12]

ERCOT has formulated the mechanisms to determine penalty price (or called shadow price caps) for transmission line constraint, detailed as follows.

The penalty price for transmission lines are affected by the maximal LMP congestion component ΔLMP_{max}^{cong} $(\$y/MWh)$ that transmission lines can handle. Once the shift

factor efficiency threshold $SF_{thershold}^{efficiency}$ (x%) is known, the maximum shadow price for transmission thermal limits constraints can be expressed as

$$SP_{\max} = \Delta LMP_{\max}^{cong} / SF_{threshold}^{efficiency} \quad (3\text{-}8)$$

Based on this method, the transmission constraint shadow price caps in SCED is :

- Base case/Voltage violation: \$5000/MW
- 'N-1' contingency case: \$4500/MW, \$3500/MW, \$2800/MW for 345/138/69 kV

3.3 Summary

This chapter describes the overview of CR in infeasible SCED both in academic area and industry practice. In addition, the concept of risk has been proposed and the application of risk-based approach in power system has been discussed in detail. Especially, risk-based OPF and risk-based SCED have been addressed, which provides the foundation for risk-based constraint relaxation in this report.

According to the literature review from industry approaches in handling infeasibility of SCED, the industry-based CR has been formulated in this chapter. In addition, how to select the penalty price in various ISOs has also been described. Thus, the solution from industry-based CR can be compared with that from risk-based CR.

4. Risk-based constraint relaxation

As discussed in Chapter 3, the industry-based constraint relaxation approach does not consider system-level security. The risk-based constraint relaxation (RBCR) is adopted in order to ensure the security at the system level when conducting constraint relaxation. In this chapter, we introduce RBCR in terms of three issues:

- The principles guiding construction of the RBCR formulation;
- The definition of risk, and how to calculate it;
- The formulation of RBCR.

4.1 Two approaches for risk-based constraint relaxation

Risk can be included within an optimization problem in two ways: (1) as a component within the objective function, where it is typically summed with a cost function; (2) as a constraint. We have investigated both approaches in this Chapter, and we refer to them as RBCR-F1 and RBCR-F2 respectively.

The strength associated with including risk within the objective function, RBCR-F1, is that it enables minimization of cost and risk simultaneously. The weakness is that it directly affects the resulting LMPs; in addition, it requires selection of a multiplier to appropriately weight the risk component relative to the cost component.

Criteria for judging the strength of the RBCR-F2 approaches are:

(1) The conditions obtained from use of RBCR-F2 should be less risky than the conditions obtained from the industry-based CR;

(2) The particular 'N-1' contingency or contingencies causing the infeasibility (called critical contingency or critical contingencies) obtained from use of RBCR-F2 should be less risky than that contingency is (or than those contingencies are) under the conditions obtained from the industry-based CR;

(3) The risk associated with a subsequent outage (an 'N-1-1' outage) of the circuit having the relaxed constraint should be less under the conditions obtained from use of RBCR-F2 than under the conditions obtained from use of the industry-based CR.

4.2 Fundamentals of risk-based constraint relaxation

4.2.1 Definition of risk metric

Risk is a probabilistic metric to quantify the likelihood and severity, which are the factors reflecting system security[26]. The severity of a post-contingency condition, can be assessed in terms of overload severity, cascading overload severity, low voltage severity and voltage instability severity[27]. Here, we consider only overload severity; however, in previous studies, we have shown that system-wide control of overload severity also benefits other forms of severity as well.

We define the risk metric for a particular contingency k resulting in post-contingency loading on circuit l as the probability of occurrence for that contingency times the thermal overload severity on circuit l resulting from that contingency, i.e., $Risk = \Pr_k Sev_l^k$.

Although contingency k could be any contingency, we restrict them to only those included within NERC's class B reliability criteria, that is to say, 'N-1' contingencies, in order to conform to industry practice.

1. Probabilities of contingencies

Based on a specific system network topology and operation state characterized by demand and dispatch, we desire to calculate risk associated with pre-defined contingencies, characterized by the outage of a particular power system component, generally a circuit or a generator.

The probabilities of contingency can be rigorously quantified based on historical data and real-time information [28]. The probability for occurrence of a contingency is defined with respect to a time interval consistent with the dispatch period. In most cases today, the dispatch time interval is 5 minutes. We normalize the chosen time interval to 1 unit. Then, we assume that the occurrence of contingency k follows the Poisson distribution. Thus, the probability of a certain contingency k is the probability that the contingency occurs at least one time in the next time period, while all other contingencies do not occur; this probability is:

$$\Pr_k = (1 - e^{-\lambda_k}) \exp(-\sum_{k \neq i} \lambda_j) \tag{4-1}$$

Where λ_k is the occurrence rate of contingency k per time interval. References [29]-[30] propose a statistical method of computing parameter λ_k that uses historical data, weather, geography, and voltage level [31, pp. 246].

When calculating the probabilities of contingencies, another important issue is that market operation procedure should be considered, that is to say, the corresponding probability for each operation point should be adapted to specific market [16]. As shown in Figure 4-1, before T_0 of midnight in Day 1, the day-ahead market will clear, providing unit commitment and SCED outcomes. In order to guarantee the necessary probabilities are available before hour t_N of Day 2, the calculation should be conducted between time interval $[t_{N-1}, t_N]$, based on the closest real-time weather information and operation status, such as forecasted load and facility condition.

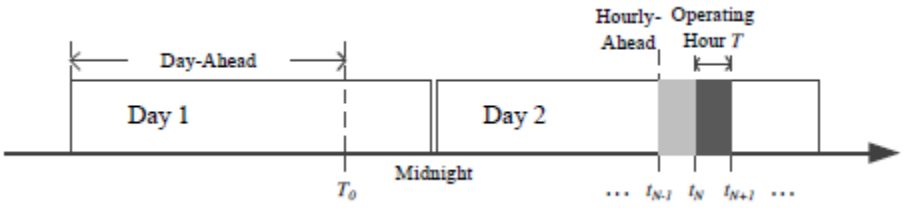

Figure 4-1 Market operation timeline

A simpler approach, which conforms in principle to conventional 'N-1' security assessment (which does not distinguish between 'N-1' contingencies in terms of probabilities), is to

assume the probabilities of all 'N-1' contingencies are identical and equal to $(1/n)(1 - Pr(Normal\ Condition))$ where n *i*s the number of 'N-1' contingencies; in this case, variation in $Risk$ from one contingency to another is entirely determined by the severity level Sev_l^k.

2. Overload severity

The overload severity function should quantify the consequence of the contingency and appropriately represent the circuit loading condition. Because severity increases with post-contingency loadings, the values of post-contingency flows in heavily-loaded circuits determine the corresponding value of severity. We quantify power flow as a percentage of rating (PR) in order to generalize the definition of overload severity function [16].

The dashed curve in Figure 4-2 illustrates an ideal overload severity function. The solid lines approximate the ideal curve; we utilize this approximation in order to maintain linearity and continuous differentiability in evaluating risk.

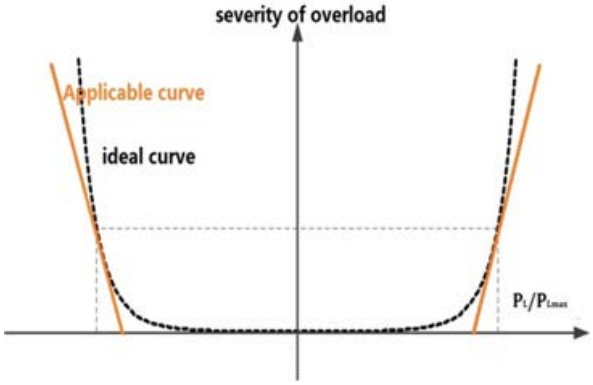

Figure 4-2 Severity function of circuit overloading

Although the dashed line is a convex representation, computational burden is increased when computing the severity of each circuit associated with all 'N-1' contingencies. Consequently, we form a piecewise-linear approximation for this function [25], as shown in Figure 4-3. The breakpoints of the approximation are chosen based on adaptive transmission ratings (ATR). ATR includes 1) Long Time Emergency (LTE) rating for loadings that can be accepted for up to 4 hours; 2) Short Time Emergency (STE) rating for loadings that can be accepted for up to 15 minutes and 3) Drastic Action Limit (DAL) for loadings that cannot be tolerated and must be immediately relieved [2].

We assume that the severity of post-contingency flow under 90% LTE is zero; thus the severity value of circuit flow between $[-0.9\text{LTE}, 0.9\text{LTE}]$ is zero. Then there are three segments: segment 1, $[0.9\text{LTE}, \text{LTE}]$ or $[-\text{LTE}, -0.9\text{LTE}]$ segment 2, $[\text{LTE}, \text{STE}]$ or $[-\text{STE}, -\text{LTE}]$ and segment 3,$[\text{STE}, \text{DAL}]$ or $[-\text{DAL}, -\text{STE}]$. The severity value when the circuit flow reaches LTE, is 1. The severity value when the circuit flow equals STE is c_1, and the maximum severity value, i.e., the value when the circuit flow equals DAL, is c_2. The value of c_1 and c_2 can be adjusted based on the perspective of the user. However, to ensure the convexity of the function, equation (4-2) and (4-3) should be satisfied.

$$c_1 > \max_l\{10 \times STE_l / LTE_l - 9\} \tag{4-2}$$

$$c_2 > \max_l\{\frac{(c_1 - 1) \times DAL_l - c_1 \times LTE_l + STE_l}{STE_l - LTE_l}\} \tag{4-3}$$

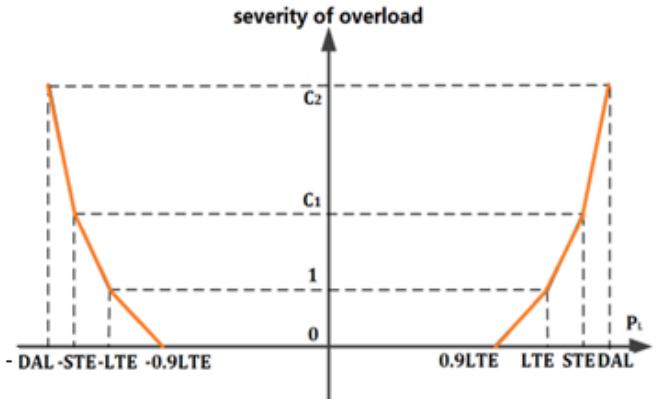

Figure 4-3 Piecewise linear function for severity calculation

As indicated by the severity function illustrated in Figure 4-3, heavily loaded circuits (for which, in our risk-based constraint relaxation procedure, dispatch action is taken) are those having flows exceeding 90% of their LTE; this is in contrast to the industry model (and to the general industry practice), which only takes dispatch action to reduce flows exceeding LTE. However, this is not a simple down-shifting of the LTE because the re-dispatch control effort made to reduce risk within the risk-based constraint relaxation does so in proportion to the severity function. Thus, higher flows, e.g., 105% of LTE, motivate more control effort than do lower flows, e.g., 91% of LTE.

4.2.2 Definition of risk indices

In order to evaluate system security level, a set of risk indices based on the risk metric are introduced, as follows:

1. *System risk*: it is a function of normalized flows for the heavier-loaded circuits, which equals to the summation over all pre-defined contingencies of each contingency probability times the contingency severity [16].

$$Risk = \sum_{k=1}^{NC} (\Pr_k \sum_{l=1}^{NL} Sev_l^k)) \tag{4-4}$$

2. *Contingency risk*: it is to evaluate the system security level under a particular contingency k.

$$CtgRisk_k = \Pr_k \sum_{l=1}^{NL} Sev_l^k \tag{4-5}$$

3. *Second contingency circuit risk*: it is the contingency risk of circuit l following the outage of a particular contingency k, i.e., this is the second contingency occurring within an 'N-1-1' outage; it is the contingency risk under 'N-1-1' condition.

$$CctRisk_l^k = \Pr_l^k \sum_m Sev_m^l \tag{4-6}$$

We observe that Pr_l^k is a conditional probability, i.e., it is the probability of losing circuit *l* given a prior loss of circuit *k*.

4. *Total second contingency circuit risk*: the summation of second contingency circuit *l* risk over all first-contingencies *k*. Thus, this is the total risk of a second contingency resulting in loss of circuit *l*.

$$TCctRisk^l = \sum_k \mathrm{Pr}_l^k \sum_m Sev_m^l \tag{4-7}$$

4.2.3 Risk limits

In the RBCR-F2 model, we constrain the risk indices not to exceed certain reference values. The RBCR procedure requires contingency risk limits for each contingency, second contingency circuit risk limits for each circuit, and a single risk limit for the system. Upper bounds for these limits are determined by identifying the associated metric under a stressed system that is considered secure under standard NERC operating criteria. In addition, there are two applications for risk indices.

- **Pre-defined contingency selection**

The 'N-1' contingency analysis is based on a predefined contingency set. If the number of contingencies are excessive, then computational burden may be a big challenge, and in this case, we may choose to include only a selected number of contingencies (e.g., based on a ranking algorithm) that are known to caused high post-contingency loadings. That is to say, we can rank the contingencies according to the contingency risk and make decisions on contingency selection.

- **Selection of the circuits not available for constraint relaxation**

There may be circuits having excessive second-contingency circuit risk, implying that a second contingency involving outage of circuit *l* following outage of circuit *k* will result in very severe consequences. If a constraint relaxation will expose the system to significantly higher risk, it is prudent to avoid constraint relaxation for such a circuit.

4.3 Risk-based constraint relaxation under formulation 1

In this section, we describe the RBCR-F1 approach where the risk term is included in the objective function.

4.3.1 Formulation of RBCR-F1

The objective function of the RBCR-F1 is to minimize the sum of production costs plus system risk, as indicated in the following formulation:

$$Min \sum_{i=1}^{NG} c_i \times P_i + \mathrm{C}_r \times Risk \tag{4-8}$$

Subject to:

$$\sum_{i=1}^{N} P_i - \sum_{i=1}^{N} D_i - Loss = 0 \tag{4-9}$$

$$P_i^{\min} \le P_i \le P_i^{\max} \tag{4-10}$$

$$\sum_{i=1}^{N} GSF_{l-i}^{0}(P_i - D_i) \le Limit_l^0, \quad for\ l \in \{all\ \ lines\} \tag{4-11}$$

$$h_l^k = \sum_{i=1}^{N} GSF_{l-i}^{k}(P_i - D_i) \tag{4-12}$$

$$\begin{cases} h_l^k - \beta_l^k = K_{c,l} Limit_l^k, \\ for\ l \in CR, k \in \{contingencies\ set\} \end{cases} \tag{4-13}$$

$$\begin{cases} h_l^k \le Limit_l^k, \\ for\ l \in NCR, k \in \{contingency\ set\} \end{cases} \tag{4-14}$$

$$Sev_l^k \ge 0 \tag{4-15}$$

$$Sev_l^k \ge a_{1l} h_l^k - 9 \tag{4-16}$$

$$Sev_l^k \ge a_{2l} h_l^k - a_{3l} \tag{4-17}$$

$$Sev_l^k \ge a_{4l} h_l^k - a_{5l} \tag{4-18}$$

(4-12) and (4-15~4-18) $for\ l \in \{all\ \ lines\}\ k \in \{contingency\ set\}$

$$Risk = \sum_{k=1}^{NC} (\Pr_k \sum_{l=1}^{NL} Sev_l^k)) \tag{4-19}$$

Here, C_r is the penalty price associated with risk; it transforms the optimization problem from multiple-objective to single objective. Constraints (4-9)-(4-12) are the same as those in the industry-based model. Constraint (4-13) introduces the relaxation level $K_{c,l}$ for each circuit l, where the slack variable β_l^k, is used as the violation indicator, identifying which circuits are overloaded under the current limit $K_{C,l} \times Limit$ (positive value implies violation, zero or negative value means no violation) and needs to be relaxed. Constraints (4-15)~(4-18) model the severity evaluation, in which parameters of $\{a_{1l}, \ldots a_{5l}\}$ could be determined by the value of parameters c_1, c_2. Equation (4-19) expresses the system risk calculation.

4.3.2 Determination of C_r

When we examine equation (4-13) and (4-15)~(4-19), we observe that $Risk$ can be expressed as a weighted linear function of β_l^k,

$$Risk = \sum_k \sum_l b_l^k \beta_l^k \tag{4-20}$$

Thus, system risk provides a way of selecting penalty function. Instead of determining penalty price for every circuit violation under a contingency, RBCR-F1 only requires a single penalty price to identify the tradeoff between production costs and risk, and thus between economics and security.

In addition, risk as the penalty function provides a reasonable re-distribution on system violations, valuated by probability of overload occurrence and corresponding consequences severity. If probability is higher or severity is higher or both are higher, the corresponding

penalty for such circuit overload is comparatively higher, resulting in reduction of such overloadings, and vice versa.

As discussed above, only need to determine one single penalty price is an attractive feature possessed by RBCR-F1, in comparison with industry-based constraint relaxation.

Considering that a low penalty price results in increasing system risk, while a high penalty price causes less relaxation and high LMP spikes. We propose two criteria to determine the range of reasonable C_r:

1. Criteria 1 is implemented to determine the upper bound of C_r , which is determined by the minimum value of C_r that could achieve the smallest value of *Risk.* The procedure is as follows:

   (1) Set $C_r = 50$, solve risk-based constraint relaxation model, then output production costs and $Risk$.

   (2) Increase current C_r with a specific ΔC_r , solve risk-based constraint relaxation model again.

   (3) Repeat step (2) until the value of $Risk$ and production costs tend to saturate, and it reaches a steady-state. The minimum value of C_r , which makes $Risk$ the smallest, is set as C_r^{upper}.

2. Criteria 2 is applied to achieve the lower bound of C_r, which is based on the evaluation on economic effects of $Risk,$, determined by $\Delta ProductionCosts/\Delta Risk$. The procedure is as follows:

   (1) Revise the risk-based constraint relaxation model: remove $Risk$ term in the objective function, add $Risk \leq Risk_{max}$ in the constraints.

   (2) Choose a tight $Risk_{max}$, which makes $Risk \leq Risk_{max}$ binding, and calculate the corresponding production costs.

   (3) Repeat (2) several times, then calculate the average $\Delta ProductionCosts/\Delta Risk$ and this value is set as C_r^{lower}.

   We can select the value of C_r from the range $[C_r^{lower}, C_r^{upper}]$.

4.3.3 Relaxation level determination

One approach to using RBCR is to set the same relaxation level for all circuits that are candidates for constraint relaxation. However, this approach may result in occurrence of some circuit overloads even though their occurrence does not contribute to alleviating the infeasibility. For example, allowing overload on a 69kV circuit in Louisiana would not alleviate an infeasibility on a 69 kV circuit in Minnesota. Thus, a preliminary problem is to determine a $\{K_{c,i}, i = 1, \dots, NL\}$ that achieves a feasible solution while minimizing increase of system-level risk.

In order to identify the relaxation level $K_{c,l}$, we make two observations. The first observation is that the risk-based constraint relaxation formulation contains β_l^k, which is the violation indicator for the infeasible SCED model. The purpose is to identify the minimum relaxation of the candidate soft constraints, while achieving the minimization of objective function.

The second observation is that, the relaxation level should be bounded, that is to say, the flow should be no more than what can be accommodated within the allowable time it will take to relieve the loading. The concept of ATR limit is thus imposed. Here, we choose 1.24LTE, which is slightly less than DAL as the bound.

We determine $K_{c,l}$ for circuit *l* as the relaxation needed to solve the SCED problem, but we do not allow a relaxation to exceed DAL. This approach is described as follows.

- Determine relaxation level 1 based on violation indicator β_l^k : Calculate $K_{c,l(1)}$ according to the maximum value of positive violation indicator $\max_{k=1,\ldots,\mathrm{NC}} \{\beta_l^k\}$;
- Determine relaxation level 2 based on ATR: Calculate $K_{c,l(2)}$ according to the value close to DAL for circuit *l*, 1.24LTE;
- Choose the smaller one between relaxation level 1 and relaxation level 2: $K_{c,l} = \min\{K_{c,l(1)}, K_{c,l(2)}\}$.

4.3.4 Procedure of RBCR-F1

The procedure for RBCR-F1 is described as follows:

Step 1: Solve the RBCR-F1 model using original limits. Identify the violated circuits based on the values of violation indicator β_l^k. The set of these violated circuits are denoted as Ω_V.
Step 2: Determine $K_{c,l}$ for each circuit flow limit, using the approach proposed in Section 4.3.3. (For those circuit flows within their limits, $K_{c,l}$ equals to 1.)
Step 3: Solve the RBCR-F1 again, and based on the result, update the set of violated circuits set Ω_V .
Step 4: Repeat Steps 2 and 3 until the set Ω_V is empty, then output the corresponding dispatch results.

If the iterations exceed a certain number, the algorithm terminates; in this case, an infeasibility exists which cannot be removed without exceeding the DAL for one or more circuits, and load shedding must be performed.

Bender's decomposition [32] method and CPLEX solver are implemented to solve this optimization problem.

4.4 Risk-based constraint relaxation under formulation 2

In this section, we describe the RBCR-F2 approach where the risk terms are included as constraints.

4.4.1 Formulation of RBCR-F2

The objective function of the RBCR-F2 model is to minimize the production costs, as indicated in the following formulation, denoted as RBCR-F2.

$$Min \sum_{i=1}^{NG} c_i \times P_i \tag{4-21}$$

Subject to:

The same as (4-9)~(4-18) in RBCR-F1

$$Risk = \sum_{k=1}^{NC} \Pr_k \sum_{l=1}^{NL} Sev_l^k \le Risk_{\max} \tag{4-22}$$

$$CtgRisk_k = \Pr_k \sum_{l=1}^{NL} Sev_l^k \le CtgRisk_{k,\max}, k \in CCS \tag{4-23}$$

$$CctRisk_k^l = \Pr_l^k \sum_{m} Sev_m^l \le CctRisk_{l,\max}^k, k \in CCS, l \in COCS \tag{4-24}$$

The first set of constraints are the same as (4-9)~(4-18) in RBCR-F1. In addition, equation (4-22) constraint the system risk under a certain level. Equation (4-23) guarantees that the contingency risk of critical contingencies must be lower than the reference value. Equation (4-24) addresses the security level for circuits where their thermal limits needs to be relaxed, and this is related to 'N-1-1' contingency condition. CCS is the set of critical contingencies, and $COCS$ is the set of critical overloaded circuits (related to second contingency[4]), which fails in the risk test on second contingency circuit risk under a particular critical contingency.

For RBCR-F2, the procedure of relaxation level determination is the same as that of RBCR-F1.

4.4.2 Procedure of RBCR-F2

The procedure for RBCR-F2 is described as follows, and shown in Figure 4-4.

Step 1: Set $\mathrm{COCS} = \emptyset$.
Step 2: Solve the RBCR-F2 model. Identify the violated circuits based on the values of violation indicator β_l^k. The set of these violated circuits are denoted as Ω_V.
Step 3: Determine $K_{c,l}$ for each circuit flow limit, using the approach proposed in Section 4.3.3. (For those circuit flows within their limits, $K_{c,l}$ equals to 1.)
Step 4: Solve the RBCR-F2 again, and based on the result, update the set of violated circuits set Ω_V.
Step 5: Repeat Steps 3 and 4 until the set Ω_V is empty, then update the corresponding relaxation results.
Step 6: Test the value of $CctRisk_l^k$, if not satisfied, update COCS, and repeat Step 2~Step 6. If satisfied, output the corresponding relaxation result.

[4] Critical overloaded circuit *l* should satisfies two conditions : 1) under critical contingency *k*, circuit *l* is overloaded and needs to be relaxed; 2)under 'N-*k*-*l*' contingency, the corresponding second contingency circuit risk for *l* exceeds the reference value.

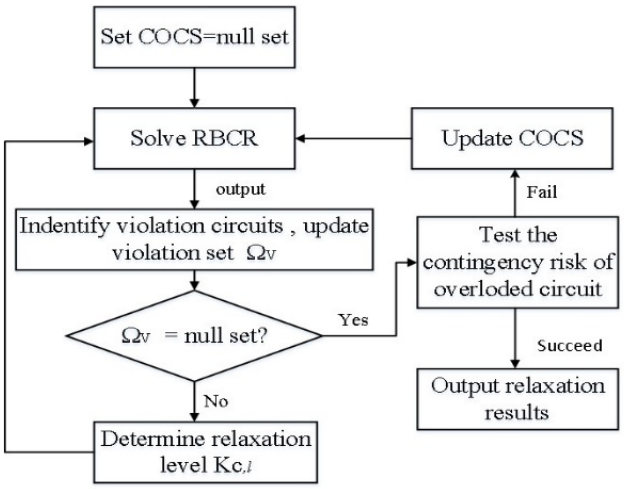

Figure 4-4 Flowchart of RBCR-F2

If the iterations exceed a certain number, the algorithm terminates; in this case, an infeasibility exists and load shedding must be performed.

As that in RBCR-F1, Bender's decomposition method and the CPLEX solver are implemented to solve this optimization problem.

4.5 Summary

In this Chapter, two approaches for performing RBCR are formulated: minimize risk or constrain risk. Corresponding formulations and solution procedures are provided. Especially, the risk indices to measure system security level under specific condition and the corresponding risk limits have been proposed.

5. Effect on LMPs of constraint relaxation approaches

5.1 Comparisons among industry-based CR and risk-based CR

As discussed in the previous chapters，the industry-based CR approach is convenient to implement, but the need to derive a reasonable penalty price for the relaxed circuits raises questions about the best way to do that which are not easily answered. Especially, use of penalty prices as have been applied within today's electricity markets results in frequent LMP spikes. In addition, the constraint relaxation results from industry-based CR do not monitor or control system-level security.

The two risk-based CR approaches do offer alternative approaches, and we have compared them to the industry-based CR in Table 5-1 using seven criteria. We have indicated in yellow, for each criterion, the most attractive approach or approaches. The basis for criteria 1-6 is provided in the discussions of previous chapters. The basis for criterion 7, the effects on LMPs, is provided in this chapter.

Table 5-1 Performance of three constraint relaxation approaches

Criteria #	Criteria	Industry-based CR	RBCR-F1	RBCR-F2
1	Implement convenience	easy	fair	fair
2	System risk considered?	No	Yes (minimizes it)	Yes (constrains it)
3	Penalty price needed?	Yes (values for every overloaded circuit)	Yes (a single value for risk)	No
4	Contingency probabilities considered?	No (treats all contingencies the same)	Yes, although not essential to do so	Yes, although not essential to do so
5	Risk of individual contingencies considered?	No	No	Yes
6	Risk of overloaded circuit under individual contingencies considered?	No	No	Yes
7	Effects on LMP	LMP spike	Smoother LMP	Smoothest LMP

5.2 Impacts on LMP calculation

Locational marginal prices (LMPs) are the economic signals used within the market-pricing approach to determine optimal dispatch (generation output) decisions, and the pricing of electricity at each node. It is defined, for each node, as the incremental cost to the system that results from re-dispatching available units to satisfy one additional unit of load at the specific node, in $/MW/time interval. The LMP mechanism has been applied in U.S. deregulated markets, e.g., in ISO-New England [33], New York ISO [34], PJM [35], California ISO, Mid-continent ISO [36], and also internationally, e.g., in New Zealand and Singapore [37].

Traditionally, LMPs are the shadow prices from the bid-based, security constrained economic dispatch model. LMP are comprised of three components: energy component, loss component and congestion component. In RBCR approaches proposed in this report (either RBCR-F1 or RBCR-F2), we find that an additional component is added in the LMP formulation; this component is related to the risk. Thus, the traditional LMP is extended to what we refer to as a Risk-based LMP, denoted RLMP.

This section will assess the effects that industry-based and risk-based constraint relaxation approaches have on LMP calculations, respectively.

5.2.1 LMP calculation under industry-based CR

In electricity markets, LMPs are calculated based on SCED both in day-ahead and real-time markets. The objective of SCED is to maximize social surplus while respecting system load demand. In addition, power balance and transmission line thermal ratings are also constrained. The objective is to maximize social surplus, which is equivalent to minimizing production (i.e., generation) costs when price-sensitive load is not represented. The SCED formulation with the industry-based CR, i.e., the penalty price approach, formulated (3-1) ~ (3-7) in Chapter 3. Here, we describe this model with Lagrange multipliers in the parentheses, as follows.

$$Min \sum_{i=1}^{NG} c_i \times P_i + \sum_{k=1}^{NC} \sum_{l=1, l \in CR}^{NL} Penalty_l^k \times \alpha_l^k$$

subject to:

$$\sum_{i=1}^{N} P_i - \sum_{i=1}^{N} D_i - Loss = 0 \qquad (\lambda_1 \geq 0)$$

$$P_i^{\min} \leq P_i \leq P_i^{\max} \qquad (\alpha_{1i}^{min}, \alpha_{1i}^{max} \geq 0)$$

$$\sum_{i=1}^{N} GSF_{l-i}^{0}(P_i - D_i) \leq Limit_l^0, \quad for\ l \in \{all\ \ lines\} \qquad (\beta_{1l}^0 \geq 0)$$

$$\begin{cases} h_l^k = \sum_{i=1}^{N} GSF_{l-i}^{k}(P_i - D_i), \\ for\ l \in \{all\ \ lines\}\ k \in \{contingency\ set\} \end{cases} \qquad (\gamma_{1l}^k \geq 0)$$

$$\begin{cases} h_l^k - \alpha_l^k \leq Limit_l^k, \\ for\ l \in CR, k \in \{contingency\ \ set\} \end{cases} \qquad (\beta_{1l,1}^k \geq 0)$$

$$\begin{cases} h_l^k \le Limit_l^k, \\ for\ l \in NCR, k \in \{contingency\ set\} \end{cases} \qquad (\beta_{1l,2}^k \ge 0)$$

The LMP is defined as a change in production costs due to an increment of load at a particular bus. Thus, the LMP at bus i can be obtained by calculating the partial derivative of Lagrange function, which is given in equation (5-1) below.

$$\begin{aligned} L_1 = & \sum_{i=1}^{NG} c_i \times P_i + \sum_{k=1}^{NC} \sum_{l=1, l \in CR}^{NL} Penalty_l^k \times \alpha_l^k - \lambda_1 (\sum_{i=1}^{N} P_i - \sum_{i=1}^{N} D_i - Loss) \\ & + \sum_{i=1}^{NG} \alpha_{1i}^{\min} (-P_i + P_i^{\min}) + \sum_{i=1}^{NG} \alpha_{1i}^{\max} (P_i - P_i^{\max}) \\ & + \sum_{l=1}^{NL} \beta_{1l}^0 [\sum_{i=1}^{N} GSF_{l-i}^0 (P_i - D_i) - Limit_l^0] - \sum_{k=1}^{NC} \sum_{l=1}^{NL} \gamma_{1l}^k \left[h_l^k - \sum_{i=1}^{N} GSF_{l-i}^k (P_i - D_i) \right] \\ & + \sum_{k=1}^{NC} \sum_{l \in CR} \beta_{1l,1}^k \left(h_l^k - \alpha_l^k - Limit_l^k \right) + \sum_{k=1}^{NC} \sum_{l \in NCR} \beta_{1l,2}^k \left(h_l^k - Limit_l^k \right) \end{aligned} \tag{5-1}$$

According to constrained optimization theory, a convex optimization problem at the optimal point must satisfy the Karush-Kuhn-Tucker (KKT) conditions, as shown in equations (5-2) ~(5-4).

$$\frac{\partial L_1}{\partial P_i} = c_i - \lambda_1 + \frac{\partial Loss}{\partial P_i} \lambda_1 - \alpha_{1i}^{\min} + \alpha_{1i}^{\max} + \sum_{l=1}^{NL} \beta_{1l}^0 GSF_{l-i}^0 + \sum_{k=1}^{NC} \sum_{l=1}^{NL} \gamma_{1l}^k GSF_{l-i}^k = 0, \ \forall i \tag{5-2}$$

$$\frac{\partial L_1}{\partial h_l^k} = \begin{cases} -\gamma_{1l}^k + \beta_{1l,1}^k = 0 \ \ \forall k, \forall l \in CR \\ -\gamma_{1l}^k + \beta_{1l,2}^k = 0 \ \ \forall k, \forall l \in NCR \end{cases}$$

(5-3) $$\frac{\partial L_1}{\partial \alpha_l^k} = Penalty_l^k - \beta_{1l,1}^k = 0, \ \forall k, \forall l \in CR$$

(5-4)

Then the LMP at bus i is expressed in equation (5-5).

$$\frac{\partial L_1}{\partial D_i} = \lambda_1 + \frac{\partial Loss}{\partial D_i} \lambda_1 - \sum_{l=1}^{NL} \beta_{1l}^0 GSF_{l-i}^0 - \sum_{k=1}^{NC} \sum_{l=1}^{NL} \gamma_{1l}^k GSF_{l-i}^k, \ \forall i \tag{5-5}$$

Taking into account that $\partial Loss / \partial D_i = -\partial Loss / \partial P_i$ and equations (5-3) and (5-4), equation (5-5) can be converted into the following form:

$$LMP_1 = \frac{\partial L_1}{\partial D_i} = \lambda_1 - \frac{\partial Loss}{\partial P_i} \lambda_1 - \left(\sum_{l=1}^{NL} \beta_{1l}^0 GSF_{l-i}^0 + \sum_{k=1}^{NC} \sum_{l \in CR} Penalty_l^k GSF_{l-i}^k + \sum_{k=1}^{NC} \sum_{l \in NCR} \beta_{1l,2}^k GSF_{l-i}^k \right), \ \forall i \tag{5-6}$$

Thus, the traditional LMP is determined by the dual variable of the power balance equation and the thermal rating constraints both under normal and contingency conditions. The LMP can be separated into the following three components: energy component, loss component and congestion component, as expressed below.

$$LMP_1^{energy} = \lambda_1 \tag{5-7}$$

$$LMP_1^{loss} = -\frac{\partial Loss}{\partial P_i}\lambda_1 \tag{5-8}$$

$$LMP_1^{congestion} = -\left(\sum_{l=1}^{NL}\beta_{1l}^0 GSF_{l-i}^0 + \sum_{k=1}^{NC}\sum_{l\in CR}\beta_{1l,1}^k Penalty_l^k GSF_{l-i}^k + \sum_{k=1}^{NC}\sum_{l\in NCR}\beta_{1l,2}^k GSF_{l-i}^k\right) \tag{5-9}$$

The full LMP expression for the industry-based CR is based on the above development. However, when SCED is based on a DC power flow formulation, the representation of losses [38], [39], [40] incurs complications (e.g., modeling the slack bus and computing loss distribution factors) that unnecessarily obscure insight into the CR problem. Thus, in the discussion of this report, which focuses on overload and constraint relaxation, the loss component is neglected to maintain simplicity in the exposition.

The difference between the LMP expression for the industry-based CR and that from the traditional SCED lies in the presence, in the industry-based CR model, the violation penalty price $Penalty_l^k$, which does not appear in the traditional SCED model. The value of $Penalty_l^k$ has an obvious and direct influence on the value of LMP, as indicated by Equation (5-6). Once there exists violation on the circuit flow, that is to say, $\alpha_l^k \neq 0$, certain values are assigned as $Penalty_l^k$. As discussed in Chapter 3, the value of $Penalty_l^k$ is typically in thousands of dollars. This tends to significantly increase the absolute value of the LMP congestion component, resulting in LMP spikes, causing high geographical and temporal variability in the LMPs.

5.2.2 LMP calculation under RBCR-F1

In our work, RBCR-F1 introduces system risk in the objective function, associated with a penalty price. Thus, the objective function is to minimize the summation of production costs and risk penalty, constrained to power balance, generation output and conductor thermal ratings both under normal and 'N-1' contingency situations. The model has been presented in Section 4.3.1. Here, we describe this model with Lagrange multipliers in the parentheses, as follows.

$$Min \sum_{i=1}^{NG} c_i \times P_i + \mathrm{C}_r \times Risk$$

Subject to:

$$\sum_{i=1}^{N} P_i - \sum_{i=1}^{N} D_i - Loss = 0 \qquad (\lambda_2 \geq 0)$$

$$P_i^{\min} \leq P_i \leq P_i^{\max} \qquad (\alpha_{2i}^{min}, \alpha_{2i}^{max} \geq 0)$$

$$\sum_{i=1}^{N} GSF_{l-i}^0 (P_i - D_i) \leq Limit_l^0, \quad for\ l \in \{all\ \ lines\} \qquad (\beta_{2l}^0 \geq 0)$$

$$h_l^k = \sum_{i=1}^{N} GSF_{l-i}^k (P_i - D_i) \qquad (\gamma_{2l}^k \geq 0)$$

$$\begin{cases} h_l^k - \beta_l^k = K_{c,l} Limit_l^k, \\ for\ l \in CR, k \in \{contingencies\ set\} \end{cases} \qquad (\beta_{2l,1}^k \geq 0)$$

$$\begin{cases} h_l^k \leq Limit_l^k, \\ for\ l \in NCR, k \in \{contingency\ set\} \end{cases} \qquad (\beta_{2l,2}^k \geq 0)$$

$$Sev_l^k \geq 0 \qquad (\mu_{1l,1}^k \geq 0)$$

$$Sev_l^k \geq a_{1l} h_l^k - 9 \qquad (\mu_{1l,2}^k \geq 0)$$

$$Sev_l^k \geq a_{2l} h_l^k - a_{3l} \qquad (\mu_{1l,3}^k \geq 0)$$

$$Sev_l^k \geq a_{4l} h_l^k - a_{5l} \qquad (\mu_{1l,4}^k \geq 0)$$

$$Risk = \sum_{k=1}^{NC} (\mathrm{Pr}_k \sum_{l=1}^{NL} Sev_l^k) \qquad (\delta \geq 0)$$

Thus, LMP at bus i can be achieved by calculating the partial derivative of the Lagrange function, which is given in equation (5-10) below.

$$\begin{aligned} L_2 = & \sum_{i=1}^{NG} c_i \times P_i + \mathrm{C}_r \times Risk - \lambda_2 (\sum_{i=1}^{N} P_i - \sum_{i=1}^{N} D_i - Loss) \\ & + \sum_{i=1}^{NG} \alpha_{2i}^{\min} (-P_i + P_i^{\min}) + \sum_{i=1}^{NG} \alpha_{2i}^{\max} (P_i - P_i^{\max}) \\ & + \sum_{l=1}^{NL} \beta_{2l}^0 [\sum_{i=1}^{N} GSF_{l-i}^0 (P_i - D_i) - Limit_l^0] - \sum_{k=1}^{NC} \sum_{l=1}^{NL} \gamma_{2l}^k \left[h_l^k - \sum_{i=1}^{N} GSF_{l-i}^k (P_i - D_i) \right] \\ & + \sum_{k=1}^{NC} \sum_{l \in CR} \beta_{2l,1}^k \left(h_l^k - \beta_l^k - K_{c,l} Limit_l^k \right) + \sum_{k=1}^{NC} \sum_{l \in NCR} \beta_{2l,2}^k \left(h_l^k - Limit_l^k \right) \\ & - \sum_{k=1}^{NC} \sum_{l=1}^{NL} \mu_{1l,1}^k Sev_k^k - \sum_{k=1}^{NC} \sum_{l=1}^{NL} \mu_{1l,2}^k \left(Sev_l^k - a_{1l} h_l^k + 9 \right) - \sum_{k=1}^{NC} \sum_{l=1}^{NL} \mu_{1l,3}^k \left(Sev_l^k - a_{2l} h_l^k + a_{3l} \right) \\ & - \sum_{k=1}^{NC} \sum_{l=1}^{NL} \mu_{1l,4}^k \left(Sev_l^k - a_{4l} h_l^k + a_{5l} \right) - \delta \left(Risk - \sum_{k=1}^{NC} (\mathrm{Pr}_k \sum_{l=1}^{NL} Sev_l^k) \right) \end{aligned} \qquad (5\text{-}10)$$

According to constrained optimization theory, a convex optimization problem at the optimal point must satisfy the Karush-Kuhn-Tucker (KKT) conditions, as shown in equation (5-11) ~(5-14).

$$\frac{\partial L_2}{\partial P_i} = c_i - \lambda_2 + \frac{\partial Loss}{\partial P_i} \lambda_2 - \alpha_{2i}^{\min} + \alpha_{2i}^{\max} + \sum_{l=1}^{NL} \beta_{2l}^0 GSF_{l-i}^0 + \sum_{k=1}^{NC} \sum_{l=1}^{NL} \gamma_{2l}^k GSF_{l-i}^k = 0, \ \forall i \qquad (5\text{-}11)$$

$$\frac{\partial L_2}{\partial h_l^k} = \begin{cases} -\gamma_{2l}^k + \beta_{2l,1}^k + \mu_{1l,2}^k a_{1l} + \mu_{1l,3}^k a_{2l} + \mu_{1l,4}^k a_{4l} = 0 \ \ \forall k, \forall l \in CR \\ -\gamma_{2l}^k + \beta_{2l,2}^k + \mu_{1l,2}^k a_{1l} + \mu_{1l,3}^k a_{2l} + \mu_{1l,4}^k a_{4l} = 0 \ \ \forall k, \forall l \in NCR \end{cases} \qquad (5\text{-}12)$$

$$\frac{\partial L_2}{\partial Sev_l^k} = -\mu_{1l,1}^k - \mu_{1l,2}^k - \mu_{1l,3}^k - \mu_{1l,4}^k + \delta \Pr_k = 0,\ \forall k, l \tag{5-13}$$

$$\frac{\partial L_2}{\partial Risk} = C_r - \delta = 0 \tag{5-14}$$

Define parameter s_l^k as follows:

$$s_l^k = \begin{cases} 0, & if\ h_l^k \in [0.9LTE, LTE] \\ a_{1l},\ if\ h_l^k \in [LTE, STE] \\ a_{2l},\ if\ h_l^k \in [STE, DAL] \\ a_{3l},\ if\ h_l^k \geq DAL \end{cases} \tag{5-15}$$

Then combine (5-12)~(5-14), we could get equation (5-16).

$$\gamma_{2l}^k = \begin{cases} \beta_{2l,1}^k + \delta \Pr_k\ s_l^k = 0\ \ \forall k, \forall l \in CR \\ \beta_{2l,2}^k + \delta \Pr_k\ s_l^k = 0\ \ \forall k, \forall l \in NCR \end{cases} \tag{5-16}$$

Then the LMP at bus i is expressed in equation (5-17).

$$\frac{\partial L_2}{\partial D_i} = \lambda_2 + \frac{\partial Loss}{\partial D_i}\lambda_2 - \sum_{l=1}^{NL} \beta_{2l}^0 GSF_{l-i}^0 - \sum_{k=1}^{NC}\sum_{l=1}^{NL} \gamma_{2l}^k GSF_{l-i}^k,\ \forall i \tag{5-17}$$

Taking into account that $\partial Loss / \partial D_i = -\partial Loss / \partial P_i$, equation (5-14) and (5-16), equation (5-17) could be converted into the following form,

$$LMP_2 = \frac{\partial L_2}{\partial D_i} = \lambda_2 - \frac{\partial Loss}{\partial P_i}\lambda_2 - \left(\sum_{l=1}^{NL} \beta_{2l}^0 GSF_{l-i}^0 + \sum_{k=1}^{NC}\sum_{l\in NCR} \beta_{2l,2}^k GSF_{l-i}^k + \sum_{k=1}^{NC}\sum_{l\in CR} \beta_{2l,1}^k GSF_{l-i}^k \right) - \sum_{k=1}^{NC}\sum_{l=1}^{NL} s_l^k \Pr_k GSF_{l-i}^k C_r,\ \forall i \tag{5-18}$$

According to the above analysis, the RLMP for RBCR-F1 is comprised of the dual variable of the power balance equation, and terms from the flow constraints and the system risk. In separating into individual components, we find three components which are similar to those of the LMP from the industry-based CR, but in addition, there is a fourth component associated with risk, as indicated in the following:

$$LMP_2^{energy} = \lambda_2 \tag{5-19}$$

$$LMP_2^{loss} = -\frac{\partial Loss}{\partial P_i}\lambda_2 \tag{5-20}$$

$$LMP_2^{congestion} = -\left(\sum_{l=1}^{NL} \beta_{2l}^0 GSF_{l-i}^0 + \sum_{k=1}^{NC}\sum_{l\in NCR} \beta_{2l,2}^k GSF_{l-i}^k + \sum_{k=1}^{NC}\sum_{l\in CR} \beta_{2l,1}^k GSF_{l-i}^k \right) \tag{5-21}$$

$$LMP_2^{risk} = -\sum_{k=1}^{NC}\sum_{l=1}^{NL} s_l^k \,\mathrm{Pr}_k \, GSF_{l-i}^k C_r \tag{5-22}$$

Again, we neglect the loss component. We observe that there is no influence of a penalty factor in the congestion component; however, the penalty price of risk, C_r has a significant effect on the value of the LMP risk component. Although $C_r$is at the same scale as that of $Penalty_l^k$ used in the industry-based CR, it is multiplied by Pr_k, which ensures that the coefficient of risk component will not be too large. This is why the RBCR-F1 results in a smoother, less geographically and temporally variable LMP than that of the industry-based CR.

5.2.3 LMP calculation under RBCR-F2

In our work, RBCR-F2 introduces the concept of controlled system risk, contingency risk, and second contingency circuit risk, which ensures that relaxation performed within RBCR-F2 makes the system and contingency less risky than that with industry-based CR. In addition, RBCR-F2 also constrains the second contingency circuit risk. The detailed model has been presented in Section 4.4.1. Here, we describe this model with Lagrange multipliers in parentheses, as follows.

$$Min \sum_{i=1}^{NG} c_i \times P_i$$

Subject to:

$$\sum_{i=1}^{N} P_i - \sum_{i=1}^{N} D_i - Loss = 0 \qquad (\lambda_3 \geq 0)$$

$$P_i^{\min} \leq P_i \leq P_i^{\max} \qquad (\alpha_{3i}^{min}, \alpha_{3i}^{max} \geq 0)$$

$$\sum_{i=1}^{N} GSF_{l-i}^0 (P_i - D_i) \leq Limit_l^0, \quad for\ l \in \{all\ \ lines\} \qquad (\beta_{3l}^0 \geq 0)$$

$$h_l^k = \sum_{i=1}^{N} GSF_{l-i}^k (P_i - D_i) \qquad (\gamma_{3l}^k \geq 0)$$

$$\begin{cases} h_l^k - \beta_l^k = K_{c,l} Limit_l^k, \\ for\ l \in CR, k \in \{contingencies\ set\} \end{cases} \qquad (\beta_{3l,1}^k \geq 0)$$

$$\begin{cases} h_l^k \leq Limit_l^k, \\ for\ l \in NCR, k \in \{contingency\ set\} \end{cases} \qquad (\beta_{3l,2}^k \geq 0)$$

$$Sev_l^k \geq 0 \qquad (\mu_{2l,1}^k \geq 0)$$

$$Sev_l^k \geq a_{1l} h_l^k - 9 \qquad (\mu_{2l,2}^k \geq 0)$$

$$Sev_l^k \geq a_{2l} h_l^k - a_{3l} \qquad (\mu_{2l,3}^k \geq 0)$$

$$Sev_l^k \geq a_{4l} h_l^k - a_{5l} \qquad (\mu_{2l,4}^k \geq 0)$$

$$Risk = \sum_{k=1}^{NC} \mathrm{Pr}_k \sum_{l=1}^{NL} Sev_l^k \leq Risk_{\max} \qquad (\tau \geq 0)$$

$$CtgRisk_k = \Pr_k \sum_{l=1}^{NL} Sev_l^k \le CtgRisk_{k,\max}, k \in CCS \qquad (\varphi_k \ge 0)$$

$$CctRisk_k^l = \Pr_l^k \sum_m Sev_m^l \le CctRisk_{l,\max}^k, k \in CCS, l \in COCS \qquad (\rho_l^k \ge 0)$$

Thus, LMP at bus i can be obtained by calculating the partial derivative of the Lagrange function, which is given in equation (5-23) below.

$$\begin{aligned}
L_3 = & \sum_{i=1}^{NG} c_i \times P_i - \lambda_3 (\sum_{i=1}^{N} P_i - \sum_{i=1}^{N} D_i - Loss) \\
& + \sum_{i=1}^{NG} \alpha_{3i}^{\min} (-P_i + P_i^{\min}) + \sum_{i=1}^{NG} \alpha_{3i}^{\max} (P_i - P_i^{\max}) \\
& + \sum_{l=1}^{NL} \beta_{3l}^0 [\sum_{i=1}^{N} GSF_{l-i}^0 (P_i - D_i) - Limit_l^0] - \sum_{k=1}^{NC} \sum_{l=1}^{NL} \gamma_{3l}^k \left[h_l^k - \sum_{i=1}^{N} GSF_{l-i}^k (P_i - D_i) \right] \\
& + \sum_{k=1}^{NC} \sum_{l \in CR} \beta_{3l,1}^k \left(h_l^k - \beta_l^k - K_{c,l} Limit_l^k \right) + \sum_{k=1}^{NC} \sum_{l \in NCR} \beta_{3l,2}^k \left(h_l^k - Limit_l^k \right) \\
& - \sum_{k=1}^{NC} \sum_{l=1}^{NL} \mu_{2l,1}^k Sev_k^k - \sum_{k=1}^{NC} \sum_{l=1}^{NL} \mu_{2l,2}^k \left(Sev_l^k - a_{1l} h_l^k + 9 \right) - \sum_{k=1}^{NC} \sum_{l=1}^{NL} \mu_{2l,3}^k \left(Sev_l^k - a_{2l} h_l^k + a_{3l} \right) \\
& - \sum_{k=1}^{NC} \sum_{l=1}^{NL} \mu_{2l,4}^k \left(Sev_l^k - a_{4l} h_l^k + a_{5l} \right) + \tau \left(\sum_{k=1}^{NC} \Pr_k \sum_{l=1}^{NL} Sev_l^k - Risk_{\max} \right) \\
& + \sum_{k \in CCS} \varphi_k \left(\Pr_k \sum_{l=1}^{NL} Sev_l^k - CtgRisk_{k,\max} \right) + \sum_{k \in CCS} \sum_{l \in COCS} \rho_l^k \left(\Pr_l^k \sum_m Sev_m^l - CctRisk_{l,\max}^k \right)
\end{aligned} \qquad (5\text{-}23)$$

According to constrained optimization theory, a convex optimization problem at the optimal point must satisfy the Karush-Kuhn-Tucker (KKT) conditions, as shown in equation (5-24) ~ (5-26).

$$\frac{\partial L_3}{\partial P_i} = c_i - \lambda_3 + \frac{\partial Loss}{\partial P_i} \lambda_3 - \alpha_{3i}^{\min} + \alpha_{3i}^{\max} + \sum_{l=1}^{NL} \beta_{3l}^0 GSF_{l-i}^0 + \sum_{k=1}^{NC} \sum_{l=1}^{NL} \gamma_{3l}^k GSF_{l-i}^k = 0, \ \forall i \qquad (5\text{-}24)$$

$$\frac{\partial L_3}{\partial h_l^k} = \begin{cases} -\gamma_{3l}^k + \beta_{3l,1}^k + \mu_{2l,2}^k a_{1l} + \mu_{2l,3}^k a_{2l} + \mu_{2l,4}^k a_{4l} = 0 \ \ \forall k, \forall l \in CR \\ -\gamma_{3l}^k + \beta_{3l,2}^k + \mu_{2l,2}^k a_{1l} + \mu_{2l,3}^k a_{2l} + \mu_{2l,4}^k a_{4l} = 0 \ \ \forall k, \forall l \in NCR \end{cases} \qquad (5\text{-}25)$$

$$\frac{\partial L_3}{\partial Sev_l^k} = \begin{cases} -\mu_{2l,1}^k - \mu_{2l,2}^k - \mu_{2l,3}^k - \mu_{2l,4}^k + \tau \Pr_k + \varphi_k = 0, k \in CCS \\ -\mu_{2l,1}^k - \mu_{2l,2}^k - \mu_{2l,3}^k - \mu_{2l,4}^k + \tau \Pr_k = 0, k \notin CCS \end{cases}, \ \forall l \qquad (5\text{-}26)$$

Here, we ignore ρ_l^k, since it does not have much influence on the LMP value.
Then the LMP at bus i is expressed in equation (5-27).

$$\frac{\partial L_3}{\partial D_i} = \lambda_3 + \frac{\partial Loss}{\partial D_i} \lambda_3 - \sum_{l=1}^{NL} \beta_{3l}^0 GSF_{l-i}^0 - \sum_{k=1}^{NC} \sum_{l=1}^{NL} \gamma_{3l}^k GSF_{l-i}^k, \ \forall i \qquad (5\text{-}27)$$

Taking into account that $\partial Loss / \partial D_i = -\partial Loss / \partial P_i$, equations (5-24)~(5-26), Equation (5-27) can be converted into the following form,

$$LMP_3 = \frac{\partial L_3}{\partial D_i} = \lambda_3 - \frac{\partial Loss}{\partial P_i}\lambda_3 - \left(\sum_{l=1}^{NL} \beta_{3l}^0 GSF_{l-i}^0 + \sum_{k=1}^{NC} \sum_{l \in NCR} \beta_{3l,2}^k GSF_{l-i}^k + \sum_{k=1}^{NC} \sum_{l \in CR} \beta_{3l,1}^k GSF_{l-i}^k \right)$$
$$- \sum_{k=1}^{NC} \sum_{l=1}^{NL} s_l^k \left(\Pr_k \tau + \varphi_k \right) GSF_{l-i}^k, \ \forall i, \varphi_k = 0 \ if \ k \notin CCS \tag{5-28}$$

The RLMP resulting formulation RBCR-F2 also has four components: energy component, loss component, congestion component and risk component, as expressed below:

$$LMP_3^{energy} = \lambda_3 \tag{5-29}$$

$$LMP_3^{loss} = -\frac{\partial Loss}{\partial P_i}\lambda_3 \tag{5-30}$$

$$LMP_3^{congestion} = -\left(\sum_{l=1}^{NL} \beta_{3l}^0 GSF_{l-i}^0 + \sum_{k=1}^{NC} \sum_{l \in NCR} \beta_{3l,2}^k GSF_{l-i}^k + \sum_{k=1}^{NC} \sum_{l \in CR} \beta_{3l,1}^k GSF_{l-i}^k \right) \tag{5-31}$$

$$LMP_3^{risk} = -\sum_{k=1}^{NC} \sum_{l=1}^{NL} s_l^k \left(\Pr_k \tau + \varphi_k \right) GSF_{l-i}^k, \ \varphi_k = 0 \ if \ k \notin CCS \tag{5-32}$$

Examining LMP_3, we observe that neither the congestion component nor the risk component has influence from a penalty factor term. This is very attractive, in that it is the reason why RBCR-F2 results in very geographically and temporally 'smooth' LMPs that do not suffer from the penalty term-induced price spikes of the industry-based CR approach.

5.2.4 LMP comparison between industry-based CR and risk-based CR

As discussed in Section 5.2.1-5.2.3, the calculation and comparison of LMP at a particular bus is shown in Table 5-2.

Table 5-2 LMP calculation

LMP	Industry-based CR	RBCR-F1	RBCR-F2
Energy component	λ_1	λ_2	λ_3
Loss component	$-\frac{\partial Loss}{\partial P_i}\lambda_1$	$-\frac{\partial Loss}{\partial P_i}\lambda_2$	$-\frac{\partial Loss}{\partial P_i}\lambda_3$
Congestion component	$-\left(\sum_{l=1}^{NL} \beta_{1l}^0 GSF_{l-i}^0 + \sum_{k=1}^{NC} \sum_{l \in CR} \beta_{1l,1}^k Penalty_l^k GSF_{l-i}^k + \sum_{k=1}^{NC} \sum_{l \in NCR} \beta_{1l,2}^k GSF_{l-i}^k \right)$	$-\left(\sum_{l=1}^{NL} \beta_{2l}^0 GSF_{l-i}^0 + \sum_{k=1}^{NC} \sum_{l \in NCR} \beta_{2l,2}^k GSF_{l-i}^k + \sum_{k=1}^{NC} \sum_{l \in CR} \beta_{2l,1}^k GSF_{l-i}^k \right)$	$-\left(\sum_{l=1}^{NL} \beta_{3l}^0 GSF_{l-i}^0 + \sum_{k=1}^{NC} \sum_{l \in NCR} \beta_{3l,2}^k GSF_{l-i}^k + \sum_{k=1}^{NC} \sum_{l \in CR} \beta_{3l,1}^k GSF_{l-i}^k \right)$

Table 5-2 LMP calculation (continued)

LMP	Industry-based CR	RBCR-F1	RBCR-F2
Risk compo-nent	/	$-\sum_{k=1}^{NC}\sum_{l=1}^{NL} s_l^k \Pr_k GSF_{l-i}^k C_r$	$-\sum_{k=1}^{NC}\sum_{l=1}^{NL} s_l^k \left(\Pr_k \tau + \varphi_k\right) GSF_{l-i}^k$
LMP spike	Substantial	Smoother LMP	Smoothest LMP

In comparison with traditional LMP or the LMP from the industry-based CR, there exists in the LMP expression for RBCR-F1 and RBCR-F2 an added component, the risk component. The risk component can be regarded as the price signal to reflect the system security level, where the value of the risk component indicates the relationship between load demand and system risk level. If the marginal risk price, i.e., the risk component, is positive, increasing the load at a specific bus would expose the system to a higher risk level; while a negative value implies that decreasing load level would expose the system to a higher risk level.

5.3 Summary

This chapter compares the proposed constraint relaxation approaches in this report, including industry-based CR and risk-based CRs, from the aspect of strengths and weaknesses. The industry-based CR is perhaps simpler and easier to implement, but it tends to cause LMP spikes. In contrast, the risk-based CR approaches result in smoother LMP distributions. Also of high significance, we believe that the RBCR results in more secure operating conditions with little increase in production cost, and perhaps even with a decrease in production costs. This suggests that the RBCR provides solutions to the SCED infeasible solution problems that yield an attractive combination between reduced risk and increased economy. We will illustrate these effects in the next chapter.

6. Case Study

6.1 Six bus network and parameter determination

In order to examine the performance of proposed CR method in addressing the infeasible SCED problem, a six-bus network [41] is presented to test and illustrate the developed approach. A single line diagram of this system is shown in Figure 6-1.

The line reactances are shown in Figure 6-1 in per unit on a 100 MVA base. The generation costs for generators connected to buses A, B and C are

$$\mathrm{Cos}t(P_A) = 5.33\times10^{-3}P_A^2 + 11.669\times P_A + 213 \quad (6\text{-}1)$$

$$\mathrm{Cos}t(P_B) = 8.89\times10^{-3}P_B^2 + 10.333\times P_B + 200 \quad (6\text{-}2)$$

$$\mathrm{Cos}t(P_C) = 7.41\times10^{-3}P_C^2 + 10.833\times P_C + 240 \quad (6\text{-}3)$$

where P_A, $P_B$and P_C are given in MW, and $Cost$ are given in dollars/5 minutes. In general, the marginal costs is $G_A \geq G_C \geq G_B$. The contingency probabilities of each line are provided in Table 6-1, providing the probability the corresponding contingency will occur during the next time period.

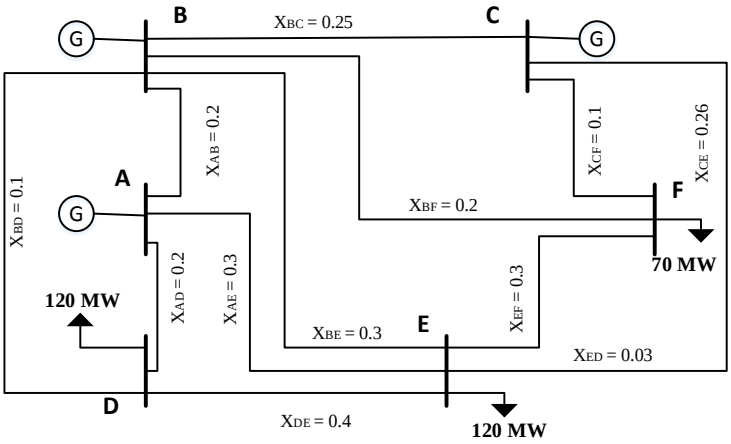

Figure 6-1 Single-line diagram for six-bus network.

Table 6-1 Contingency probability

Ctgcy	A-B	A-D	A-E	B-C	B-D	B-E
Prob	0.0077	0.0107	0.0115	0.0096	0.0008	0.0015
Ctgcy	B-F	C-E	C-F	D-E	E-F	
Prob	0.0176	0.0001	0.0138	0.0153	0.0115	

Under such a system operation status, the violation in line B-D is detected under the 'N-1' contingency condition, which makes the SCED problem infeasible. So contingency B-D is

the critical contingency. Define the contingency set includes all 'N-1' contingency, and here the loss of component refers to line outage. We do not consider trip of generators.

Solve this problem under the industry-based CR and risk-based CR, and the corresponding results are described and analyzed in Section 6.2.

1. Risk Limits

According to the risk indices from industry-based model, and shrink them as 90% of the original value, we can achieve the risk limits for RBCR-F2, as follows:

(1) *Contingency risk limits:* this is the limit to constrain the value of contingency risk, here, we only consider critical contingency B-D，so $CtgRisk_{B-D,max}$ =0.0065；

(2) *Second contingency circuit risk limits*: this is the limit to constrain the value of second contingency circuit risk, here, we only consider such circuit risk under critical contingency B-D， so $CctRisk^{B-D}_{A-B,max} = 0.0000$，$CctRisk^{B-D}_{A-D,max} = 0.0018$；$CctRisk^{B-D}_{A-E,max} = 0.0021$；$CctRisk^{B-D}_{B-C,max} = 0.0002$，$CctRisk^{B-D}_{B-E,max} = 0.0007$；$CctRisk^{B-D}_{B-F,max} = 0.0038$，$CctRisk^{B-D}_{C-E,max} = 0.0015$，$CctRisk^{B-D}_{C-F,max} = 0.0022$；$CctRisk^{B-D}_{D-E,max} = 0.0000$，$CctRisk^{B-D}_{E-F,max} = 0.0002$.

(3) *System risk limits:* this is the limit to constrain the value of system risk, and $Risk_{max}$=1.35.

2. The determination of C_r

To select C_r, according to criterion 1 set forth in Section 4.3.2, we solve RBCR-F1 under multiple values of C_r from 50 to 500 with a step size of 20, and calculate corresponding production costs and $Risk$. The 3-D scatter plot in Figure 6-2 shows that, with increasing value of C_r (50~250), the $Risk$ component is decreasing and the production cost is rising in the form of a step function. When $C_r \geq 250$, the value of $Risk$ and production costs tend to saturate, and it reaches a steady-state. So we select $C_r^{upper} = 250$. According to criterion 2, C_r^{lower}=$\Delta ProductionCosts/\Delta Risk$ =166. So our choice range for C_r is 166 to 250; we choose $C_r = 250$, because at this value, the risk is minimum with relatively little rise in production costs.

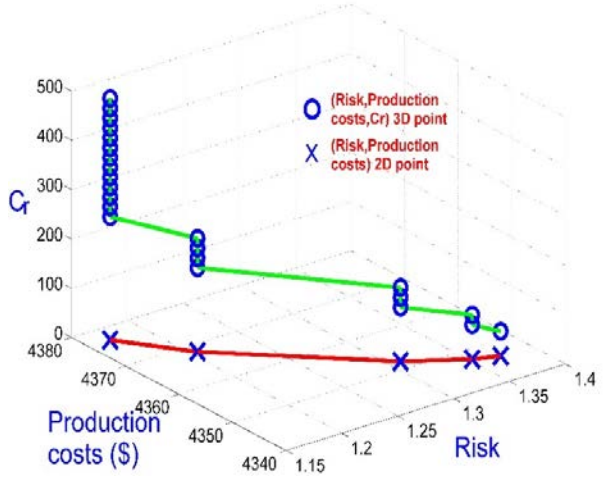

Figure 6-2 The C_r curve

3. The determination of $Penalty_l^k$

As introduced in Chapter 3, the penalty price of the industry model is on the scale of thousands of dollars, a value that is driven by the magnitude of total energy sales. However, the system we are using for illustration has only six buses and the total energy sale is not so large, so there is no need to use a large penalty price.

In addition, the value of penalty price has significant effects on LMP. In order to fairly compare the LMPs from the two models, we should select penalty prices according to a consistent attribute characterizing the system of interest. To this end, we select the risk penalty to equal the summation of violations times the selected penalty price for the industry-based CR. According to this, we select the penalty price for the industry-based CR model to be $Penalty_l^k = 50$.

6.2 Constraint relaxation results

6.2.1 Distribution of heavily-loaded post-contingency flows

In order to examine the distribution of heavily-loaded post contingency flows, the security diagrams under pre-defined contingencies [42] are drawn for each constraint relaxation method, as shown in Figure 6-3(a)~(b). The sector angular spread is proportional to the probability of the particular contingency, and the radial distance from the center is proportional to the loading value. Figure 6-3(a) compares the industry-based CR approach (model CR-F1) with the risk-based CR approach where risk is in the objective function (model RBCR-F1). Figure 6-3(b) compares the industry-based CR approach (model CR-F1) with the risk-based CR approach where risk is constrained (model RBCR-F2). In both comparisons, the total risk of CR-F1 exceeds that of the corresponding RBCR case.

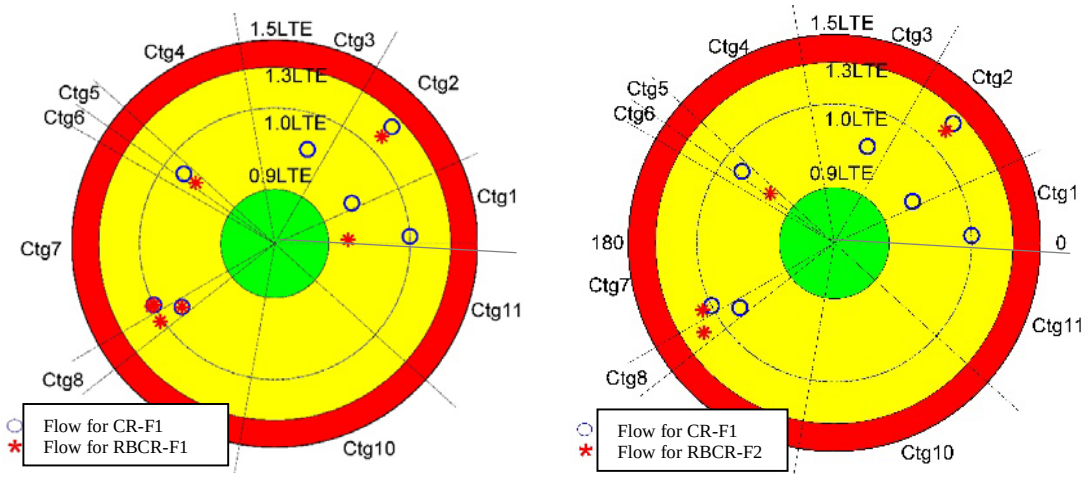

(a) CR-F1 and RBCR-F1 (b) CR-F1 and RBCR-F2

Figure 6-3 Heavily-loaded flow distribution (≥ 0.9LTE)

Figure 6-3 (a) indicates that CR-F1 shows flows in excess of 0.9LTE for 7 out of the 11 contingencies, whereas RBCR-F1 shows flows in excess of 0.9 LTE for only 6 out of the

11 contingencies. Of these 6 heavily-overloaded flows, there is only one where the RBCR-F1 flow exceeds the CR-F1 flow; this is for contingency 8, a very low probability contingency. The reason for this is that, whereas the industry-based approach CR-F1 only exerts dispatch control for the circuits having flows exceeding 1.0 LTE, the risk-based approach RBCR-F1 exerts dispatch control for all flows exceeding 0.9LTE, in proportion to its overload severity and the probability of its occurrence.

Figure 6-3 (b) is similar in that CR-F1 shows flows in excess of 0.9LTE for 7 out of 11 contingencies, whereas RBCR-F2 shows flows in excess of 0.9LTE for only 4 out of the 11 contingencies. Of these 4 heavily-loaded circuits, there are two where the RBCR-F2 flow exceeds the CR-F1 flow; this is for contingencies 7 and 8. Again, contingency 8 is very low probability. Although contingency 7 is not low probability, the difference between the flow from CR-F1 and that from RBCR-F2 is relatively small. The result verifies that CR-F1 only exerts dispatch control for the circuits having flows exceeding 1.0 LTE.

6.2.2 Dispatch decision

For system operators, dispatch decision is an important result deriving from SCED model, Table 6-2 summarizes the dispatch decision for these three models.

Table 6-2 Dispatch decision (unit: MW)

Model	Industry-based CR	RBCR-F1	RBCR-F2
Gen. at bus A	192	177	159
Gen. at bus B	46	55	58
Gen. at bus C	72	78	93

Table 6-2 shows that more output is dispatched from the cheaper generator G_B, and less from the more expensive generator G_A in RBCR. For industry-based CR, the output from G_B has to be reduced due to the congested line B-D. However, in the risk-based approaches, the power flow has been redistributed such that more output could be anticipated from cheaper generators G_B , G_C , and less from the more expensive generator G_A.

6.2.3 Costs analysis

Economics is an important evaluation factor in power system operation. The costs of these three models are listed in Table 6-3.

Table 6-3 Costs analysis

Model	**Industry-based CR**	**RBCR-F1**	**RBCR-F2**
Production costs($/5 minutes)	4407	4377	4348
Total costs ($/5 minutes)	5377	4670	4348

According to Table 6-3, RBCR-F2 has the lowest production costs, while that of RBCR-F1 is higher and that of industry-based CR is the highest. RBCR redistribute the overload

and the generation re-dispatch has better economic effects, resulting lower production costs. Especially, the production costs of RBCR-F2 is slightly lower due to the fact that RBCR-F2 allows slightly higher risk, that is to say, this enhancement of economy is at the sacrifice of system risk.

In addition, the order of the total costs is the same as that of production costs. The reason is that RBCR-F2 has no additional costs in total costs function, and risk penalty in RBCR-F1 is lower than violation costs in industry-based CR.

In conclusion, the relaxation result of RBCR-F2 is the most economic, while RBCR-F1 is less and industry-based CR is the least.

6.2.4 Risk index comparison and relaxation level

Table 6-4 gives the value of risk indices and Table 6-5 is the result of relaxation level, which is determined by the criteria in Section 4.3.3.

Table 6-4 Value of risk indices

Model	Industry-based CR	RBCR-F1	RBCR-F2
System risk	1.500	1.170	1.350
Contingency risk of line B-D	0.007	0.002	0.000

Table 6-5 Value of $K_{C,l}$

Line	Industry-based CR	RBCR-F1	RBCR-F2
A-B	1.10	1.10	1.10
A-D	1.10	1.10	1.10
A-E	1.10	1.10	1.10
B-C	1.10	1.10	1.10
B-D	**1.34**	**1.23**	**1.26**
B-E	1.10	1.10	1.10
B-F	1.10	1.10	1.10
C-E	1.10	1.10	1.10
C-F	**1.10**	**1.13**	**1.25**
D-E	1.10	1.10	1.10
E-F	1.10	1.10	1.10

The RBCR models have less system risk. The reason is that the industry-based CR does not consider system-level risk; RBCR adopts the risk metric to quantify system-level security, and conducts constraint relaxations. Furthermore, RBCR could re-dispatch the overflow circuits in an optimized way, which brings less degradation on system-level security. As described in Table 6-5, industry-based CR relax line B-D to $1.34 \times Limit_{BD}^{0}$, while RBCR-F1 (F2) relax line B-D to $1.23(1.26) \times Limit_{BD}^{0}$ and line C-F to $1.13(1.25) \times Limit_{CF}^{0}$, to remove infeasibility of SCED. So RBCR is associated with less stress on system risk. In addition, the contingency risk of the critical contingency k is also smaller, since we have constraints to indirectly (RBCR-F1) or directly (RBCR-F2) control

critical contingency risk.

In conclusion, the system is less risky than it is with industry-based CR; the critical contingency is also less risky than it is with industry-based CR and the overloaded circuit under particular contingency is less risky than it is with industry-based CR. The mechanism of RBCR, realizes the requirements of the structured design as described in section 4.1.

6.2.5 Effects on LMP

As mentioned in Section 6.1, we set $Penalty_l^k = 50$, to decrease the large LMP spike resulting from the huge value of $Penalty_l^k$, providing a basis for comparing the industry-based CR approach with the RBCR approaches. In order to conduct comparisons, we also solve the industry-based CR model with the very high value of penalty price typical of industry today, and the corresponding results are expressed in Table 6-6.

Table 6-6 LMP for industry-based CR under two penalty price (unit: $/MW)

LMP	Penalty price from industry	Penalty price based on RBCR
A	13.53	13.53
B	11.23	11.24
C	11.83	11.83
D	1727.50	53.73
E	405.40	21.42
F	654.10	26.33

As shown in Table 6-6, buses D, E, and F have relatively higher LMPs than other buses in the network, resulting from congestion in line B-D. With penalty price based on RBCR, the LMPs at buses D, E and F are much lower, but the spiking tendency is still obvious.

The LMPs computed with the industry-based CR method are compared with the LMPs computed from the RBCR method in Figure 6-4 and Table 6-7.

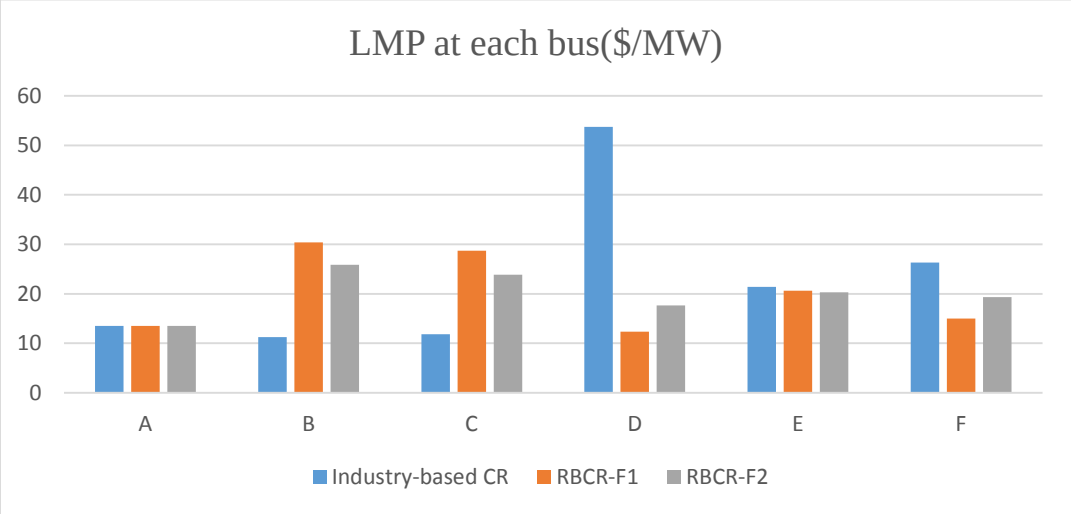

Figure 6-4 LMP at each bus

Table 6-7 LMP at each bus

Model	Bus	(R)LMP	(R)LMP Energy	(R)LMP Congestion	(R)LMP Risk	(R)LMP Variance
Industry-based CR	A	13.53	13.53	0	-	262
	B	11.24	13.53	-2.29	-	
	C	11.83	13.53	-1.70	-	
	D	53.73	13.53	40.20	-	
	E	21.42	13.53	7.89	-	
	F	26.33	13.53	12.80	-	
RBCR-F1	A	13.53	13.53	0.00	0.00	62
	B	30.37	13.53	16.53	0.30	
	C	28.69	13.53	12.62	2.54	
	D	12.33	13.53	10.98	-12.18	
	E	20.63	13.53	10.74	-3.65	
	F	14.97	13.53	13.35	-11.91	
RBCR-F2	A	13.53	13.53	0.00	0.00	19
	B	25.89	13.53	11.81	0.54	
	C	23.84	13.53	9.02	1.28	
	D	17.66	13.53	7.85	-3.72	
	E	20.28	13.53	7.68	-0.93	
	F	19.32	13.53	9.54	-3.74	

As indicated in Table 6-7 and Figure 6-4, high LMPs are observed at bus D for industry-based CR, due to the constraint violations. The price spike comes from the congestion component in the LMP. For RBCR, there is no price spike, and the volatility is much lower (as reflected in the variance) since congestion has been significantly reduced and re-distributed over the system. Although LMP increase a bit due to congestion component, the risk component smooths LMP at each bus. In addition, we observe the fact the LMP variance of RBCR-F2 is lower than that of RBCR-F1. This is the consequences of penalty price in the component, descried in equation (5-22). Thus, RBCR-F2 is free of penalty price, and can further smooth LMP distribution.

In addition, from the risk component in LMP, there are three observations, which verifies the conclusion made in [16].

(1) A bus will see higher price (than industry-based LMP) if it is at the source of a congested line and the risk component is positive;
(2) A bus will see lower price (than industry-based LMP) if it is at the sink of a congested line and the risk component is negative;
(3) The RLMP in other buses may increase or decrease, depending on the calculation result.

6.3 Summary

The results from six-bus network indicates that risk-based CR has better performance than industry-based CR in handling infeasible SCED problem. RBCR could re-distribute overload flow in a more uniform way, thus improving system security and reducing economic production costs. RBCR also decreases geographical and temporal variability in LMPs.

7. Conclusion and future work

7.1 Conclusion

The infeasible SCED is solved successfully by the proposed method---Risk-based constraint relaxation (both formulation 1 and formulation 2). It introduces risk metric to quantify the system security. The relaxation level determination considers the value of violation indicator, ATR constraint and circuit post-contingency risk, which could determine an optimized decision on how much relaxation level for each candidate branch, with the least (for RBCR-F1, controlled for RBCR-F2) system-wide security stress imposed on system operation. Also, LMP calculated by RBCR is more stable and with less volatile. So RBCR is a promising way to addressing infeasible SCED problem.

The advantage of applying RBCR in solving infeasible SCED is that it utilizes a metric—the concept of risk, to quantify the effects on system security by allowing overflow on transmission lines. Then it's possible to compare which approach is a better way to solving infeasible SCED problem in terms of system-wide security. With the constraint on system risk, we can also control the relaxation actions, making which are guaranteed to satisfy the reliability requirements of system operation. Besides, the approach of RBCR-F1 can give some reference on determining the penalty price in industry approach; while RBCR-F2 is free of penalty price.

One challenge of approach RBCR-F1 is that we should determine reasonable weights for the components in objective function, that is to say, the penalty price, which can lead to a much more optimized solution in terms of guaranteeing system security. To achieve the weight, we already propose some criteria to constraint the range of penalty price. Another challenge is that the thermal limits of conductor would vary with the voltage level and ambient condition. The formulation of RBCR approach should be able to reflect such situations. Besides, what we have done only considers constraint relaxation under contingency situation, and it would be more helpful if the risk-based constraint relaxation approach can also be applied in addressing pre-contingency constraints, that is to say, the thermal limits under normal situation. When we consider both pre-contingency and post-contingency constraints, we should choose reasonable weights to combine them together.

7.2 Future work

There will be a follow-up project from PSERC---*Risk Assessment of Constraint Relaxation Practices*. We are in the process of further developing our work in three directions, as described in the remainder of this section.

- **Constraint relaxation by dynamic line rating**

Static line ratings (SLR) are typically computed under conservative weather conditions (ambient temperature, wind speed, wind direction, and solar radiation [43]) by season. If real-time measurements are available, then dynamic line ratings (DLR) may be used, where ratings are computed as a function of i)current through the conductor, ii)conductor size and type, and iii) measured and telemetered weather conditions (as described above). DLRs

therefore vary with time. Lines equipped with DLR measurement devices may be limited to only those which are known to frequently require constraint relaxations.

- **Risk-based constraint relaxation under normal conditions**

The work described in this report is focused on risk-based constraint relaxation under contingency conditions, which considers the thermal limits under normal conditions as hard constraints that cannot be violated. However, the thermal limits under normal conditions are set based on credible, but highly conservative weather conditions.

Under the assumption that the market solution results in a corresponding network condition (and therefore the market solution will actually occur), then a normal condition violation differs from a contingency violation, because the normal condition occurs with probability almost 1.0, but the contingency condition occurs with very low probability. This difference should be reflected in the amount of overload allowed or in the amount of time an overload is allowed, or both.

We conclude by recognizing that there are two approaches for treating a normal condition overload, and there are two options under each approach, as follows:

Approach 1, Modify bus injections:

a. Re-dispatch: This option is preferred if it is available; if it is not (or if it is too expensive), then either option 1b or approach 2 must be used.
b. Interrupt load: This is the least preferred option.

Approach 2, Apply constraint relaxation:

a. Increase allowable rating based on DLR: This option is attractive if DLR has been deployed for the line for which the constraint relaxation will be applied.
b. Take short-term risk: The risk of allowing a temporary increase in rating can be assessed if (i) some weather information (not DLR measurements) is available so that it can be characterized with probability distribution functions; (ii) the speed of re-dispatch capability to relieve the overload can be assessed. A constraint relaxation can then be assessed based on quantitative risk assessment.

- **Risk-based constraint relaxation for corrective SCED**

The risk-based constraint relaxation approach described in this report uses a preventive risk-based SCED formulation, which does not account for the possibility of corrective action following the constraint relaxation. On the other hand, this influence can be included within a corrective SCED formulation. Incorporating adaptive transmission rates within such a formulation would provide that the transmission rates are a function of the time required to relieve them. A risk-based corrective SCED formulation [44] would ensure that transmission rate increases do not pose excessive system risk.

References

[1] MISO Market Subcommittee Presentation, 'Constraint Relaxation Status Updates'. [Online]. https://www.misoenergy.org/Library/Repository/Meeting%20Material/Stakeholder/MSC/2011/20110628/20110628.

[2] S. Maslennikov and E. Litvinov, 'Adaptive Emergency Transmission Rates in Power System and Market Operation,' IEEE Transactions on Power Systems, vol.24, no.2, pp.923-929, May 2009.

[3] B. Stott and E. Hobson, 'Power System Security Control Calculations Using Linear Programming, Part II,' IEEE Transactions on Power Apparatus and Systems, vol.PAS-97, no.5, pp.1721-1731, Sept. 1978.

[4] B. Stott and J. Marinho, 'Linear Programming for Power-System Network Security Applications,' IEEE Transactions on Power Apparatus and Systems, vol.PAS-98, no.3, pp.837-848, May 1979.

[5] M. Irving and M. Sterling, 'Economic Dispatch of Active Power with Constraint Relaxation,' IEE Proceedings C on Generation, Transmission and Distribution, vol.130, no.4, pp.172-177, July 1983.

[6] S. Zhang and M. Irving, 'Analytical Algorithm for Constraint Relaxation in LP-based Optimal Power Flow,' IEE Proceedings C on Generation, Transmission and Distribution, vol.140, no.4, pp.326-330, Jul 1993.

[7] O. Alsac, J. Bright, M. Prais, and B. Stott, 'Further Developments in LP-Based Optimal Power Flow,' IEEE Transactions on Power Systems, vol.5, no.3, pp.697-711, Aug 1990.

[8] California ISO (CAISO),'Parameter Tuning for Uneconomic Adjustments in the MRTU Market Optimizations'. May, 2008. [online] https://www.caiso.com/Documents/DraftFinalProposal-Parameter Tuning Uneconomic AdjustmentsinMRTUMarketOptimization09-Jun-2008.pdf

[9] Mid-continent ISO (MISO), 'Filing of the Midcontinent Independent System Operator, Inc., to Revise Its Tariff to Add a Transmission Constraint Demand Curve', FERC Docket No. ER13-2295-000.

[10] Mid-continent ISO (MISO), 'Constraint Relaxation Update', Market Subcommittee, May 1, 2012. [online]https://www.misoenergy.org/Library/Repository/Meeting%20Material/Stakeholder/MSC/2012/20120605/20120605%20MSC%20Item%2003a%20Constraint%20Relaxation.pdf

[11] Electric Reliability Council of Texas (ERCOT), 'Setting the Shadow Price Caps and Power Balance Penalties in Security Constrained Economic Dispatch', Wholesale Market Operations, Oct 20, 2010.

[12]Electric Reliability Council of Texas (ERCOT), 'SCED Power Balance Penalty Curve'. ERCOT Business Practice.

[13] ISO-New York (ISO-NY), '2009 Assessment of the Electricity Markets in New England', External Market Monitor, June 2010.

[14] Pennsylvania-Jersey-Marylandd (PJM), 'Order On Compliance Filing,' issued April 19, 2012.

[15] M. Ni, J. McCalley, V. Vittal, S. Greene, C. Ten, V. Gangula, and T. Tayyib, "Software Implementation of on-line risk-based security assessment," IEEE Transactions on Power Systems, Vol. 18, No. 3, August 2003, pp 1165-1172.

[16] Qin Wang, 'Risk-Based Security-Constrained Optimal Power Flow: Mathematical Fundamentals, Computational Strategies, Validation and Use Within Electricity Markets,' Ph.D. dissertation, Dept. of ECpE, Iowa Sate Univ., Ames, IA, 2013.

[17] V. Miranda and L. Proenca, 'Why Risk Analysis Outperforms Probabilistic Choice as the Effective Decision Support Paradigm for Power System Planning', IEEE Transactions on Power Systems, vol.13, no.2, pp. 643-648, May 1998.

[18] P. Linares, 'Multiple Criteria Decision Making and Risk Analysis as Risk Management Tools for Power System Planning', IEEE Transactions on Power Systems, vol.17, no.3, pp. 895-900, Aug. 2002.

[19] W. Li, P. Choudhury, D. Gillespie, and J. Jue, 'A Risk Evaluation Based Approach to Replacement Strategy of Aged HVDC Components and its Application at BCTC', IEEE Transactions on Power Delivery, vol.22, no.3, pp. 1834-1840, 2007.

[20] A. Janjic and D. Popovic, 'Selective Maintenance Schedule of Distribution Networks Based on Risk Management Approach', IEEE Transactions on Power Systems, vol.22, no.2, pp. 597-604, 2007.

[21] G. Strbac, R. Moreno, D. Pudjianto, and M. Castro, 'Towards a Risk-Based Network Operation and Design Standards', IEEE Power and Energy Society General Meeting. Detroit, MI, July 2011.

[22] T. Zheng and E. Litvinov, 'Operational Risk Management in the Future Grid Operation', IEEE Power and Energy Society General Meeting. Detroit, MI, July 2011.

[23] P. Varaiya, F. Wu and J. Bialek, 'Smart Operation of Smart Grid: Risk-Limiting Dispatch', Proceedings of IEEE, vol.99, no.1, pp. 40-57, Jan. 2011.

[24] Q. Wang , J. McCalley, T. Zheng and E. Litvinov, 'A Computational Strategy to Solve Preventive Risk-Based Security-Constrained OPF,' IEEE Transactions on Power Systsms, vol.28, no.2, pp.1666-1675, May 2013.

[25] Q. Wang, G. Zhang, J. McCalley, T. Zheng and E. Litvinov, 'Risk-Based Locational Marginal Pricing and Congestion Management,' IEEE Transactions on Power Systems, vol.29, no.5, pp.2518-2528, Sept. 2014.

[26] M. Ni, J. McCalley, V. Vittal, etc. 'Software implementation of online risk-based security assessment,' IEEE Transactions on power systems, vol.18, no.3, pp.1165-1172, Aug. 2003.

[27] J. McCalley, V. Vittal, and N. Abi-Samra, 'An overview of risk based security assessment,' IEEE Power Engineering Society Summer Meeting, 1999, vol.1, no., pp.173-178 , Jul 1999.

[28] D. Niebur and A.J. Germond, 'Power System Static Security Assessment Using the Kohonen Neural Network Classifier', IEEE Transaction on Power Systems, vol.7, no.2, pp.865-872, May 1992.

[29] F. Xiao, J. McCalley, Y. Ou, et al., 'Contingency Probability Estimation Using Weather and Geographical Data for On-Line Security Assessment,' Int. Conf. on Prob. Methods Applied to Power Syst., Stockholm, June 2006.

[30] J. McCalley, F. Xiao, Y. Jiang, et al., 'Computation of Contingency Probabilities for Electric Transmission Decision Problems,' Proc. of the 13th Int. Conf. on Intelligent Syst. Appl. to Power Syst., Arlington, Nov. 2005.

[31] G. Grimmett and D. Stirzaker, Probability and Random Process, 3rd ed., Oxford University Press, 2001

[32] A. Geoffrion, 'Generalized Benders decomposition', Optimization Theory Application., vol. 10, no. 4, pp. 237–260, 1972.

[33] 2013 Annual Markets Report, ISO New England, May 2013. http://www.isone.com/markets/mkt_anlys_rpts/annl_mkt_rpts/2013/2013_amr_final_050614.pdf

[34] State of the Markets Reports, New York ISO, May 2014. https://www.potomaceconomics.com/uploads/nyiso_reports/NYISO_2013_SOM_Report.pdf

[35] PJM Training Materials (LMP 101), PJM. http://www.pjm.com/Globals/Training/Courses/ip-lmp-ftr-101.aspx

[36] 2011 State of Market Report for the MISO Electricity Markets Midcontinent ISO, May 2011. https://www.potomaceconomics.com/uploads/midwest_reports/2011_SOM_Report.pdf

[37] B. Chakrabarti, C. Edwards, C. Callaghan, and S. Ranatunga, Alternative Loss Model for the New Zealand Electricity Market using SFT, 2011 IEEE Power and Energy Society General Meeting, Detroit, USA.

[38] L. Chen, H. Suzuki, T. Wachi, and Y. Shimura, 'Components of Nodal Prices for Electric Power Systems,' IEEE Transaction on Power Systems, vol. 17, no. 1, pp. 41- 49, 2002.

[39] T. Orfanogianni and G. Gross, 'A General Formulation for LMP Evaluation,' IEEE Transaction on Power Systems, vol. 2, no. 3, pp. 1163-1173, 2007.

[40] A. Conejo, E. Casillo, R. Minguez, and F. Milano, 'Locational Marginal Price Sensitivities,' IEEE Trans. Power Sys., vol. 20, no. 4, pp. 2026-2033, 2005.

[41] A. Wood and B. Wollenberg, Power Generation, Operation and Control, 2nd . New York, NY, USA: Wiley, 1996.

[42] F. Xiao and J. McCalley, 'Risk-Based Security and Economy Tradeoff Analysis for Real-Time Operation,' IEEE Transactions on Power Systems, vol.22, no.4, pp.2287-2288, Nov. 2007.

[43] IEEE Power Engineering Society, Transmission and Distribution Committee, 'IEEE Standard for Calculating the Current-temperature Relationship of Bard Overhead Conductors,' IEEE STD 738-2012, New York: Institute of Electrical and Electronic Engineers, 2013.

[44] Q. Wang, J. McCalley, T. Zheng, and E. Litvinov, 'Solving Corrective Risk-based Security-Constrained OPF with Lagrangian Relaxation and Benders Decomposition,' under review by International Journal of Electrical Power and Energy Systems.